Controlled Molecular Release through Polymeric Vehicle

Anindita Laha

A Dissertation Submitted to
Indian Institute of Technology Hyderabad
in Partial Fulfillment of the Requirements for
The Degree of Doctor of Philosophy

भारतीय प्रौद्योगिकी संस्थान हैदराबाद
Indian Institute of Technology Hyderabad

Department of Chemical Engineering

November 2017

Declaration

I declare that this written submission represents my ideas in my own words, and where others' ideas or words have been included, I have adequately cited and referenced the original sources. I also declare that I have adhered to all principles of academic honesty and integrity and have not misrepresented or fabricated or falsified any idea/data/fact/source in my submission. I understand that any violation of the above will be a cause for disciplinary action by the Institute and can also evoke penal action from the sources that have thus not been properly cited, or from whom proper permission has not been taken when needed.

Anindita Laha
CH12P001

Approval Sheet

This thesis entitled **"Controlled Molecular Release through Polymeric Vehicle"** by **Anindita Laha** is approved for the degree of Doctor of Philosophy from IIT Hyderabad.

Dr. KV Venkatesh
IIT Bombay
External Examiner

Dr. Chandra Shekhar Sharma
IIT Hyderabad
Internal Examiner

Dr. Saptarshi Majumdar
IIT Hyderabad
Advisor

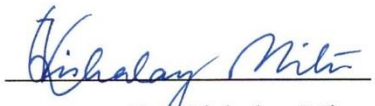

Dr. Kishalay Mitra
IIT Hyderabad
Co-Advisor

Dr. Subha Narayan Rath
IIT Hyderabad
Chairperson

Acknowledgements

The PhD program is truly like a marathon event, one which I would not have been able to complete without the constant support of the innumerable people over the past five years.

First, I would like to convey my deepest gratitude to my thesis advisor Dr. Saptarshi Majumdar for his supervision, scientific discussions and support in all matters, academic or otherwise. I consider myself extremely fortunate to have received a chance to work under your supervision as you have shown me how to stand my ground and prepare for the kind of career that I have always wished for in my life. I will forever be grateful to you for your guidance and kindness. You have always been patient and encouraging when it came to discussing new scientific ideas as well as persevering in the face of many difficulties. I consider the lessons I learnt from you about research and life an asset and I hope to pass on what you have taught me to many others.

I would also like to extend my gratitude to my thesis co-advisor, Dr. Kishalay Mitra for his valuable suggestions and especially, for his extremely motivational and helpful attitude. Apart from technical help, I prize your lessons on how to approach research from a calm and steady position and this has helped me tackle work during stressful days. Your kind words and cheerful nature has certainly given me a lot of confidence and hope towards doing better work. It has been a pleasure to have you as my co-advisor.

My sincere thanks to Dr. Chandra Shekhar Sharma for the productive collaborations, guidance, support and encouragements. I am truly grateful to him for his valuable comments throughout my PhD work. I deeply appreciate your expertise in the field of nanotechnology that influenced and motivated me to work in this field. I consider myself extremely fortunate to get his guidance as an honorary thesis advisor. I would like to thank him from the bottom of my heart for having faith in me at every stage of this journey. My heartiest regards to you, sir, for your promptness, encouragement, care and hard work. Thank you for being such a wonderful mentor and a great role model.

I would like to extend my appreciation to all members of my doctoral committee for the varied technical support I have received from them throughout this program. I would like to express my sincere gratitude to Dr. U. B. Desai, Director of IIT Hyderabad, for providing good research environment. I would like to express my sincere gratitude to Dr. Narasimha Mangadoddy, Head of the Department of Chemical Engineering, for all kind of help and support. I would like to thank Dr. Basant K Patel, Head of the Department of Biotechnology, for being part of my doctoral committee as an external member. Despite his extremely busy schedule divided among research, teaching and administrative work; he has taken time out to review the annual progress of my work carefully.

I would also like to thank Dr. Debaprasad Shee for his valuable suggestions and expertise, which helped me immensely during this journey. I am extremely grateful to him for allowing me to avail the latest equipment that has facilitated the progress of my PhD thesis smoothly. I consider myself extremely lucky to have him as part of my doctoral committee.

I would also like to thank Dr. Lopamudra Giri for her valuable suggestions and appreciation of our work. I genuinely admire your kind and humble nature. I would like to convey my thanks to Dr. Mudrika Khandelwal, Assistant professor, Department of Materials Science and Metallurgical Engineering for the collaborative work. My sincere thanks to Dr. Pinaki Prasad Bhattacharjee, Head of the Department of Materials Science and Metallurgical Engineering, Dr. G Prabu Sankar, Associate professor, Department of Chemistry for giving me an opportunity to access their lab facilities for characterizing my samples. I would also like to thanks all the anonymous reviewers who has given excellent suggestions during the review process of journal publications. Although I have faced several rejections from their journals but it has always helped me to improve the quality of the article every single time.

I would like to thank my M.Tech thesis advisor Dr. Sekhar Bhattacharjee, Professor and former Dean of Technology, thesis co-advisor Dr. Sampa Chakrabarti, Head of the Department and Dr. P. Roy, retired Professor, Department of Chemical Engineering, Calcutta University, for encouraging me to pursue a PhD. My deepest gratitude to Dr. Seeram Ramakrishna, Director of Center for Nanofibers & Nanotechnology, NUS for your kind words during GIAN course. I would like to

mention here that your books and articles that I avidly read influenced my interest and work in the area of nanofiber. However, meeting you in person and being part of a collaboration with you became a different level of experience altogether. I consider myself extremely fortunate to have received this opportunity. I would also like to extend my appreciation to Dr. Kajori Kargupta, Professor, Department of Chemical Engineering, Jadavpur University for inspiring me. I would like to express my sincere gratitude to Dr. Abhijit Majumdar, Assistant Professor, Department of Chemical Engineering, IIT Bombay and Dr. Rabibrata Mukherjee, Associate Professor, Department of Chemical Engineering, IIT Kharagpur for their motivating speech during Chemference 2015. Although I have only had the chance of a very short conversation with them, their words have been a great source of motivation for me. I would also like to express my regards to Dr. Nandini Ramesh Sankar, Assistant Professor, Department of Liberal Arts, IIT Hyderabad who has also inspired me indirectly and continues to amaze with her kindness. Although, I have never met her and have only heard of her from my friends, I truly admire her sensitive and down-to-earth persona.

Further, I would like to thank all my co-workers, past and present members, of our Poly-Nano-Bio (PNB) research group for their help and support throughout this journey. I also would like to thank Dr. Chandra, Dr. Debaprasad and Dr. Kishalay's group members for their support. Special thanks to Utkarsh, Deepak, Manohar. K for their help during the process of setting up our research lab. Utkarsh and I had started our journey together from procuring instruments to building up our first experimental research lab in the permanent campus. I would also like to extend my thanks to Shital and Mrunalini for the productive collaborative work. Thank you for all night outs and fun we had in our lab. Many thanks to the other lab mates Anitha di, Srinadh, Pinaki, Prateek, Akash, Karthik, Kali Suresh, M. Suresh, N. Jyothi, Karan, Prerna for all the good memories. Each of you have helped me persevere through the long and isolating process of PhD. I wish all of you great success in life.

My countless thanks to all the staff members of the Academic, Administration, Library, Store, and Account section for their help and cooperation during this period. My deep regards to all security guards and bus drivers who have always been nice and have made my work at the lab during late hours comfortable and safe.

In addition, I would like to thank my friends who have made this difficult journey bearable. I would like to start with my beloved roommate, Neethi who has been a great source of strength for me always. Honestly, without her selfless love and friendship, I would not have survived here. It makes me wonder how a complete stranger becomes such a close friend as she has stuck with me through thick and thin of both my personal and academic life. I would like to thank Nilanjana for being such a sweet and empathetic friend. I will never forget the fun we had during our Creative Arts courses, while swimming or simply wandering about the campus, wondering about life. I would also like to thank Utpal from the core of my heart for his friendship and support in times of need. Thank you for being there for me and for the endless conversations over tea. My sincere thanks to Sreeparvathi, Anudeep, Santanu, Saswati, Soumya, Dan, and Anand for making this experience unforgettable. I would also like to thank my school friends Manali, Nandana, Purbasha, Oeindrila for their love and support through the years. My note of gratitude would be incomplete without the mention of Manojit, Abhi da, Subham da, and Arnab for their friendship and constant support. Thank you.

Finally yet most importantly, I would like to thank my parents for their endless sacrifice, encouragement and support. I would like to thank my elder brother, Anirban with all my heart for trusting me and convincing our parents in my favour for me to be able to pursue my dreams. You have been always an invaluable support system and a source of joy for me.

Dedicated to

Ma, Baba and Dada

Abstract

Controlled drug delivery systems (DDS) have gained a lot of attention recently due to their added advantages such as improving therapeutic efficacy in delivering the drug molecules at a predetermined rate to the targeted site for a prolonged period. Designing a polymer based DDS involves an in-depth understanding of drug-carrier interactions, and good control over the parameters that can modulate transportation of drug molecules according to the therapeutic requirement.

Delivering less soluble drug molecules encapsulated in hydrophilic polymer matrix in zero-order manner is usually a challenge. To counter this challenge, we used Piperine, a model hydrophobic drug and Amphotericin B (Amp-B), a model amphiphilic drug in order to develop a polymer based DDS. We also used FDA approved natural polymer gelatin (type A) as an excipient because of its biocompatibility, biodegradability, muco-adhesiveness and easy availability. Despite of all the advantages of gelatin, it is extremely hydrophilic and has poor mechanical stability in an aqueous solution that limits its application and long-term usage. To overcome this challenge, we used Glutaraldehyde (GTA) as a crosslinker to modify gelatin. Although GTA is widely used as a crosslinker because of its excellent efficiency in stabilizing collagenous material, higher concentration of GTA solution (25 % v/v) and longer exposure in saturated vapor of GTA (more than 24 h as reported in literature) may have adverse cytotoxic effects. We successfully used a highly diluted concentration of GTA solution (0.01-0.25 % v/v) and reduced the exposure time to only 6 minute to saturated GTA vapor for crosslinking to achieve the desired stability of the fabric. In summary, this thesis investigates the full potential of natural polymer (gelatin, type A) based cast-film (GCF) and electrospun nanofiber film (GNF) as DDS, particularly for less soluble drug molecules.

The thesis starts with the fabrication of GCF as a potential drug-carrier for hydrophobic molecule, piperine, by solvent evaporation method. Piperine was selected because of its viable features such as its bio-enhancer properties, and anti-oxidant, anti-depressant, anti-inflammatory and anti-tumor activities. Thus, piperine was wrapped into GCF in order to protect the bioactive molecule from enzymatic

degradation in gastrointestinal (GI) tract. To increase the water repulsion capability of the vehicle, we used higher concentration of polymer during fabrication and GTA solution for crosslinking. Higher concentration of polymer led to longer diffusional path, which caused less swelling followed by less degradation. On the other hand, GTA increased the molecular entanglement that not only promoted better stability, but also controlled the initial fast release of drug molecules. The concentration of polymer and crosslinker used for the system were the main cause of drug release i.e. due to diffusion or degradation. The distribution of drug was found on the surface as well as in bulk of the GCF, which resulted in initial fast release followed by sustained release. We developed an overall understanding about the drug-polymer interactions, roles of crosslinker on swelling, as well as release study from the GCF vehicle. After exploring different aspects of drug loaded cross-linked GCF in terms of morphology, biodegradation, thermal stability of the drug loaded vehicle, the vehicle still needed further modifications such as, (a) creating porous structured vehicle, to reduce usage of GTA solution for crosslinking, (b) controlling the initial burst release of drug in lower pH and (c) achieving zero-order drug release for prolonged time.

In the next step, with the previous understanding of drug-polymer interactions, we tried to develop a DDS based on GNF due to its unique structural features. Electrospinning has become the most common and cost-effective nanofiber production technique due to its capability of fabricating ultrafine continuous fibers with very high surface-to-volume ratio and with interconnected porosity as well as tunable pore dimensions. Nanofibrous structure, which is made of natural, biodegradable, biocompatible polymer, has tremendous applications in different biomedical fields.

The purpose of the present study is to fabricate a large surface area-to-volume GNF device for drug delivery application. The work involves three main steps i.e., (a) fabricating less soluble drug encapsulated hydrophilic GNF, (b) modulating the stability by crosslinking and finally, (c) modifying the vehicles with different crosslinking strategies and multi-layered structure so as to achieve zero-order release of the hydrophobic drug, piperine.

In keeping with the above-mentioned steps, firstly, continuous long nanofibers were fabricated and drug-polymer interactions were checked using Fourier transform

infrared spectroscopy (FTIR). Similar to GCF, we found that piperine was intact in the GNF with no reaction with the polymer matrix. The morphology of the fibers was also examined using Scanning Electron Microscopy (SEM) imaging instrument after gold coating the samples for 10 seconds. Long and continuous fibers with average diameter of 150 nm and characteristic peaks of piperine in GNF provided the evidence of the drug encapsulation in the polymer matrix. Due to the highly porous structure and hydrophilicity of the polymer, GNF were cross-linked with saturated vapor of GTA for only 6 minutes. This porous structure not only reduced the usage of GTA solution but also drastically reduced the duration of exposure in saturated vapor of GTA from a few hours to a few minutes. The fusion of nanofibers at the crossing points of fiber network was due to the water vapor in GTA solution, which was evident from the SEM images. Interestingly, we found that the presence of the hydrophobic molecules significantly reduces the fusion of GNF while crosslinking with GTA vapor. Thus, an exposure of only 6 minutes was not only adequate to control the early degradation with intact fiber morphology, but it also significantly marginalized any adverse effects associated with the use of GTA.

After the fabrication of the device, *In-vitro* release study was done to analyze the effect of the release medium, and the duration of crosslinking on the drug release from GNF. While the amount of drug release decreased with increase in crosslinking time, the same increased with higher pHs. The release profile showed bi-staged curves i.e., sudden release of drug followed by sustained release, which was far from zero-order kinetics. One very quick fix was to increase the crosslinking timing, which is not desirable because of the toxicity of GTA that would reduce the overall total release. Thus, we incorporated new strategies to control the rapid release of drug during the initial hours. Fabricating a multi-layered structured GNF with 6 and 8 minutes crosslinking with GTA was our next attempt in order to increase the diffusional barrier between the drug molecules and release medium to tone down the initial rapid release. Piperine loaded GNF layer was kept as a core layer where two barrier layers were protecting from both sides. It was evident that, increase in barrier layer decreases the initial release and the drug loading. Consequently, different variations of barrier and core layer were tried, which greatly improved the release profile. Despite the improved release profile, achieving zero-order release was

challenging. Thus, the concept of sequential crosslinking was used to achieve a near zero-order release profile with higher drug loading. Non-uniformity of crosslinking within the layers in the case of single time cross-linked sample (6 minutes) was the main hindrance in achieving zero-order release of drug. The top layers were exposed more to the GTA vapor, which led to more fused fibrous structure where in-between layers were not crosslinked well due to the low mobility of GTA molecules. Increased crosslinking time was one option that we ruled out due to the cytotoxicity effect of GTA. As an alternative, in-between layer of the mesh were crosslinked in a sequential manner keeping the total crosslinking time same. To increase the compactness of the fiber mesh uniformly within the layers, fiber mesh was crosslinked each time for 2 minutes after depositing barrier layer, core layer and finally the barrier layer on the opposite side. This drastically improved the release kinetics by achieving zero-order release for 48 hour in the case of the higher drug loaded DDS.

This study has drawn attention by (a) successfully fabricating drug encapsulated GNF based DDS, (b) crosslinking the vehicle with only 6 minutes of exposure to GTA vapor and (c) achieving zero-order release pattern using sequential crosslinking method. However, this newly developed vehicle was far from the realistic tablet with proper therapeutic dose. Therefore, after developing this understanding about controlling the release of a model hydrophobic drug molecule using nanofibers based DDS, our next objective was to use this knowledge in developing a real case scenario. To achieve this, we loaded a higher dose of Amphotericin B (Amp-B) in compressed nanofiber based oral tablet (CNOT) form for anti-fungal treatments. Amp-B is an anti-fungal drug, which is very difficult to deliver orally due to its low solubility in water. This is a polyene macrolide, which is almost 3 times bigger than piperine in terms of molecular weight. Due to high toxicities and poor prognosis of the drug, there is a great need for developing new DDS, which can encapsulate the drug molecules and can safely deliver correct dose preventing over-dosing. To the best of our knowledge, except for one recent report, Amp-B loaded GNF based DDS has not been explored in detail. After checking drug-polymer interactions and morphology, the drug-encapsulated fabric was crosslinked with GTA vapor for 6 minutes and then manual hydraulic press helped to form a compressed oral tablet. This

newly engineered CNOT was monitored for *in-vitro* degradation and release study in different physiological pHs for more than 72 h.

This study, therefore, establishes the potential viability of biodegradable, electrospun nanofibers as an oral DDS with promising controlled release features.

Graphical Abstract

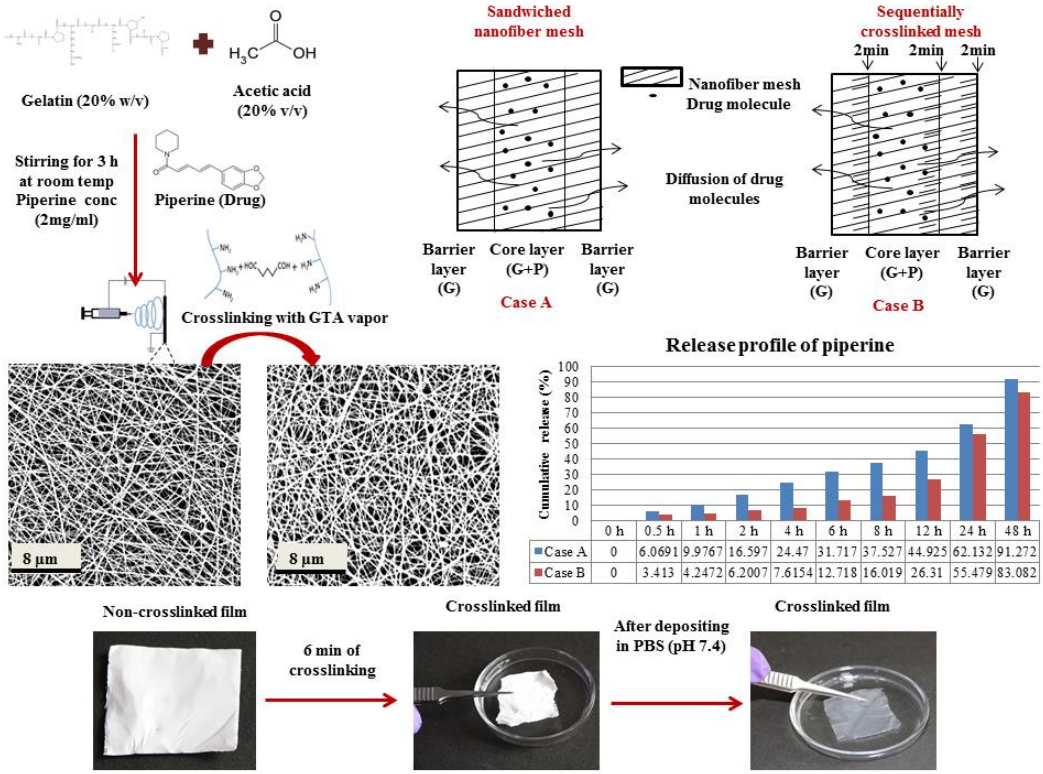

List of Publications

Journal Publications from the present study

1. **A. Laha**, U. Bhutani, K. Mitra and S. Majumdar, Fast and slow release: synthesis of gelatin cast-film based drug delivery system, Mater. Manuf. Processes **(2015)** 223-230.

2. **A. Laha,** S. Yadav, S. Majumdar, C. S. Sharma, *In-vitro* release study of hydrophobic drug using electrospun cross-linked gelatin nanofibers, Biochem. Eng. J. 105 **(2016)** 481-488.

3. **A. Laha**, S. Majumdar, C. S. Sharma, Controlled drug release formulation by sequential crosslinking of multilayered electrospun gelatin nanofiber mat, MRS Advances 1(29) **(2016)** 2107–2113.

4. **A. Laha,** C. S. Sharma, S. Majumdar, Sustained drug release from multi-layered sequentially crosslinked electrospun gelatin nanofiber mesh, Mater. Sci. Eng. C 76 **(2017)** 782–786.

5. **"**Amphotericin-B loaded Compressed Nanofiber Oral Tablets as a Potential Drug Delivery Vehicle" (manuscript under preparation)

Journal publications from other work

1. S. K. Adepu, N.s Dhiman, **A. Laha**, C. S. Sharma, S. Ramakrishna, M. Khandelwal, Three-dimensional bioprinting for bone tissue regeneration, Curr Opin Biomed Eng. 2 **(2017)** 22–28.

2. U. Bhutani, **A. Laha**, K. Mitra and S. Majumdar, Sodium alginate and gelatin hydrogels: viscosity effect on hydrophobic drug release, Mater Lett.164 **(2016)** 76-79.

Conference proceeding

1. A. Laha, C. S. Sharma, S. Majumdar, Electrospun gelatin nanofibers as drug carrier: effect of crosslinking on sustained release, Materials Today: Proceedings 3 **(2016)** 3484–3491.

Conferences

1. GIAN course on "Biomaterials Engineering and Digital Manufacturing" at Indian Institute of Technology, Hyderabad, India (12th -21st December, 2016).
2. Oral presentation on “Controlled Drug Release Formulation by Sequential Crosslinking of Multilayered Electrospun Gelatin Nanofiber Mat” on Materials Research society (MRS) 2016, Phoenix, Arizona, U.S (28th March- 1st April, 2016).
3. Oral presentation on “Electrospun gelatin nanofibers as drug carrier: effect of crosslinking on sustained release” on ICABET 2016, International conference on Advances in Bioprocess Engineering and Technology, organized by Heritage Institute of Technology, Kolkata, India (20th – 22nd January, 2016).
4. RSC Best Poster Award on “In vitro study on Gelatin nano fiber based Oral drug delivery vehicle for hydrophobic drug” on Macro 2015, International symposium on Polymer Science and Technology, organized by Indian Association for the Cultivation of Science (IACS), Kolkata, India (23rd -26th January, 2015).
5. Conference paper presentation on “Release Study of Hydrophobic Drug from Electrospun Cross-linked Gelatin Nanofiber Mat” on Workshop on Nanoengineering in Medicine, organized by AIIMS, at New Delhi, India (17th -19th December 2014)
6. Paper presentation on “Rapid and Controlled Release of Drug through Polymeric Thin” on International Conference on Polymeric Biomaterials, Bioengineering & Biodiagnostics (Biomaterials 2014) organized by (IIT) Delhi, Asian Polymer Association (APA), ENEA, and CNR Italy, at New Delhi, India (27th - 30th of October, 2014.)

Nomenclature

Amp-B	Amphotericin-B
CNOT	Compressed nanofiber oral tablet
DDS	Drug delivery system
FDA	Food and Drug Administration
GCF	Gelatin cased-film
GCF XY	Gelatin cased-film and X is polymer concentration and Y is crosslinker concentration
GCF-P	Gelatin cased-film with piperine
GCF-P XY	Gelatin cased-film with piperine where, X is polymer concentration and Y is crosslinker concentration
GNF	Gelatin nanofiber
GNF C4	Gelatin nanofiber with 4 min crosslinking with GTA vapor
GNF C6	Gelatin nanofiber with 6 min crosslinking with GTA vapor
GNF C8	Gelatin nanofiber with 8 min crosslinking with GTA vapor
G-P NF	Piperine loaded gelatin nanofiber
G-P NF C4	Piperine loaded gelatin nanofiber 4 min crosslinking with GTA vapor
G-P NF C6	Piperine loaded gelatin nanofiber 4 min crosslinking with GTA vapor
G-P NF C8	Piperine loaded gelatin nanofiber 4 min crosslinking with GTA vapor
GI	Gastrointestinal
GTA	Glutaraldehyde
h	Hours (Unit of time)
min	Minutes (Unit of time)
NC	Non-crosslinked
RPM	Rotation per minute

List of Figures

List of Tables

Contents

Chapter 1

Overview of Controlled Drug Delivery Systems

1.1 Introduction to controlled drug delivery system

In the last few decades, researchers have witnessed a remarkable research growth aimed at developing new drug delivery systems (DDS). Developing controlled DDS has been the cutting edge research area of science where the knowledge streams from chemistry, material science and chemical engineering have merged for the benefit of human health care. Controlled release of drug is an efficient process of delivering pharmaceutical molecules from an engineered system under specific physiological conditions. Researchers have designed the DDS in order to enable the maintenance of the drug concentration in the body within its therapeutic range for a prolonged time period, which in turn aids in less amount of drug administrations. Thus, controlled DDS has become a subject of cutting-edge research in the field of biomedical sciences and pharmacy for several reasons [1, 2].

Controlled DDS provides the following advantages compared to conventional DDS, as discussed below:

1. Controlled DDS can release drug molecules in a predetermined or constant rate, which helps in maintaining drug concentration within the therapeutic window.
2. Single administration of drug can control the desired drug concentration for a prolonged time period, which increases patient's compliance and comfort.
3. Site-specific drug delivery can reduce systemic drug level and drug over-dosage as well.

4. Controlled DDS can also protect the drug molecules from enzymatic degradation and can be delivered at the absorption site, which facilitates drug efficacy.

Briefly, the motivation for developing controlled DDS is to improve the drug efficacy, which not only reduces drug over-dosage but also improves patient's compliance. To understand these benefits, a comparative study of different kinds of release profiles are presented in Figure 1.1.

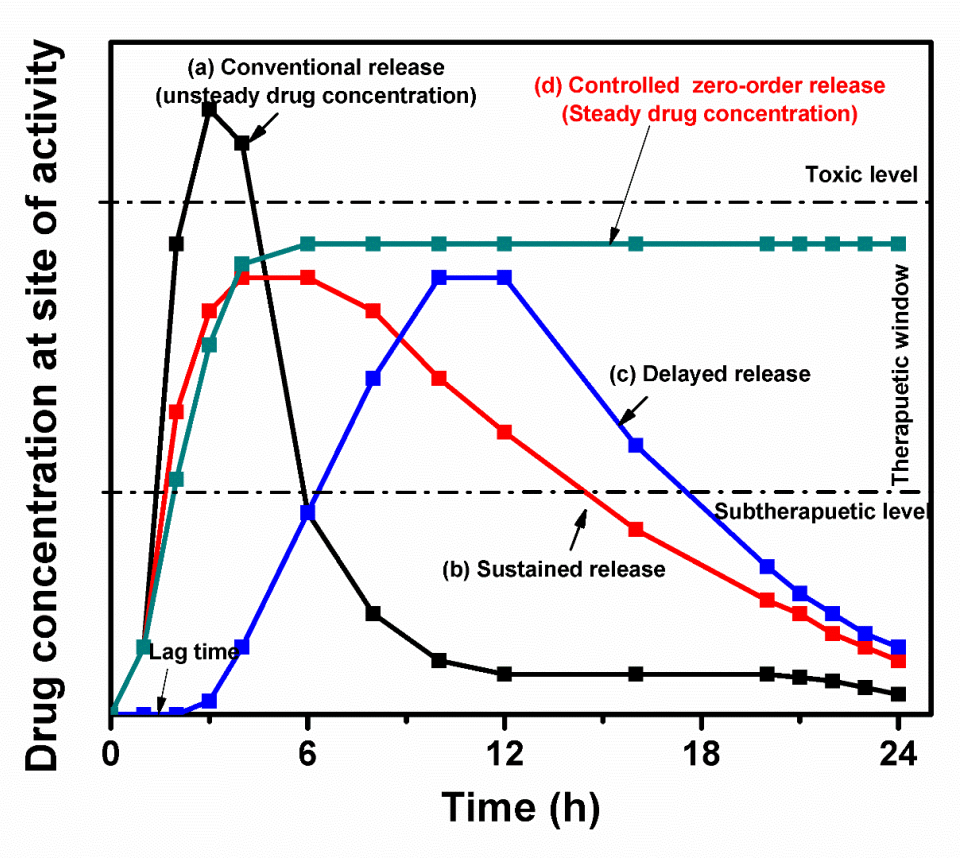

Figure 1.1: Different kind of drug release profiles: (a) Conventional release, (b) Sustained release, (c) Delayed release, (d) Controlled zero-order release

Figure 1.1 highlights the benefits and side effects of different drug release profiles. As every drug has its own therapeutic range, above which it creates a toxic effect and below which it is inefficient, maintaining drug concentration within this range for a prolonged time-period is naturally desirable. In the case of conventional method (curve a), after ingestion or injection of the drug, concentration in the blood level rises, and then it reaches a peak and starts decreasing. In this case, immediately after the drug administration, the drug shoots

beyond the upper limit of the therapeutic range and starts declining soon after. This shows unsteady drug concentration and maintenance of effective drug concentration for a lesser duration of time. This kind of system needs frequent administration of the drug, which causes an undesirable oscillation of the drug concentration between ineffectiveness and toxicity. However, sustained release certainly improves the efficacy of the drug when compared to conventional systems (curve b). In the case of site-specific drug release, delayed release profile is more accurate (curve c). To reduce immediate burst release, the drug molecule is wrapped in a well-designed system so that it can release at the active or the absorption site after a time gap. However, controlled release of drug molecules can sustain the drug concentration within the therapeutic range for a desired duration even with a single administration. In controlled DDS, the vehicle is fabricated in such a way that it releases the drug molecules in zero-order for a long period (curve d). In this case, the rate of drug release synchronizes with the rate of drug elimination from the body, which reaches a steady rate of drug concentration within the therapeutic window [3, 4].

Presently, the conventional system has been modified in order to achieve pulsatile release profiles, which can keep the drug concentration within the therapeutic range (not shown in Figure 1.1). For example, molecules like insulin need pulsatile release during the specific time when the blood glucose level increases [5]. As an example for controlled DDS, controlled release of non-steroid anti-inflammatory drug (NSAID), tramadol can significantly reduce pain due to osteoarthritis through a single administration of drug in a day [6]. However, delayed release profiles are appropriate in the case of colon specific DDS. In this case, the concentration of the drug reaches the desired range after a time gap and can release at the specific site [7]. In short, drug-releasing systems are designed in order to get specific release profiles without crossing the toxic concentration level.

1.2 A Brief history of controlled drug delivery systems

The need for developing an effective controlled drug release system has occupied researchers for the past six decades. Smith Kline & French company made the first successful attempt in this field in 1952 for a 12-hour delivery of dextroamphetamine sulfate (Dexedrine) using spansules [8, 9]. The word spansule is a combination of two words – span and capsule [9, 10]. Hence, this kind of formulation can release drug for different span of time [9, 11]. Therefore, spansules were considered as the *first controlled-release formulation*, which were later modified with stable and slowly dissolving synthetic polymers. Around the same time,

Folkman found the anesthetic gas could be diffused through the silicon tubes and would be absorbed by the rabbit's blood [12]. Through this mechanism, Folkman and Long in 1964 first proposed the concept of the sealed capsule, which can be *implanted* in order to give *prolonged release*. This was the very first time that the concept of a reservoir mechanism of DDS was reported [13]. This *reservoir-based system* showed excellent control of the release rate of the drug and achieved exceptional *zero-order release profiles* [14].

Following this, in 1968 Alejandro Zaffaroni founded a company named ALZA (ALejandro ZAffaroni), the first of its kind which focused on developing controlled drug delivery devices [14]. The company fabricated many controlled drug-releasing devices, which enormously contributed to the field of controlled DDS research and application. The ophthalmic insert called Ocusert became the first commercial product of the ALZA corporation to gain approval by the FDA in 1974 [14-16]. Other examples of controlled DDS include, the poly(ethylene co vinyl acetate) based rate controlling membrane system which showed controlled release of the anti-glaucoma drug, pilocarpine, for a duration of 1 week [16]. Immediately after, in 1976, procedures using intrauterine device (IUD), Progestasert showed zero-order release of the contraceptive steroid progesterone for the duration of a month [14]. The population council laboratories in New York, developed another controlled DDS birth control device, Norplant showed 5 years of controlled release of progestin from silicon rubber made implanted tubes which was approved for clinical trial in U.S around 1980 but eventually it was withdrawn from the global market in 2008 [14, 17]. Instances of these controlled DDS through the years, using non-degradable implants have become very successful commercially because of its *zero-order controlled release* of drug molecules for a prolonged duration.

In 1971, ALZA first introduced controlled drug delivery through transdermal patches and patented the skin patch as the "bandage of administering drug". This reservoir drug system showed initial burst release followed by zero-order release [18]. In 1990, FDA approved self-administrated transdermal fentanyl patch (Duragesic) for chronic pain relief up to 72h[19-21]. With time, research in controlled DDS via the transdermal patch branched out to deliver through different media in order to increase the drug permeability in the body. As a result, of these recent developments, in 2008, biosensor patch (Symphony) and micro-needle based patches have gained a lot of success due to its continuous blood glucose monitoring ability and a painless process of blood collection [21, 22].

The idea of osmotically driven oral DDS systems primarily came from Rose-Nelson[23, 24], Higuchi-Leeper [23, 25] and Higuchi-Theeuwes pumps [26] in the early 1950s. Based on the principle of the osmotic pump, osmotic-controlled release oral delivery systems (OROS) were developed. Due to the osmotic pressure difference between the release medium (GI tract body fluid) and the inner constituents of the device, water molecules would penetrate through the semi-permeable membranes displacing the drug molecules from the device. In 1974, Theeuwes and other researchers from ALZA introduced a compressed tablet known as the elementary osmotic pump (EOP). Derived from this idea, the first two products indomethacin, Osmosin [27] and phenylpropanolamine, AcutrimTM [28], were launched in the 1980s. In the 2000s, a new design with push-stick osmotic pumps (PSOP) based formulation (ConcertaTM) was launched in order to deliver methylphenidate to children with attention-deficit hyperactivity disorder (ADHD) [11, 29]. Furthermore, in 2013, an attempt to deliver insulin orally was reported by using the oramed insulin pill [30].

In the late 1970s, the concept of polymer-drug conjugates or nano-therapeutics for developing new controlled DDS rendered immense promise. Since the 1980s, three key technologies have greatly influenced the development and clinical success of nano-therapeutics. These three key technologies are (a) PEGylation, (b) “active targeting” and (c) “enhanced permeation and retention effect” (EPR). PEGylation is the conjugation of the drug with poly(ethylene glycol) or PEG. Around the 1980s and 1990s, PEGylation company, Enzon and Shearwater Polymers were founded which introduced a number of PEGylated products for clinical practice. This invention was considered a great influence for nano-therapeutics. Recently, antibody-drug conjugated formulation Kadcyla was approved by the FDA in 2013. Kadcyla was formulated by conjugating monoclonal antibody trastuzumab with the potent cytotoxic drug, mertansine (DM1) and its application proved to be a great success in treating certain kinds of breast cancers [21, 31].

In conclusion, the journey of developing controlled drug delivery devices, which began in the early 1950s, has continued with the deployment of new technical methods, and has led to a better understanding of the myriad biological processes which could be utilized in the process [32]. Subsequent challenges in the future will further expand the field of controlled drug delivery and will result in better and enhanced systems. The evolution of drug-carriers starting from the scale of the *macro*, moving to *micro* and further to the *nano* level has contributed to targeting biological problems with increased accuracy [33]. With an enhanced comprehension of biology and pharmacology, the drug delivery scientist will be able to innovate new vehicles that can deliver the drug with greater precision and efficiency. Thus,

considering the history of the development of DDS through the years, the past innovations and concepts become stepping-stones towards the requirement for smarter formulations of controlled drug delivery vehicles in the present.

1.3 Different routes of drug delivery

Drug delivery scientist and engineers have attempted to deliver drug molecules through different routes to counterbalance the bioavailability and adverse effects of therapeutically active medicine. Although, oral consumption is the most common and convenient route of delivering drug molecules, researchers have designed different drug releasing vehicles in order to deliver drugs via the eyes, nose, lung, skin, vascular system, vagina, buccal membrane and brain.

The oral route, used extensively for drug delivery, is the most common and well-researched area for delivering drug molecules [34]. Despite abundant research regarding oral drug administration, developing an oral delivery system particularly for poor water-soluble drugs and macromolecules like protein and peptides has remained a challenging feat [35]. The possible approaches, which may improve the bioavailability of proteins like insulin, are: (1) modification of the physicochemical properties of macromolecules; (2) addition of novel function to macromolecules; and (3) use of improved delivery carriers. Clearly, it is essential that these approaches maintain the biological activity of the proteins [30, 35]. To carry proteins across the epithelium in the GI tract and to protect it from protease degradation, the use of microspheres, bio-adhesive patch has also been suggested [36-38].

Apart from oral routes, other drug delivery routes has also gained a lot of attention in order to deliver drug in targeted area by bypassing the first-pass metabolism. The controlled release of the anti-glaucoma drug through the eyes was the first attempted route, as has been previously mentioned in the section discussing the brief history of controlled DDS. Subsequent research and developments since then have contributed towards the treatment of glaucoma, age-related macular degeneration, diabetic macular edema and retinal vascular occlusions [39, 40]. Since last decade, many researches with bio-adhesive polymer, chitosan in the form of powder, micro-particle, nano-particle, micro-emulsion, nano-emulsion, and microsphere has been done to deliver the drug to the brain using the nasal route [41-44]. Apart from administration through the nasal route to deliver the drug to the brain, direct polymeric implantation during brain tumor neurosurgery has also been established [34, 45]. Furthermore, the lungs are also considered as an excellent route due to the possibility of a non-invasive administration of the drug via inhalation of aerosols, which bypasses the first-

pass metabolism, facilitates local drug delivery and renders the availability of a huge surface area for drug absorption [34, 46]. Another pathway used is the transdermal DDS, which has been studied and clinically practiced due to numerous advantages. Transdermal patches have become commercially successful for the treatment of hypertension, birth control, analgesia, motion sickness, hormone replacement, and smoking cessation [21]. As another alternative drug delivery route, the vaginal route has also gained popularity by delivering drug through the virginal epithelial layers by using of adhesive polymer gel or creams [47]. Finally, vascular DDSs have also become an effective way to deliver the drug at the targeted site [48]. For carrying out drug delivery through the vascular route, liposome, dendrimer, polymeric micelles, polymersomes, polymer-drug conjugates, solid particle based nanofabrication are used in order to design endothelium-targeted DDSs [49]. The vascular DDS has been used extensively in both diagnosing and curing cardiovascular diseases, pulmonary, oncological diseases, and other disease conditions [50].

1.4 Types of drug delivery systems

Extensive research and the conscious effort of engineers, pharmacologists and chemists have led to state-of-the-art techniques in polymeric drug delivery vehicles. From the adaptation of a novel idea, which originates in a research lab, to formulating a commercially successful DDS is very long process including several intermediate clinical trials [21]. In the process of developing a new DDS, scientists have often addressed certain key aspects of controlled DDS such as, (a) constant drug concentration within therapeutic window over a long time, (b) biocompatibility and biodegradability of the system, (c) protection of drug molecules from early degradation and (d) releasing drug molecules at absorption site. From the perspective of a pharmacologist, delivering drug molecules with low solubility in a biological condition has always been a challenge. Added to these factors, to get commercial success, the new DDS must meet conditions such as, (a) reduced frequency of drug administration that will result higher patient compliance, (b) affordability and (c) easy or self-administration of drug [51]. Despite a lot of new ideas and research that have emerged at the laboratory level, the affordability and effectivity of the controlled drug-releasing carriers are still to be considered. Among all different kinds of DDS, oral thin films, hydrogel, nano and macro particles, liposome and micelles, nanofibers are widely used in the field of drug delivery, tissue engineering and wound dressing. Few of such important vehicles have been discussed in the following section.

1.4.1 Polymeric thin film and hydrogel

In the past few decades, polymeric thin films have been used extensively in the form of fast dissolving oral films [52], controlled release in absorption site [53], buccal film or patches [54] and transdermal patch [55]. Thermo-sensitive [56] ,pH- sensitive [53], biodegradable and muco-adhesive [54] polymers are used to fabricate these thin films. Various methods like solvent casting, semisolid casting, hot melt extrusion, solid dispersion extrusion, rolling, dip coating, Langmuir Blodgett are used to fabricate polymeric film with micro to nano thickness [52, 57]. The drug release from the oral film is directly influenced by various factors like (a) film composition, (b) film thickness, (c) drug loaded amount, (d) duration of crosslinking, (e) porosity of the film, (f) pH and ionic strength of the release medium [53]. Oral based films can be used as both local and site-specific DDS with flexible release profiles [53, 57].

Hydrogels are a three-dimensional, soft, flexible, porous, hydrophilic, biocompatible and biodegradable polymeric network, which demonstrate excellent water absorption capability [58]. Hydrogels are fabricated with water-soluble, non-toxic, natural and synthetic polymers [4, 59]. Hydrogels are called “physical gel” when its molecular entanglements are largely based on hydrogen bonds (generally lower energy molecular interactions). In contrast to that, a “chemical gel” is formed when the hydrogel builds stronger covalent bonds between the macromolecules. Physical gels are mostly reversible in nature, whereas chemical gels show permanently cross-linked nature [58]. As hydrogels can absorb huge amounts of water and can hold it inside the polymeric matrix, crosslinking plays a very important role from preventing early dissolution of the polymer chain [59, 60]. Researchers have done extensive work in order to fabricate smart or stimuli-sensitive hydrogels, which have tremendous applications in the field of drug delivery, tissue engineering, and wound dressing [59-61]. Recently, hydrogel based soft contact lenses have shown promising results not only by correcting vision but also through controlling drug release for a prolonged time [59]. In addition to that, environment sensitive hydrogels have also shown enormous potential as site-specific DDS, controlled DDS, biosensor, and bio separator [62]. In order to design stimuli-sensitive smart hydrogel, materials like pH-sensitive, temperature-sensitive, glucose-sensitive, electric signal-sensitive, light-sensitive, pressure-sensitive, specific ion-sensitive, specific antigen-responsive polymers are extensively used [4, 59, 61-63].

1.4.2 Liposome and micelle

In 1960s, a famous biophysicist tried to disperse phospholipids in water, and it immediately resulted in a closed spherical structure with a hydrophilic core surrounded by a phospholipid bilayers shell and the structure that this experiment gave rise is known as a

liposome [64]. Liposomes can be synthesized from non-toxic surfactants, cholesterols, long chain fatty acids and proteins. Since this discovery, the colloidal vehicle has shown immense capability for carrying drug molecules with low-solubility, small molecules and bioactive lipids. Drugs with a wide variation of lipophilicities can be encapsulated either in the hydrophobic phospholipid bilayers shell side or in the hydrophilic core. Liposomes can be of two types based on the number of bilayers: (a) unilamellar vesicles and (2) multilamellar vesicles. Again based on side, unilamellar vesicles can be of two types: (a) small unilamellar vesicles and (b) large unilamellar vesicles. The size of the liposome can vary from very small (25nm) to large vesicle (2.5µm). Nano-liposomes have shown excellent control on pharmacokinetics and the co-delivery of two chemotherapeutic agents. It has also showed improved oral mucosal delivery of peptide molecules with prolonged retention in the GI tract and better penetration capability into the mucus layers [65] . Thus, liposome-based DDS has showed remarkable improvement in delivering hydrophobic drugs, intracellular drug delivery, sustained drug release, gene therapy, site-avoidance delivery, site-specific targeting, and intraperitoneal administration [64-70].

Recently with the advancement of novel DDS, micelle has also shown promising improvement in terms of delivering hydrophobic drugs [71]. Polymeric micelles are a combination of two segments: (a) an outer shell that controls in-vivo pharmacokinetics behavior of the system and an inner shell that protects the drug molecules and releases them at the targeted site [72]. In brief, amphiphilic polymer based multi-functional micelles with its unique hydrophobic core and its hydrophilic shell structure, have shown promising results by targeting the cancerous tumors with therapeutic agents. The usages of micelle in MRI to monitor targeting efficacy certainly improve the therapeutic outcome of drug delivery [73].

1.4.3 Nano-particles

With the rising of nanoscale technologies in the 1970s, there has been the dawning of a new era of research in terms of disease diagnosis, treatments and preventions. Nanoscale devices are an outcome of the persistent efforts of engineers, biologists, chemists and physicists. Nanoparticles used as drug-carriers are generally submicron (<1 µm) colloidal particles. Nanoparticle-based DDS have already shown great success in the field of drug delivery and still have tremendous potential in the delivery of protein, peptide, vaccine, antibiotics, anti-tumor therapy and also in crossing blood-brain barrier as vehicles [74, 75]. Generally, nanoparticles are made from natural or synthetic polymers, which are biocompatible and biodegradable in nature. Drug release from the nanoparticles are caused by diffusion, swelling or degradation, particularly in the absorption site. In the case of oral

drug delivery, muco-adhesive polymer based nanoparticles increases the adhesion of drug-loaded particles to the mucosa in the GT tract. This improves the bioavailability of the drug extensively [74]. In addition to that, for low-soluble drugs, nanoparticle based DDS can show targeted release in order to improve bioavailability and reduce side effects of the active molecules. Nano-suspension of drug-loaded nanoparticles has also shown remarkable improvement in bioavailability of low soluble drugs by oral, injectable, local or pulmonary administration [74-81].

1.4.4 Nano-gel

Nano-gels are submicron sized three-dimensionally crosslinked hydrophilic polymer network, which has both the features of hydrogels and nanoparticles [82]. Nano-gels are physically or chemically crosslinked nanoparticles which have tremendous ability to absorb water or biological fluid without deforming its original shape. The presence of hydrophilic groups such as –OH, –CONH–, –$CONH_2$–, and –SO_3H in the polymer matrix helps to absorb water inside the matrix resulting swelling like hydrogels. However, crosslinking helps to maintain the shape of the nano-gel matrix. The advantages of nano-gels are: (a) the non-toxic, biocompatible and biodegradable polymer formulation, (b) tunable release profiles, (c) ability to encapsulate both hydrophobic and hydrophilic kind of drug molecules, (d) ability to respond to different environmental stimuli (pH, ionic strength and temperature) (e) high drug loading capability and (f) high stability of the matrix [83, 84]. Despite several advantages, nano-gels interact between drug and polymer through electrostatic binding, hydrophobic interaction, and hydrogen bond, which decrease the solubility of the matrix limiting its application [84, 85]. Presently, well designed multi-responsive and self-crosslinked nano-gels are used widely as a targeted drug-carrier with wide range of pharmaceutical molecules [86, 87].

1.4.5 Nanofiber

Electrospinning is a cost effective and simple method for the production of nanofibers from an electrostatically driven jet of polymer solution. Fabrication of polymer fibers with a diameter of a few nanometers to several micrometers, by an electrostatic force was first reported in 1934 [88]. In the interim period of 70 years, a number of developments have led to the fabrication of continuous fibers through the use of different kinds of natural and synthetics polymers. Since the 1980s, electrospun polymeric fibers have regained the attention of the scientific community due to its exceptional properties such as its (a) large ratio to surface area-to-volume, (b) highly porous three-dimensional fibrous structure and (c) tunable inter-fibrous porosity [88]. The fiber properties are dependent on three main factors: (a)

polymer solution parameters (viscosity, surface tension, conductivity etc.), (b) process parameters (voltage, federate and tip-to-collector distance) and (c) ambient conditions (humidity and temperature) [89, 90]. The applications of electrospun nanofibers include wound dressing, drug delivery, nano-sensor, ophthalmology, development of artificial organs, tissue-engineering scaffolds [90]. Among all of these various applications, electrospun nanofibers as drug-carriers constitute its fastest growing and most promising use [90].

To engineer electrospun nanofiber based DDS, natural, synthetic and hybrid polymer blends have been used [88]. Selection of polymer, solution parameters and process parameters play a great role in determining the fiber diameter size and morphology [89]. To understand the science behind the fiber formations, researchers have done extensive work with various kind of polymers, solvents and drugs. In addition to that, biodegradable natural polymers have also gained attention in the field of tissue engineering and regenerative medicine. Although natural polymers suffer from poor mechanical properties but the ability to recognize cell sites because of cell affinity gives it the upper hand [89, 90]. In case of tissue engineering or artificial organ, extra-cellular matrix (ECM) plays a very important role by giving the cells a physical structure and support. ECM helps in cell attachments, cell proliferation and differentiation [88]. Interestingly, the 3D structure of nanofiber scaffold can mimic the structure of ECM and the use of this kind of scaffold is extensive in damaged tissues for the healing process [88]. Thus, biomaterials, which show biocompatibility, biodegradability, non-toxicity, hydrophilic with required mechanical strength, are widely used in drug delivery and tissue engineering.

Since 2005, the application of electrospun nanofibers in drug delivery has attracted special attention (Figure 1.2) because of its unique properties such as (a) high ratio of surface area-to-volume, (b) high drug loading, (c) multi-drug delivery, (d) ease of operation, (e) and cost-effectiveness [88-90].

Although, nanofiber based DDS is one of the most recent and potential drug-carriers, however, this system needs to go through many experiments under physiological or in-vivo conditions to make it marketable. Thus, a very close collaboration between drug delivery scientists and pharmaceutical companies is required to fully understand the budding potential of the vehicle and render this transition from lab to bed practicable.

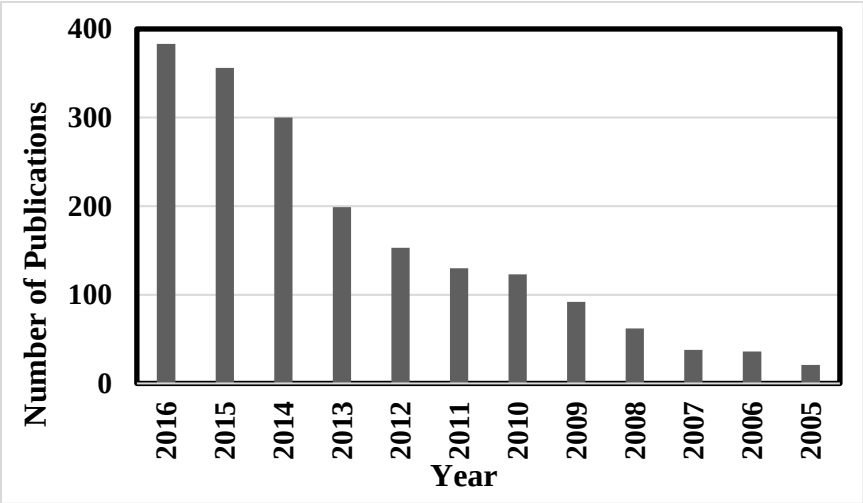

Figure 1.2: Publications related to "nanofibers in drug delivery" since 2005 (Data extracted from Web of Science)

1.5 Polymers used in controlled drug delivery systems

The selection of the polymer plays a very important role in fabricating or designing controlled DDS. Polymers are classified according to their origin (i.e. natural or synthetic), backbone stability (biodegradable or non-biodegradable) and water solubility (hydrophobic and hydrophilic) [51, 88]. Biomaterial is the polymeric system that is used in the field of biomedical science. William defined biomaterial in his article [91] as:

''A biomaterial is a substance that has been engineered to take a form which, alone or as part of a complex system, is used to direct, by control of interactions with components of living systems, the course of any therapeutic or diagnostic procedure, in human or veterinary medicine.''

Engineered polymeric biomaterials (tagged as 'biomaterials' in this thesis), which are used for biomedical applications, must be made of biocompatible polymers. William defined the term biocompatible in his article [92] as:

"*Biocompatibility refers to the ability of a biomaterial to perform its desired function with respect to a medical therapy, without eliciting any undesirable local or systemic effects in the recipient or beneficiary of that therapy, but generating the most appropriate beneficial cellular or tissue response in that specific situation, and optimizing the clinically relevant performance of that therapy."*

In brief, the most common biocompatible, biomaterials which are widely used in the fabricating DDSs are classified in Table 1.1 [51, 89, 93].

Table 1.1: Different kinds of biomaterials used in DDSs

Natural polymer				
	Biodegradation	**Mechanical stability**	**Water affinity**	**References**
Gelatin	**Enzymatic**	**Weak**	**Hydrophilic**	**[94]**
Chitosan	**Enzymatic**	**Weak**	**Hydrophilic**	**[95]**
Alginate	**Enzymatic**	**Weak**	**Hydrophilic**	**[96, 97]**
Hyaluronic acid	**Enzymatic**	**Weak**	**Hydrophilic**	**[98]**
Collagen	**Enzymatic**	**Weak**	**Hydrophilic**	**[99-102]**
Silk fibroin	**Enzymatic**	**Strong**	**Hydrophilic**	**[103]**
Dextran	**Enzymatic**	**Weak**	**Hydrophilic**	**[104, 105]**
Cellulose acetate	**Non-degradable**	**Weak**	**Hydrophilic**	**[106]**
Synthetic polymer				
	Biodegradation	**Mechanical stability**	**Water affinity**	**References**
Poly(glycolic acid) (PGA)	**Hydrolytic**	**Strong**	**Hydrophilic**	**[107]**
Polycaprolactone (PCL)	**Hydrolytic**	**Strong**	**Hydrophobic**	**[108]**
Poly(lactic acid) (PLA)	**Hydrolytic**	**Strong**	**Hydrophilic**	**[107]**
Poly(lactic-co-glycolic acid) (PLGA)	**Hydrolytic**	**Strong**	**Less Hydrophilic**	**[109-112]**
Poly(vinyl alcohol) (PVA)	**Enzymatic**	**Strong**	**Hydrophilic**	**[113]**
Poly(ethylene oxide) (PEO)	**Enzymatic**	**Weak**	**Hydrophilic**	**[114]**

In summary, polymer blending of synthetic and natural kinds have been recently used in DDS to increase the mechanical stability of the vehicles. Alternatively, crosslinking of natural polymers to slow down the degradation speed of the vehicle is also another option.

However, using crosslinker may increase the risk of toxicity, which may lead to limiting of the usage of the drug vehicle. In an attempt to counter this, researchers have extensively studied the application of natural polymer as biomaterials in DDS with minimal usage of crosslinkers and synthetic polymers.

Based on the perspective gain from this literature review, we have selected gelatin as an excipient because of biocompatibility, biodegradability and hydrophilic nature. Natural biomaterial gelatin based DDS has also been crosslinked to reduce the early degradation of the vehicle. The minimum usage of the crosslinker is one of the main aim of this study. Since, delivering a drug with low-solubility is a challenging feat, in this study, we have selected hydrophobic drug (Piperine) and amphiphilic drug (Amphotericin-B) as model drugs. Subsequently, we have attempted to deliver these drugs using a hydrophilic polymer gelatin based drug vehicle.

1.6 Objectives

The main objective of the thesis is to develop a low-cost, polymeric drug-carrier, which is fabricated with a biocompatible, biodegradable, natural polymer to achieve controlled and sustained release of low soluble drug molecules in a zero-order manner for a prolonged time.

The primary objectives of the thesis include:

- Fabrication of a natural polymer (gelatin) based, simple design, low-cost drug vehicle (cast-film and nanofibers are fabricated in this thesis)
- Delivering less soluble drugs like Piperine (model hydrophobic drug) and Amphotericin-B (Amp-B: model amphiphilic drug) using gelatin based drug-carriers
- Achieving zero-order drug release for at least 24-48 h in different physiological pHs similar to GI tract
- Fabricating a less toxic polymeric vehicle by reducing the usage of toxic cross linkers
- Understanding the science behind the successfully encapsulation of drug in different polymeric vehicles keeping all the properties of the drug intact, and to be able to control the parameters, which play key role in the release behavior of the drug molecules

- Fabricating a novel drug delivery vehicle that permits flexibility in drug release as per the requirements of varied therapies, particularly with respect to less water-soluble drug molecule

Delivering less soluble drugs is always a challenge and that is one of the main motivating factor for the work. Developing a genetic formulation of drug-polymer carrier, which can promote any kind of release profiles including zero-order release for different kind and size of drug molecules, is the objective of this thesis.

1.7 Layout of thesis

As the title of the thesis implies, the objective of this work is to provide a comprehensive idea of controlled drug delivery processes using polymeric drug delivery vehicles. This thesis includes different experimental techniques with an understanding of developing the process of polymeric drug delivery vehicles.

The thesis starts with the introduction to controlled DDSs followed by a brief history of controlled DDS, various routes of drug administration, types of drug-carriers for controlled DDS, different kinds biomaterials used in drug delivery vehicles. Chapter 1 includes research objectives and the layout of the thesis. Chapter 1 serves as a starting point toward the overall understanding of the thesis in general.

Chapter 2 discusses the fabrication and release study of the hydrophobic model drug piperine from the natural polymer, gelatin-based cast-film (GCF). The main objective of this chapter is to understand the drug-polymer interactions and the effect of cross linkers on drug release from the GCF. This chapter gives an overall understanding of the release kinetics of piperine, which is solely dependent on two factors viz. modification of the polymeric vehicle and the environment of the release medium.

Based on our previous understanding of stability and release pattern of hydrophobic molecules from GCF, we tried to work on the deficiencies of the previous vehicles by introducing nanostructured DDS in Chapter 3. This chapter includes basic theories on the electrospinning process, and on fabricated, hydrophobic drug-loaded gelatin nanofiber (GNF) based DDS. The importance of the chapter lies in its examination of how we successfully improved the water repulsion capability of the vehicle by crosslinking it for a few minutes, which significantly marginalized any adverse effects, associated with the toxic cross linker.

All the aspects of the newly developed DDS in terms of thermal, structural and drug-polymer interactions are studied in this chapter.

Chapter 4 begins with the possible solutions aimed at reducing the burst release of drug by introducing a multi-layered structured GNF based DDS. This chapter describes the different formulations of drug-loaded core and barrier layers in order to get zero-order release of the drug. This chapter not only focuses on the detailed design of fabricating a core-barrier for the system but also documents the improvements in release profiles. At last, the role of different strategies of crosslinking to achieve zero-order release of hydrophobic drug is examined in this chapter.

Chapter 5 discusses the effect of different crosslinking strategies i.e. one-time and sequential crosslinking of different GNF based systems based on drug release profiles. The chapter also presents a comprehensive study of different kinds of drug-polymer formulations to identify the key parameters of modifying the drug release profile. This chapter includes in-depth understanding of the role of different crosslinking strategies for single and multi-layered GNF based DDS. The aim of this chapter is to fabricate a general GNF based DDS, which can be tuned according to the desired release profiles particularly for hydrophobic drug molecules.

With the previous experience with GNF based DDS using hydrophobic drug, chapter 6 attempts to present a realistic approach to fabricating compressed nanofiber based oral tablets (CNOT) using a model amphiphilic drug, Amphotericin B (Amp-B). This chapter describes the fabrication, characterization and release performance of anti-fungal drug Amp-B loaded GNF and CNOT. Here the aim is to show the potential application of the nanofiber based DDS for molecules with larger size and with different nature (amphiphilic kind of drug). To meet the realistic scenario, Amp-B based CNOT is fabricated matching the therapeutic dose of the drug. The significance of taking a generic approach of fabricating CNOT, which can be applicable for different kinds of low soluble drugs, is discussed in chapter 6.

Finally, chapter 7 reviews the newly engineered polymeric drug delivery vehicles with concluding remarks of the thesis. This chapter also includes the possibility of future works in the field of polymeric drug delivery vehicles particularly for low soluble drug molecules.

Chapter 2

Fabrication of Gelatin Cast-Film based DDS

2.1 Literature review

While chapter 1 provides a historical overview of controlled DDS, different polymeric vehicles, different biomaterials used for DDS and different drug administration routes, chapter 2 narrows down the focus to developing gelatin based cast-film as a potential drug delivery vehicle particularly for low soluble orally administrable drug piperine.

As introduced in chapter 1, controlled delivery of drug occurs when bioactive molecules are encapsulated in a well-engineered system so that the drug can be released in a predetermined manner under specific physiological conditions [1, 2]. Consequently, the development of new biopolymers has become a rapidly emerging area of research which has in turn proved to be a driving force for revolutionizing polymer based DDS [3, 115, 116]. Compared to other drug delivery routes, the oral administration process is preferred because it is painless, patient-friendly and easy for self-medication [56, 117, 118]. In spite of this, oral administration of the drug is considered challenging because GI fluids cause hydrolysis and enzymatic degradation of the active molecules [35]. Thus, in order to protect the drugs from the harsh conditions of the GI tract, they are usually wrapped with biocompatible polymers known as excipients [51, 116]. To overcome early degradation of drug molecules and to deliver the drug at the absorption site with better bioavailability, researchers have developed

various kinds of biodegradable and biocompatible polymeric vehicles as a suitable means for controlled DDS.

Over the years, drug delivery scientists have designed a wide array of drug-carriers to overcome these issues concerning conventional drug delivery methods. These have been discussed in chapter 1. Among various drug delivery vehicles, *polymeric cast-films* are gaining considerable attention as alternatives to tablets [119]. Oral cast-films are simple in design and are easy to administer particularly to very young and elderly patients. For creating effective polymeric cast-films, researchers have engineered different kinds of drug loaded oral films with various types of biomaterials [120-122]. Likewise, chemists have synthesized multiple varieties of biomaterials, which can control the interaction between the polymer chain and the biological components. With these newly developed biocompatible biomaterials, chemical engineers presently design the drug-carrier or vehicle in such a way so that it is able to maintain the drug concentration within the therapeutic level. Both engineers and pharmaceutical scientists pay very close attention to the designing of the drug-carrier in order to meet the desired release profiles. It is therefore evident that the selection of an appropriate biomaterial and a drug delivery vehicle is very important to make the vehicle therapeutically effective and commercially successful.

From the two kinds of available biomaterials, namely, synthetic and natural polymers as discussed previously, we have chosen natural polymer gelatin as an excipient of the drug-carrier [102, 123, 124]. The properties of gelatin may differ depending upon several factors (such as collagen source, the type of hydrolytic treatment and the method of extraction) during its synthesis [102]. Gelatin is a hydrophilic polypeptide, which can be extracted either from acid or alkali or even from the hydrolysis of collagen. This collagen is usually sourced from the skin, bone, cartilage, and connecting tissue of different animals. The synthesizing process and concentration of crosslinker hugely influences the mechanical properties, swelling degrees, physio-chemical properties and thermal stability of gelatin. The versatility of gelatin, therefore, makes it the most viable option for designing the drug-carrier. In this proposed work, we have selected gelatin cased-film (GCF) as the drug delivery vehicle, which can be administrated orally.

There have been myriad reports on different kinds of oral films, with many classes of encapsulated drug molecules that target a broad spectrum of release profiles. For instance, there are reports regarding fast dissolving and muco-adhesive oral films for buccal administration, and targeted oral films, which are used for a prolonged duration [54, 76, 119,

125, 126]. In the case of muco-adhesive or fast dissolving oral films, the administrative route is mostly through the buccal cavity which bypasses the first pass-metabolism and avoids the adverse conditions of the GI tract [52, 118]. In the case of oral films with prolonged release however, the design is critically important, particularly for targeted drug release [125, 126]. Here, as discussed in chapter 1, the challenge is to maintain the drug concentration within the therapeutic level for a prolonged duration. In order to accomplish this task, there are three options available. The first is to; increase the drug load, which may however cross the upper limit or the toxic level of the drug. The second option is frequent administration of drug, which could prove to be inconvenient to the patients. Finally, the third option is to encapsulate the drug in a polymer matrix so that it can easily survive though the harsh condition of the GI tract and can be released at the absorption site. Taking up the aforementioned challenge, we have aimed to fabricate a polymer carrier, encapsulated with molecules of interest, which can provide a wide range of drug release profiles. Our next challenge is to deliver molecules with low-solubility using hydrophilic polymer based GCF. Gelatin has been extensively studied as an oral drug-carrier and the efficacy of the vehicle with many different drugs has been reported in literature [116, 122]. Despite extensive research on gelatin based DDS, delivering a low-soluble drug remains a challenge in the field of drug delivery.

In this study, we have selected piperine as a low-soluble model drug. Piperine has been used in alternative and complementary therapies because of its bio-enhancer properties, and its anti-oxidant, anti-depressant, anti-inflammatory, anti-thyroid, and anti-tumor activities [127]. It has been reported that piperine increases the bio-availability of curcumin, an anti-cancerous drug, by 2000% in humans [128]. The gelatin-based hydrophilic matrix increases the solubility of the vehicle, which in turn releases the drug. However, gelatin's poor structural consistency in an aqueous medium is a considerable drawback. To improve its stability in wet conditions, polymer blending and crosslinking are two reported methods [129, 130] but, due to the low biocompatibility and cell affinity of synthetic polymers, polymer blending as a probable solution was eliminated at this stage for this study. Alternatively, drug impregnated GCF was cross-linked at various degrees of concentrations to improve the structural property of the vehicle. Among different crosslinking agents reported in the literature to improve water resistivity of gelatin [94, 131-133], glutaraldehyde (GTA) has been used in this study owing to its easy availability, low cost, and excellent crosslinking capacity within a short time period. However, GTA is used at a very low concentration to minimize its cytotoxic effects [133].

In this chapter, we have anticipated that hydrophobic drug encapsulation will prevent the biopolymer matrix from early degradation and enhance the release possibility at the

absorption site. Thus, on the one hand, the designed hydrophilic matrix protects the active molecules from gastric fluids, and on the other hand, it releases the drug due to enzymatic degradation in the lower intestine. However, the challenge is to crosslink the vehicle to the correct degree so that it can provide the desired mechanical strength and can release the drug in a controlled manner. The advantage of using GTA crosslinked gelatin matrix is primarily because of its swelling properties and its capacity for time-programmed degradation. Naturally, crosslinking plays a very important role in the swelling rate and the desired sustainability of the vehicle. The covalent bonding, hydrogen bonding, and the physical interaction facilitate the longevity of the vehicle. Eventually, due to the external stimuli (like: pH and ionic strength of the dissolution medium), the polymer relaxation leads to swelling, which results in the diffusion of the drug molecules from the vehicle to the release medium [122, 131-133]

This study aimed to examine all aspects of the drug loaded cross-linked GCF in terms of morphology, biodegradation, thermal stability of the drug loaded vehicle and achieve control over the drug release profiles using this vehicle. In order to check the overall morphology, and to find the presence of drug in the polymer film, Optical Microscope was used. Fourier Transform Infrared (FTIR) spectroscopy and Differential Scanning Calorimetry (DSC) investigated the presence of drug and thermal stability respectively. Finally, *In-vitro* release study was undertaken (for several cases with varying concentrations of polymer and crosslinker) in different physiological conditions that mimicked the stomach and intestinal pHs. In summary, the effort was to demonstrate the mechanism for preparing GCF of different dissolution rates (fast and slow). This was carried out through changing the concentrations of gelatin and GTA and facilitate the release of hydrophobic drug (Piperine) for a variety of release requirements i.e. from fast to slow release of drug molecules.

2.2 Materials and Methods

2.2.1 Materials

Gelatin (Type A, 175 bloom), Piperine (98%), Hydrochloric acid (ACS, 36.5-38.0%), Glutaraldehyde (25% v/v aqueous solution), Phosphate buffer saline (PBS: pH 7.4), Sodium hydroxide pallets (98%) were purchased from Alfa Aesar. Deionized water (DI) (Milli Q water 18.1Ω) was used throughout the experiments.

2.2.2 Fabrication of cast-film

GCF were fabricated by solvent casting method. First, different concentration (A: 2.5% w/v, B: 5% w/v, C: 10% w/v and D: 15 % w/v (gm/ml)) of 5 ml aqueous gelatin solution were made in magnetic hot plate maintaining the temperature at 50^{o}C and the rotation speed at 600 RPM. After 2 h, piperine (2mg/ml) as a model drug was loaded in the homogenous gelatin solution and was kept for stirring for another hour. In the next step, the solutions were poured in (60×15 mm) petri dishes and kept in dry air oven for 24 h, maintaining the temperature at 30^{o}C. After 24 h, the completely dried, drug-loaded, gelatin cast-films (GCF-P X where, X=A/B/C/D) were removed from the petri dish.

2.2.3 Crosslinking

After fabricating GNF-P X, the films were cross-linked with different concentrations of GTA (1: 0.01% v/v, 2: 0.02% v/v, 3: 0.05% v/v, 4: 0.1 % v/v, and 5: 0.25 % v/v) for 10 min. The different concentration of crosslinking led to various degrees of cross-linked samples (GCF-P XY where, X=A/B/C/D and Y=1/2/3/4/5). Following this, these crosslinked samples were kept in a hot air oven for another 24 h with the temperature being maintained at 30^{o}C. Gelatin has polyampholyte nature because of the presence of positively and negatively charged amino acids [122]. Further on, GCF-P X were cross-linked using different concentrations of GTA solution in order to improve the water sensitivity and thermal stability. The carbonyl groups (C=O) of aldehyde group (-CHO) present in GTA react with amine groups (-NH2) of lysine, one of the amino acid present in gelatin [133]. These cross-linked gelatin molecules have covalent bonds between molecules which cause remarkable water resistivity for the system. Figure 2.1 shows digital images of GCF-P D0 and GCF-P D4. Although, the crosslinked sample GCF-P D4 was dipped for only 10 min in 0.1% v/v of GTA, it showed good water resistivity and thus was sufficient to protect the film from degradation. The nomenclature of samples with different polymer concentration and various GTA concentration is displayed in Table 2.1.

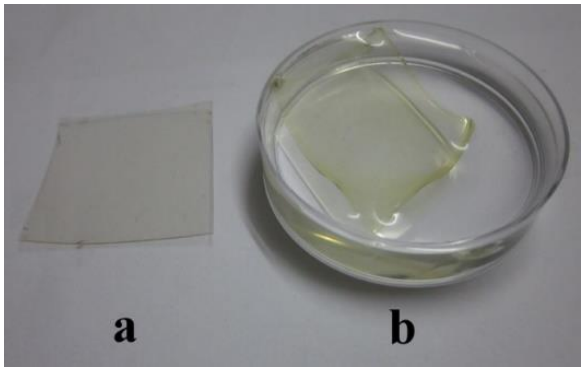

Figure 2.1: Digital images of (a) non-crosslinked sample (GCF-P D0) and crosslinked sample (GCF-P D4) immersed in PBS (pH 7.4)

Table 2.1: Nomenclature of samples used in this chapter

Polymer Concentration (gm/ml)	**Non-crosslinked**	**Crosslinker GTA solution concentration Y= 1/2/3/4/5**				
X=A/B/C/D	**Y=0 (0% v/v)**	**Y=1 (0.01% v/v)**	**Y=2 (0.02% v/v)**	**Y=3 (0.05% v/v)**	**Y=4 (0.1% v/v)**	**Y=5 (0.25% v/v)**
A=2.5% w/v	**GCF-P A0**	**GCF-P A1**	**GCF-P A2**	**GCF-P A3**	**GCF-P A4**	**GCF-P A5**
B=5.0% w/v	**GCF-P B0**	**GCF-P B1**	**GCF-P B2**	**GCF-P B3**	**GCF-P B4**	**GCF-P B5**
C=10% w/v	**GCF-P C0**	**GCF-P C1**	**GCF-P C2**	**GCF-P C3**	**GCF-P C4**	**GCF-P C5**
D=15% w/v	**GCF-P D0**	**GCF-P D1**	**GCF-P D2**	**GCF-P D3**	**GCF-P D4**	**GCF-P D5**

2.3 *In-vitro* biodegradation study

The motivation behind the *In-vitro* biodegradation was to check the water resistant properties of the system in different pH solutions while maintaining physiological conditions. Thus, GCF-P X were cross-linked using different concentration of GTA solution for better stability in aqueous conditions. All the dried cross-linked films (GCF-P XY where, X=A/B/C/D and Y=1/2/3/4/5) were kept in 50 ml solutions of pH 1.2, 6, 7.4 and 8 in a mechanical shaker (Remi RIS-24 plus) for 24 h, at 37 ^{O}C and 100 RPM. *In-vitro* biodegradation results for GCF-P XY (where, X=A/B/C/D and

Y=1/2/3/4/5) are summarized in Table 2.2. The non-cross-linked (NC) drug loaded gelatin films (GCF-P X0 where 0= NC) dissolved within few minutes for all the concentration of gelatin (GCF-P X0 where X=A/B/C/D and 0=NC) because of the hydrophilic nature of the polymer.

All the different concentration of gelatin samples (A: 2.5% w/v, B: 5% w/v, C: 10% w/v and D: 15 % w/v) cross-linked with 0.05% v/v of GTA solution (that is sample GNF-P X 3) and above were intact even after 24 h in all pH conditions. Cross-linked samples below 0.05% w/w (GCF-P X3 where, X=A/B/C/D and 3=0.05% v/v) were partially degraded within 24 h. In case of sustained release for more than 24 h, these samples were not recommended as a vehicle. Thus we have taken GCF-P X3 where, X=A/B/C/D and 3=0.05% v/v as the baseline.

Table 2.2 shows that with the same amount of crosslinking (0.02% v/v of GTA that is sample GCF-P X2 where, X=A/B/C/D and 2=0.02% v/v) even the stability of the vehicle can be improved by increasing the concentration of gelatin. This is because of the increase in the thickness of the film. The thickness of different samples (GCF-P X where X=A/B/C/D) were measured by Digimatic micrometer, Mitutoyo, and are presented in Table 2.2. Thus, it can be understood that longer diffusion path for water ingression leads to difficulty in swelling followed by less degradation, which confirms better stability of the vehicle. Another possible explanation can be that with a higher concentration of gelatin the crosslinking is better with GTA due to the presence of more lysine protein in the matrix, which can react with GTA and thus increase the molecular entanglement, leading to better stability. The gelatin cast-films of 10% w/v and above (that is sample GCF-P C2 and CGF-P D2 where, 2= 0.02% v/v) are quite stable with even minimal crosslinking (0.02% v/v of GTA) for all the physiological pH for a period of 24 h. However, the sample GCF-P A2 and GCF-P B2 showed partial degradation in lower pHs.

Finally, we conclude that, samples GCF-P XY where X=A/B/C/D and Y=2/3/4 showed good stability in different pH solutions. These selected samples were used for further experiments. The selected samples are highlighted in the Table 2.2.

Table 2.2: Summary of *In-vitro* biodegradation study for sample GCF-P XY where, X= A/B/C/D and Y=0/1/2/3/4/5

pH of solution	A=2.5% w/v GCF-P and crosslinking time= 10min (Thickness: 0.0518 ± 0.0 mm)						Main cause of drug release
	A0 (0%v/v)	A1 (0.01 %v/v)	A2 (0.02 %v/v)	A3 (0.05 %v/v)	A4 (0.10 %v/v)	A5 (0.25 %v/v)	
1.2	-	+	+	*	*	*	Degradation
6	-	+	+	*	*	*	Degradation
7.4	-	+	+	*	*	*	Degradation
8	-	+	+	*	*	*	Degradation
pH of solution	B=5% w/v GCF-P and crosslinking time= 10min (Thickness: 0.103 ± 0.01 mm)						
	B0 (0%v/v)	B1 (0.01 %v/v)	B2 (0.02 %v/v)	B3 (0.05 %v/v)	B4 (0.10 %v/v)	B5 (0.25 %v/v)	
1.2	-	+	+	*	*	*	Diffusion
6	-	+	+	*	*	*	Diffusion
7.4	-	+	+	*	*	*	Diffusion
8	-	+	*	*	*	*	Diffusion
pH of solution	C=10% w/v GCF-P and crosslinking time= 10min (Thickness: 0.181 ± 0.01 mm)						
	C0 (0%v/v)	C1 (0.01 %v/v)	C2 (0.02 %v/v)	C3 (0.05 %v/v)	C4 (0.10 %v/v)	C5 (0.25 %v/v)	
1.2	-	+	*	*	*	*	Diffusion
6	-	+	*	*	*	*	Diffusion
7.4	-	+	*	*	*	*	Diffusion
8	-	+	*	*	*	*	Diffusion
pH of solution	D=15% w/v GCF-P and crosslinking time= 10min (Thickness: 0.305 ± 0.01 mm)						
	D0 (0%v/v)	D1 (0.01 %v/v)	D2 (0.02 %v/v)	D3 (0.05 %v/v)	D4 (0.10 %v/v)	D5 (0.25 %v/v)	
1.2	-	+	*	*	*	*	Diffusion
6	-	+	*	*	*	*	Diffusion
7.4	-	+	*	*	*	*	Diffusion
8	-	+	*	*	*	*	Diffusion

Where, '-' means dissolved completely in the solution. '*' means not dissolved and '+' means slightly dissolved in the dissolution medium after soaking for 24 h.

2.4 Characterization

After checking the stability of the cross-linked samples in biological conditions, we have investigated the effect of crosslinking on thermal stability using Differential Scanning Calorimetry (DSC 1 Stare system, Mettler Toledo: Switzerland, model no: B25063033) in nitrogen atmosphere. The experiment was performed in the range to 35 to 300 $^{\circ}$C at a heating rate of 10 $^{\circ}$C /min. Surface morphology of the drug loaded film was confirmed using Optical microscope (Carl Zeiss Axio Imager M2m) under 5X optical lens in bright field mode. In order to examine the presence of drug and the effect of crosslinking on the film, samples were characterized using Attenuated Total Reflectance (ATR)-Fourier transform infrared (FTIR) spectrometer (Bruker Alpha-P) in the 4000-500 cm^{-1} range.

2.4.1 Thermal characterization

DSC was performed for the maximum concentration of gelatin and maximum concentration of GTA i.e. 15% w/v of GCF-P cross-linked with 0.10% v/v of GTA (sample: GCF-P D4), which was the most stable sample in all the pH conditions. Figure 2.2 shows very distinct two stage endothermic peaks within the range of 35 to 250 ^{o}C. The first peak between 85 to 110 ^{o}C refers to the helix to coil transition and the second peak indicates the degradation and decomposition of gelatin in the range of 200 to 250 ^{o}C [129]. The denaturation temperature of NC film (GCF-P D0) is 89.5 ^{o}C (approx.), whereas the same for the cross-linked one is 96 ^{o}C. Finally, we can conclude that crosslinking helps in entanglement of the polymer molecules and leads to better thermal stability of the polymeric vehicle.

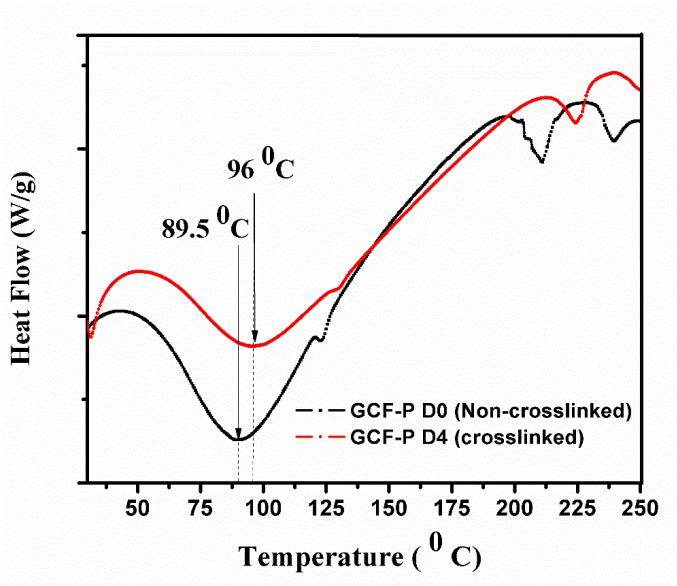

Figure 2.2: DSC thermogram of GCF-P D0 and GCF-P D4

2.4.2 Structural characterization

Figure 2.3 shows the optical microscopic images of NC gelatin sample without drug molecules (GCF D0) and with drug molecules (GCF-P D0). In the case of GCF D0, the sample showed a smooth morphology (Figure 2.3 a). However, for sample GCF-P D0, the presence of drug molecules were clearly visible in Figure 2.3 b. As drugs were loaded during the formation of the film, they were distributed both in core and surface of the film. Figure 2.4 showed the morphology of swelled sample GCF-P D4 in different time intervals of immersion in PBS solution. The presence of the drug in the matrix as well as on the surface is very clear. When the sample starts swelling due to diffusion, the drug molecules start moving towards the release medium. We have assumed that the drugs molecules, which are attached to the uppermost surface of the film, will show an initial fast release profile due to partial degradation of the film. Drug molecules within the layers of the film will lead towards sustained release profile. In this case, the diffusional force remains the main factor in releasing molecules from core of the cross-linked film. These drug molecules from the core will be responsible for the delayed or sustained release of drug molecules. Optical microscopic images not only gave an overall idea of the topography of the samples but also gave an image of drug distribution and drug transportation for swelled samples.

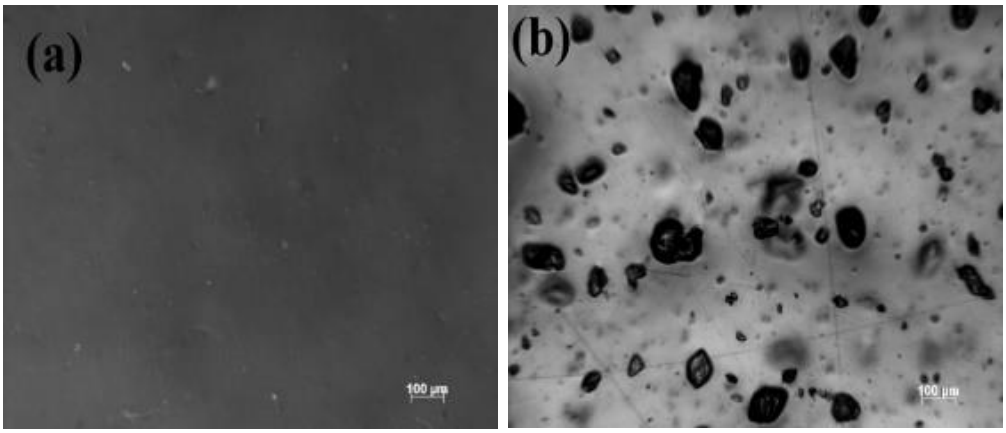

Figure 2.3: Optical microscopic image of (a) GCF D0, (b) GCF-P D0

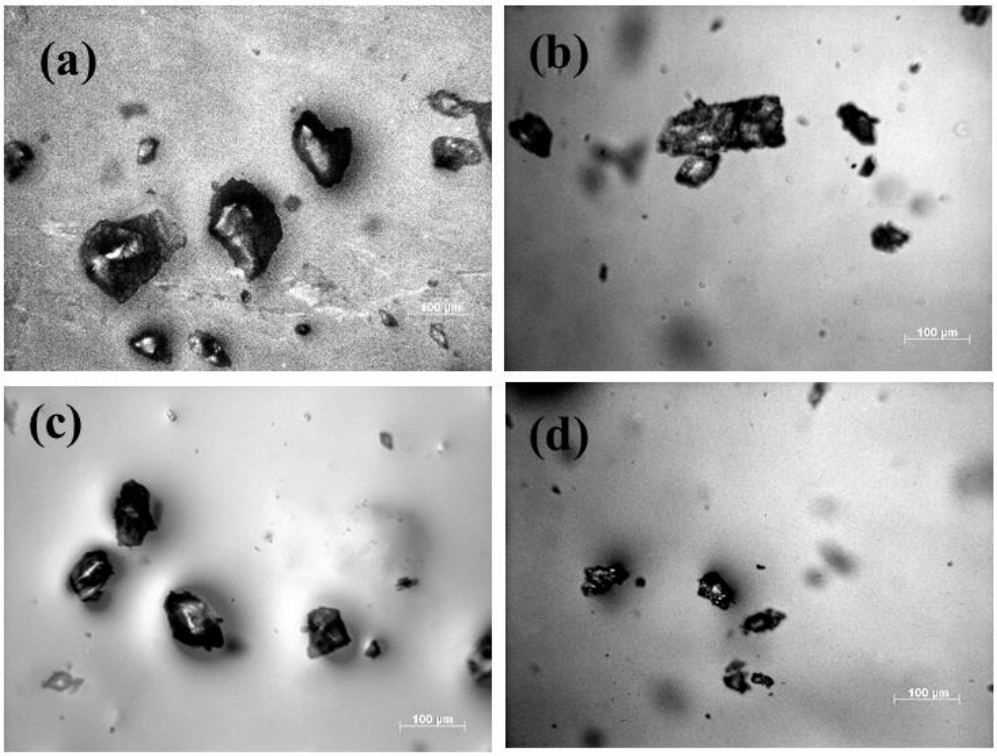

Figure 2.4: Optical Microscopy images of GCF-P D4 at various time intervals i.e. (a) 1 h, (b) 8 h, (c) 12 h and (d) 24 h of immersion in PBS solution (pH 7.4) maintaining 37 ^{O}C

2.4.3 Drug-polymer compatibility

To understand the effect of crosslinker on the polymer and the interaction between the drug and polymer matrix, ATR/ FTIR were done. Figure 2.5 shows the results of ATR/FTIR for the non-crosslinked and crosslinked films with and without drug (a. GCF D0, b. GCF D4, c. GCF-P D0, d. GCF-P D4). The absorption bands at 3271 cm^{-1} (N-H stretching), 1626 cm^{-1} (amide I, C=O and C-N stretching), 1535 cm^{-1} (amide II,

N-H bend and C-H stretch) and 1236 cm^{-1} (amide III) are the characteristic bands of non-crosslinked GCF which are shown in Figure 2.5 (a) [126]. The aldehyde group (-CHO) of GTA reacts with the lysine's amino group present in gelatin. New covalent (C-N) bonds form due to the reaction of amino group of gelatin with carbonyl group of GTA [133].

Figure 2.5 (a) and 2.5 (b) shows the minor peak shifting for non-crosslinked (GCF D0) and crosslinked (GCF D4) gelatin film from 3271 cm^{-1} (N-H stretching) to 3273 cm^{-1} due to hydrogen bonding between amino group of gelatin and carbonyl group of GTA. Similar peak shifting was observed at amide I (C=O and C-N stretching) from 1626 cm^{-1} to 1630 cm^{-1} as well as in amide II and III peaks of gelatin, which confirm the crosslinking of gelatin with GTA.

Figure 2.5 (a) and 2.5 (c) shows the presence of piperine in non-crosslinked gelatin film. The peaks due to N-H stretching have shifted from 3271 cm^{-1} to 3274 cm^{-1} that is an indication of very weak interaction between piperine and gelatin. There is no major peak shifting that occurs due to the presence of piperine which is an indication of the successful encapsulation of drug without reacting with the polymer matrix. Next, we compared non cross-linked (GCF-P D0) and cross-linked (GCF-P D4) GCF with piperine in Figure 2.5 (c) and 2.5 (d). Similarly, minor change in peaks can be observed in N-H, amide I, II, III peaks that indicates less crosslinking of gelatin. This crosslinking was good enough for the stability of polymer film in biological conditions, which has been discussed in section 2.3. Therefore, it is clear from the FTIR studies that drug molecules are neither strongly attaching with the polymer nor forming new molecules, i.e. drug is encapsulated in polymer matrix without reacting with the matrix.

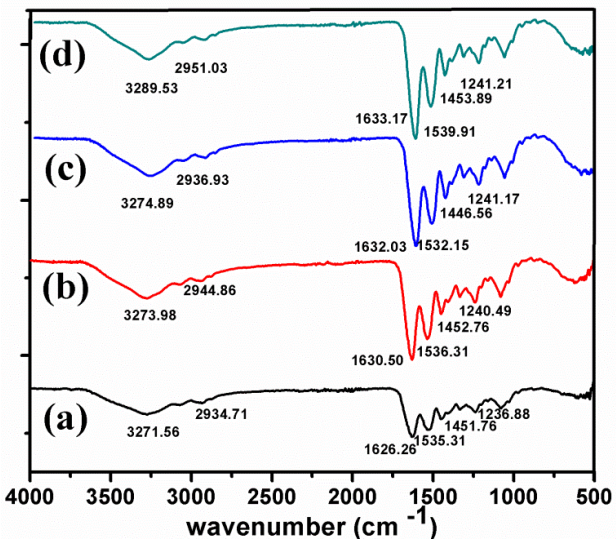

Figure 2.5: ATR/FTIR spectra for (a) GCF D0, (b) GCF D4, (c) GCF-P D0, (d) GCF-P D4

2.5 Drug release performance

In this section, we tried to bind all the previous observations from the morphology study, *In-vitro* biodegradation, thermal stability and drug-polymer interaction studies to predict the desired release profiles. To study the *In-vitro* release of piperine from GCF, films were kept in 50ml of PBS and 0.1N HCl solution at different physiological pH levels (pH 1.2: similar to stomach; pH 7.4: similar to intestine). The temperature and stirring of the system were maintained at 37 ^{O}C and at 50 RPM respectively. 3ml samples were taken at certain time gaps and analysed using an UV spectrophotometer (Perkin Elmer Lambda 35) at 342nm as λ_{max} for Piperine. Fresh 3ml release solution was replaced in the release medium to maintain the total volume as constant. Standard curve for piperine in PBS is shown in Appendix C.

Release profile of piperine from different cross-linked film (GCF-P XY where X= A/B/C/D and Y= 2/3/4) are shown in Figures 2.6 and 2.7. Concentration of polymer and crosslinker and pH of the release medium plays an important role in these release profiles [122]. Release of drugs can be influenced by the diffusion of drug molecules from the matrix as well as the partial degradation of polymer matrix. Swelling of the matrix is also a very important factor for the drug release study [129]. From the *In-vitro* biodegradation study, we got an idea of the stability for crosslinked sample. Based on degradation study, we selected few samples (highlighted in Table 2.2 and the samples were GCF-P XY where X= A/B/C/D and Y= 2/3/4) which were suitable for the drug release study. The swelling and degradation of the matrix can be toned-down by changing the concentration of gelatin and GTA. The water molecules from the release medium diffuses inside the film and starts swelling. For lower concentration of gelatin and GTA, the binding forces in the crosslinked gelatin matrix were less which led to faster degradation followed by fast release of drug. To take control over the degradation due to hydrolysis, films were cross-linked with higher concentration of GTA and higher concentration of gelatin. Similar to *In-vitro* biodegradation of film, thickness of the film played an important role in the drug release phenomena as well. Firstly, with same drug loading for different films, lower concentration polymer showed faster release due to the lesser diffusional path. The lesser diffusion path led to higher mobility of water molecule and thus the faster degradation of the film. Secondly, with lower concentration of polymer, the presence of amine group, which can react with GTA, is also less. Less entanglement between the polymer chain and crosslinker may cause faster degradation of film, which results swelling of the matrix. Due to less

crosslinking of the matrix, the hydrophilic chains attracts water molecules, which easily invites water molecules inside the matrix causing swelling of the film. The swelled film causes partial degradation as well as diffusion of drug molecules from the matrix. Naturally, the penetration of water molecules through the matrix is very much dependent on the entanglement between the polymer chain and crosslinking. In case the crosslinking is not strong enough, the water molecules starts entering from the release medium to the matrix causing swelling. Due to the high osmotic pressure, the matrix experiences early degradation, which leads to sudden release of drugs. On the other hand, the release pattern can be controlled by increasing the concentration of gelatin and GTA both. Therefore, the perfect amount of crosslinker and polymer concentration is required to fabricate a GCF based vehicle, which can sustain for a longer period and can release drug without initial sudden release.

From *In-vitro* biodegradation of cased-film, we concluded that, crosslinking more than 0.01% v/v of GTA to less than 0.25% v/v of GTA (GCF-P XY where X= A/B/C/D and Y= 2/3/4) was sufficient for it to remain stable under all the pH conditions for 24 h. DSC thermogram had already confirmed the thermal stability due to the crosslinking effect. The ATR/FTIR had also clearly represented the presence of drug in gelatin matrix without reacting with the vehicle. These analyses get further support *In-vitro* drug release study.

The *In-vitro* drug release patterns for the samples GCF-P XY where X=A/B/C/D and Y=2/3/4 in different physiological pH conditions (pH 7.4, pH 1.2) are shown in Figures 2.6 and 2.7. The drug concentration (µg/ml) Vs time (min) data is presented in Appendix B (Table B1 and B2). The drug release pattern for GCF-P AY (where, Y=2/3/4) showed initial sudden release in the first 3-4 h compared to GCF-P DY (where, Y=2/3/4) samples (Figure 2.6 a). The inter- and intra- molecular bonds between gelatin molecules in higher concentration of gelatin film show less swelling followed by less amount of drug release compared to the case of lower concentration of gelatin film.

With the increase in the polymer concentration, the cumulative drug release was decreased and the initial release was controlled. Polymer concentration influences the film thickness, which resulted in longer diffusional path for the drug molecules to release. Therefore, the presence of drug molecules in the core of the film causes slow release. The reason is, due to the higher concentration of polymer and crosslinker, the drug molecules experience constraints and slow down the mobility or transportation of the drug molecules. The drugs present in the core of the mesh, come out to the release

medium due to diffusional force. For example, the sample GCF-P D4 shows sustained release compared to GCF-P D1. Less crosslinking causes partial degradation which leads to faster release for GCF-P D1 compared to GCF-P D4.Whereas the reason of sustained drug release from the sample GCF-P D4 is diffusional force. However, sample GCF-P AY (where, Y=2/3/4) exhibits similar release pattern for all the different concentration of GTA solution. This might be because of the less molecular entanglement in the polymer matrix in general, which easily causes partial degradation (Table 2.2) [122, 131-133].

Figure 2.7 represents similar case studies in pH 1.2. It is observed that the drug release amount is less in all the cases in pH 1.2 solutions compared to pH 7.4. The explanation of the phenomenon is due to the presence of H+ ions, the polymer matrix gets protonated and this leads to less swelling of the film [122, 129]. Lesser drug release in pH 1.2 is desirable, as main absorption of drug will take place in intestine (pH 7.4). If the release is less in stomach (pH 1.2) and the vehicle is stable in that condition, the drug loss will be less. Typically, in the stomach, the retention time is generally 3-4 h. Nevertheless, we have studied it for 8 h to check the drug release pattern. The maximum drug released in pH 1.2 for the sample GCF-P A1 (i.e. 0.02% v/v of GTA and 2.5%w/w of gelatin) is approx. 24% over 8 h. Further, the drug release in lower pH is taken care of by increasing the concentration of GTA and polymer. As a result, the total drug release gets reduced (only approx. 14% of total drug) by almost 10% for the sample GCF-P D4 (i.e. 0.1% v/v of GTA and 20%w/w of gelatin) over 8 h.

Finally, by controlling the crosslinker and gelatin concentration, we can engineer the vehicle in such a way that we get desired drug release profiles. From the *In-vitro* drug release study, we can conclude that the GCF-P XY (where, X= A/B/C/D and Y= 2/3/4) is stable in the harsh conditions (pH 1.2) of the GI tract and is able to release the drug in a controlled manner in absorption site (pH 7.4). Thus, GCF-P XY (where, X= A/B/C/D and Y= 2/3/4) can be a potential oral drug delivery vehicle to get—fast and slow—both kinds of drug release patterns for specific use.

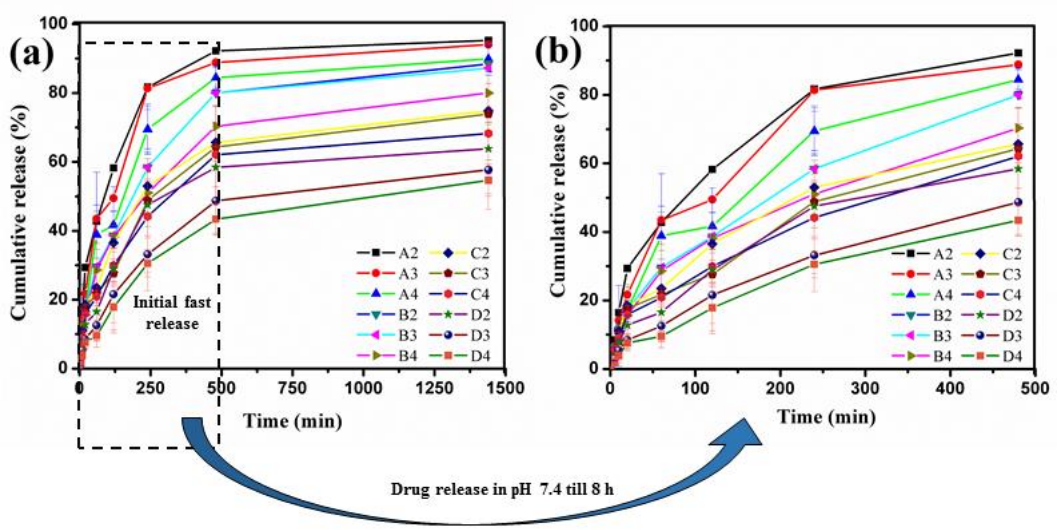

Figure 2.6 (a): Cumulative release of piperine for GCF-P XY (X=A/B/C/D and Y=2/3/4) in pH 7.4 for 24 h and (b): for 8 h, (where, A= 2.5%w/v of gelatin, B= 5% w/v of gelatin, C= 10%w/v of gelatin, D= 15%w/v of gelatin film; 2= 0.02%v/v of GTA, 3=0.05%v/v of GTA and 4= 0.1% v/v of GTA)

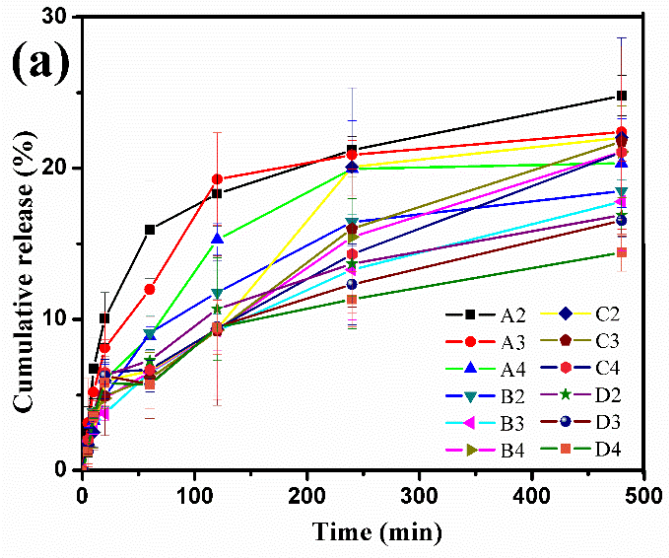

Figure 2.7: Cumulative release of piperine for (a) GCF-P XY (X=A/B/C/D and Y=2/3/4) in pH 1.2 for 8 h, (where, A= 2.5%w/v of gelatin, B= 5% w/v of gelatin, C= 10%w/v of gelatin, D= 15%w/v of gelatin film; 2= 0.02%v/v of GTA, 3=0.05%v/v of GTA and 4= 0.1% v/v of GTA)

2.5.1 Drug release mechanism

To understand the drug release kinetics and the mechanism, data were analysed with various mathematical models such as zero-order, first order, Higuchi and respective co-efficient as presented in Table 2.3 and 2.4. It can been clearly observed from Table 2.2, the samples fitted best in the Higuchi model, among all others, based on the higher R^2 values.

The equation of Higuchi model is:

$$F = K_H\, t^{1/2}$$

Where, F = amount of drug release at time t, K_H = Higuchi dissolution constant.

The decreases in K_H values were found for all the samples in both the release medium (pH 7.4 and pH 1.2), which indicates the increase in diffusional barrier. With the increase of polymer and crosslinker concentration, the diffusion process has slowed down drastically, which finally toned down the drug release (Figures 2.6 and 2.7). From Tables 2.3 and 2.4, it can be noted that with the same polymer concentration, the K_H value has decreased with increase in crosslinking concentration. On the one hand, polymer concentration helped increase the diffusion path of the film; while on the other hand, crosslinking prevented the polymer matrix from swelling. As a result, we gained control over the swelling as well as over the partial degradation due to diffusion, which finally helped us achieve sustained release [134, 135].

Table 2.3: List of drug release co-efficient fitted in different kinetic models (For pH 7.4)

Samples (pH 7.4)						
Release Models	**Zero-order**		**First Order**		**Higuchi model**	
Sample names	**k**	R^2	**K**	R^2	K_H	R^2
A2	**0.0393**	**0.8831**	**0.0066**	**0.9833**	**5.3554**	**0.9959**
A3	**0.0376**	**0.9139**	**0.0065**	**0.9701**	**5.0402**	**0.9901**
A4	**0.0321**	**0.9092**	**0.0046**	**0.9577**	**4.3078**	**0.9862**
B2	**0.0275**	**0.9061**	**0.0034**	**0.9698**	**3.7062**	**0.9981**
B3	**0.0275**	**0.9061**	**0.0034**	**0.9698**	**3.7062**	**0.9981**
B4	**0.0249**	**0.8786**	**0.0028**	**0.9312**	**3.4068**	**0.9966**
C2	**0.0249**	**0.9008**	**0.0029**	**0.9615**	**3.371**	**0.9949**
C3	**0.022**	**0.9075**	**0.0025**	**0.9472**	**2.9544**	**0.9841**
C4	**0.0208**	**0.8926**	**0.00223**	**0.9479**	**2.8263**	**0.9958**
D2	**0.0213**	**0.9503**	**0.0025**	**0.9828**	**2.7962**	**0.983**
D3	**0.0151**	**0.9463**	**0.0016**	**0.9768**	**1.9987**	**0.9895**
D4	**0.0134**	**0.9669**	**0.00144**	**0.9826**	**1.7443**	**0.9704**

Table 2.4: List of drug release co-efficient fitted in different kinetic models (For pH 1.2)

Samples (pH 1.2)						
Release Models	**Zero-order**		**First Order**		**Higuchi model**	
Sample names	**k**	R^2	**K**	R^2	K_H	R^2
A2	**0.0112**	**0.7672**	**0.000898**	**0.7088**	**1.5921**	**0.9623**
A3	**0.0108**	**0.8291**	**0.000934**	**0.8037**	**1.5097**	**0.9824**
A4	**0.0096**	**0.9117**	**0.000898**	**0.9203**	**1.2897**	**0.9937**
B2	**0.0079**	**0.8839**	**0.000693**	**0.8972**	**1.082**	**0.9977**
B3	**0.0063**	**0.9033**	**0.000547**	**0.9286**	**0.8512**	**0.9997**
B4	**0.007**	**0.9033**	**0.000642**	**0.951**	**0.9323**	**0.9905**
C2	**0.0085**	**0.9492**	**0.000841**	**0.9492**	**1.1052**	**0.954**
C3	**0.0071**	**0.9201**	**0.000644**	**0.9498**	**0.9547**	**0.9848**
C4	**0.0067**	**0.8547**	**0.000556**	**0.8675**	**0.9239**	**0.9802**
D2	**0.0067**	**0.8336**	**0.000553**	**0.8182**	**0.9406**	**0.9809**
D3	**0.006**	**0.8238**	**-0.00021**	**0.7998**	**0.8367**	**0.9687**
D4	**0.0057**	**0.8075**	**0.000446**	**0.7727**	**0.7972**	**0.9678**

2.6 Summary

In order to investigate the importance of crosslinker and polymer concentration on the release profile of piperine at different pH, we studied the surface morphology, *In-vitro* biodegradable study, thermal stability and chemical interactions of the drug and the polymer. Optical microscopic images gave us an idea about the polymer morphology and confirmed the presence of drugs in the samples. *In-vitro* Biodegradation and DSC showed the water resistibility and thermal stability of the system. The ATR/FTIR study showed no presence of strong drug-polymer interaction. The *In-vitro* release study showed that drug release can be controlled by changing the concentration of crosslinkers and gelatin. At lower pH, slower release of drug was observed. Finally, drug release from GCF-P XY (where, X= A/B/C/D and Y= 2/3/4) can have both fast and slow release profiles based on the concentrations of crosslinker, the polymer, and the pH conditions of the release medium. Thus, from the *In-vitro* release data, we can draw an inference that the piperine loaded gelatin cast-film (GCF-

P XY, where, X= A/B/C/D and Y= 2/3/4) is able to deliver the hydrophobic drug in a desired release pattern i.e. from fast release to a release for prolonged duration.

2.7 Highlights of this work and motivation for the next chapter

1. Gelatin based cast-film (GCF) is low-cost and simple to fabricate.
2. GCF can successfully encapsulate the low-soluble drug piperine and can deliver the drug at the absorption site (intestine) by protecting it from early release in stomach.
3. Piperine is stable in the polymer matrix.
4. Crosslinking provides the thermal and mechanical stability to the system.
5. Crosslinking and polymer concentration results in flexible drug release profiles for 24 h.
6. GCF exhibits pH sensitive features, which is desirable.

These results certainly validate the use of biopolymer gelatin as an excipient for oral DDS and confirms the stability of the drug in the matrix. This study also gives a clear understanding of the role of crosslinker for the release study. These preliminary results provide us a platform, which motivates us to meet the other objectives mentioned in chapter 1 section 1.6.

The primary impulse behind the improvement of these existing vehicles is to reduce the usage of toxic GTA and to achieve sustained or a zero-order release of piperine for a prolonged duration (24-48 h).

Chapter 3

Fabrication of Gelatin Nanofibers based DDS

3.1 Introduction

The key results from chapter 2 regarding the applicability of piperine-loaded gelatin based drug-carrier motivates us to carry forward the work using the same excipient and drug in an attempt to improve the drug vehicle. The sole focus of this chapter then, is to discuss the fabrication of a drug-carrier, which can reduce the usage of the toxic crosslinker and to discuss how the sustained drug release of low-soluble drug piperine for a period of 24-48 h can be achieved. To meet the aforementioned aim, firstly, we introduced a nanofiber based DDS, which was crosslinked with GTA vapor for only 6 min, and secondly, we fabricated a pH sensitive drug-carrier that could release piperine for 24 h. This section, therefore, discusses the background of the electrospun nanofiber DDS experiment in detail to explicate and highlight the novelty of this work.

3.2 Literature review

As mentioned in chapter 1, oral film and hydrogel is a widely acceptable drug-carrier. Moreover, nanofiber based DDS has also gained considerable attention in the last few decades. Several applications of nanofiber based DDS in the field of drug delivery and tissue engineering have reported that their large surface area-to-volume ratio and controllable

porosity results in high drug loading capacity [88, 136-155]. In 2002, for the first time, Kenawy et al. reported the sustained release of the model drug tetracycline hydrochloride using poly(lactic acid) and poly(ethylene-co-vinyl acetate) blend nanofiber mesh [143]. Since then, electrospun nanofibers have been successfully used as drug-carriers, and have shown fast release, bi-phasic, controlled release, delayed release, zero-order release of various kinds of drugs. Active pharmaceutical molecules like antibiotic, antiseptics, NSAID, anti-cancer and biomolecules like protein and nucleic acid have also been successfully encapsulated in nanofibers and the efficiency as drug-carrier has been investigated [88, 89]. Nanofiber based DDSs have also shown remarkable sustained and prolonged release of anti-cancer drug paclitaxel over a period of more than 60 days [88, 90, 136]. Besides that, the capability to encapsulate both hydrophilic anti-cancer drug doxorubicin and lipophilic anti-cancer drug paclitaxel in the matrix and enabling different drug release kinetics justifies the effectiveness of multi-drug delivery and combination therapy [139-144, 147, 148]. In addition to that, the application of nanofiber based DDS as transdermal and oral drug-carrier, with different kinds of phytochemical or natural/ayurvedic medicines have also been studied [137, 145, 148-150]. . For example the herbal compound, shikonin loaded biodegradable synthetic polymer poly-caprolactone (PCL) nanofiber mesh has showed excellent control release for 24 h. Shikonin is found in the roots of Lithospermum erythrorhizon plant and it is widely known for its wound healing, anti-tumor, antioxidant, and anti-inflammatory properties [137]. In another study PCL nanofibers with herbal drugs have shown excellent anti-bacterial properties and wound healing capability. PCL nanofibers have been fabricated with herbal extracts from Tecomella undulata, Glycyrrhiza glabra, Asparagus racemosus and Linum usitatissimum and anti-bacterial studies have been performed against common pathogenic bacteria namely, Staphylococcus aureus and Klebsiella pneumonia. Researchers have claimed this wound dressing product to be 50% more effective in controlling dermal bacterial infection than the commercial dressing products available [149]. In additional natural polymer based nanofiber wound dressing has also been reported [145, 150]. For example, wound healing compound, asiaticoside (extract of centella asiatica herb) loaded natural polymer gelatin nanofiber has showed an excellent release for 7 days [145].

The FDA-approved, biopolymer gelatin has been largely accepted in different forms as a drug-carrier for therapeutic applications. The entire focus of this thesis is exclusively on fabricating a vehicle that can increase the dissolution rate of low-soluble drugs. As majority of the drugs are highly hydrophobic with low solubility and low permeability, delivering these drugs orally is still a challenge [142]. Polymer based solid dispersion (SD), is one of the

methods to improve oral absorption of the low-soluble drug, which has been extensively studied in pharmaceutical industries [139, 140, 142]. Electrospinning is also one of the methods to prepare drug-polymer solid dispersions [140, 156]. Under high electric field, drug loaded polymer solution can be transformed into nano-micron sized fibers through the electrospinning method [157]. This method can produce extraordinarily porous nano-fibrous structure with high surface area, which directly influences the bioavailability of the poorly soluble drug through increase in the dissolution rate of the drug [140]. Various FDA approved synthetic and natural polymers have been used by many researchers for the preparation of solid dispersions [142]. In addition, nano-fibrous structured device can provide rapid, immediate, delayed, or modified dissolution, with sustained and /or pulsatile release characteristics [140, 158, 159]. Following this path, in this chapter, we have fabricated gelatin based electrospun nanofiber DDS in order to release the low-soluble drug piperine in a sustained way for a prolonged time.

Although electrospun gelatin nanofiber with different synthetic polymer blends has been used extensively in the field of tissue engineering and drug delivery, there are very few studies available solely on the use of gelatin nanofibers as a drug-carrier [160-163]. Moreover, to the best of our knowledge, there is no report on the controlled release of hydrophobic drug using electrospun gelatin nanofiber except for a recent demonstration of slow release of nystatin, an anti-fungal reagent [160]. More importantly, there is a need for a systematic effort in literature to study the release of hydrophobic drug and correlate it with physiochemical conditions as well as structural properties of pure gelatin based electrospun fiber mat.

Electrospun gelatin nanofibers are water soluble which limits their applications and long term use [164]. Crosslinking agent like formaldehyde [132], genipin [131, 138, 154], glutaraldehyde (GTA) [129, 133, 164] etc. have been reported in the literature, to modify gelatin via its amino, carboxyl, or hydroxyl group respectively. GTA is most widely used because of its efficiency in stabilizing collagenous materials [164] and reducing the biodegradation of such materials.

In this study, gelatin nanofibers were prepared using electrospinning (with as well as without piperine) and were cross-linked using saturated GTA vapor. Further, *In-vitro* release studies were performed at varying pH conditions that matched the human GI tract environment. Thus, we have tried to corelate the morphology, *In-vitro* biodegradation study, stability of hydrophobic drug, and the effect of crosslinking with the *In-vitro* release study of the hydrophobic drug through hydrophilic gelatin nanofiber. This study attempts to draw

much needed attention towards exploring the full potential of electrospun nanofibers as a DDS, particularly for hydrophobic drugs.

3.3 Introduction to electrospinning

Electrospinning is a simple, straightforward and cost-effective method to prepare electrospun fibers ranging from diameters of nano- to micrometers. An electrospinning setup consists of three main parts: a high voltage supplier, a syringe pump and a collector as shown in Figure 3.1. The polymer solution loaded capillary tube with a blunt needle is placed with the syringe pump facing the collector. In this process, high voltage is applied to the polymer solution so that this can induce the charge in the solution. The electrified polymer solution drop distributes charges over the surface. The mutual charge repulsion on the surface directly opposes the surface tension of the fluid. When the intensity of the electric field increases, due to the stronger repulsion force of similar charges, the polymer drop at the tip of the needle elongates to form a conical shape known as Taylor cone. Further, with increase in the voltage difference between the needle and collector, which crosses the threshold value, the drop experiences a highly repulsive electrostatic force. At the point when the electric force overcomes the surface tension of the polymer solution, a multiple charged jet of fluid is ejected from the elongated Taylor cone. This jet then travels toward the region lower with potential, which is collector in most cases. Before reaching the collector, the jet is continuously stretched and whipped and this produces very long, continuous, micro- to nanometer thin fibers. During this process, due to excessive stretching, the surface area increases drastically. Through the elongation process, the solvent evaporates quickly and dry solid fibers are deposited on the collector [157, 159].

The morphology and diameter of the fiber depends on several parameters. Generally, these parameters are divided into three categories i.e. polymer solution parameter, process parameter and ambient condition. In the case of polymer solution parameters, polymer viscosity, surface tension, conductivity and solvent volatility are the main features. For process parameters, applied voltage, tip-collector distance and flow rate are the most decisive aspects. The effects of ambient conditions such as temperature and humidity are also significant [89, 90, 147, 159].

The polymer concentration is responsible for the solution viscosity, which determines the spinnability of the solution. Polymer concentration also refers to the entanglement of the polymer chains which directly influences the polymer fiber morphology. The surface tension

of the polymer solution is also dependent on polymer concentration. The concentration of polymer should be high enough so that it can form uniform continuous fibers. In the case of low viscosity, and high surface tension, the fiber will not form and it will break up into droplets. In the case of highly conductive solution, the fiber diameter tends to decrease.

The process parameters are also extremely important as they determine the diameter and morphology of the fibers. With higher applied voltage, the jet starts and it tends to form thinner fibers with optimized flow rate. However, if the flow rate is not optimized, higher voltage will lead to thick diameters for the fibers. The flow rate should be perfect enough so that it can ensure the continuous formation of the Taylor cone. The distance between tip and the collector should be modulated so that the solvent can be evaporated and the dry solid fibers deposited on the collector. The influences of polymer solution parameters, process parameters and ambient conditions on the diameter of the fiber are presented in Table 3.1 [89, 147, 159].

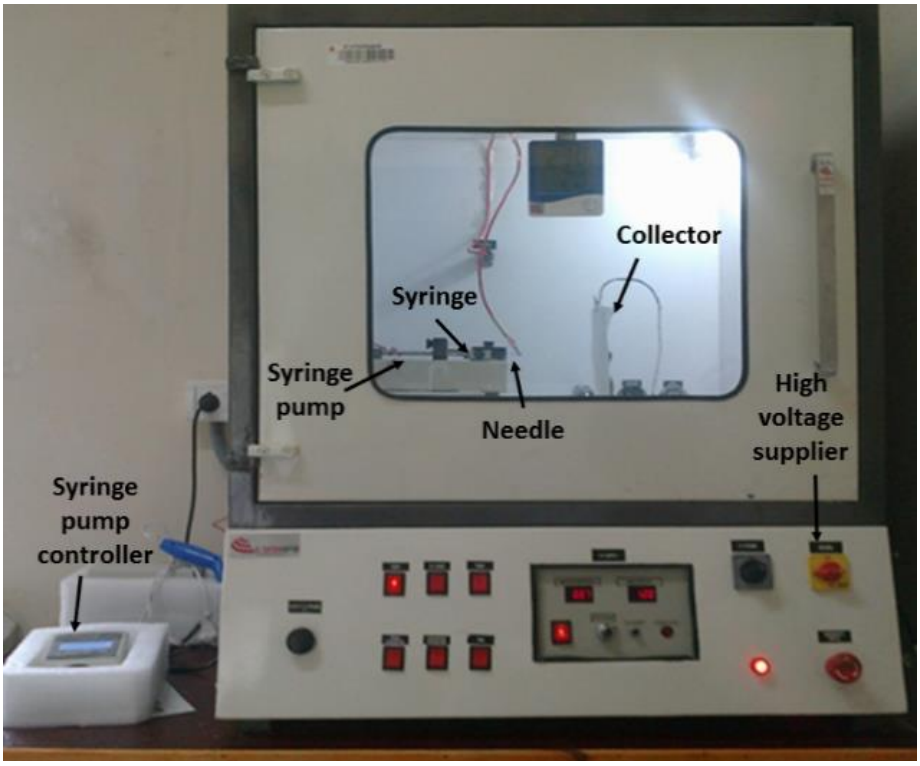

Figure 3.1: Digital image of electrospinning setup

Table 3.1 Effect of electrospinning parameters on fiber morphology

Parameters	Fiber morphology
Polymer solution parameter	
Polymer concentration or viscosity	**Fiber diameter increases with increased viscosity**
conductivity	**Fiber diameter decreases with increased conductivity**
Surface tension	**Initials the jet but no conclusive correlation with diameter**
Solvent volatility	**Porous fibers with increased volatility (higher surface area)**
Process parameter	
Applied voltage	**Fiber diameter decreases with higher voltage**
Distance between tip and collector	**Fiber diameter decreases with longer distance**
Flow rate	**Fiber diameter increases with higher flow rate**
Ambient condition	
Temperature	**Fiber diameter decreases with higher temperature**
Humidity	**Fiber diameter increases with more humidity**

3.4 Materials and Methods

3.4.1 Materials

Gelatin (Type A, 175 bloom), Piperine (98%), Hydrochloric acid (ACS, 36.5-38.0%), Glutaraldehyde (25% v/v aqueous solution), Acetic acid (glacial, ACS, 99.7 +%), Sodium hydroxide pallets (98%), phosphate buffer saline (pH 7.4) were purchased from Alfa Aesar (A Johnson Matthey Company, India). Deionized water (DI) (Milli Q water 18.1 Ω) was used throughout the experiments.

3.4.2 Fabrication of nanofibrous mesh

Preparation of electrospinning solution

Gelatin (Type A) was dissolved in acetic acid solution (20%, v/v in distilled water) at 20% (w/v). The solution was stirred on a magnetic stirrer for 3 h at room temperature to

get a clear and homogenous solution, which was used to prepare gelatin nanofibers (GNF). In the prepared gelatin solution, piperine (2 mg/ml) was added and stirred for 2 h, to prepare piperine loaded gelatin nanofibers (G-P NF).

Electrospinning process

Electrospun nanofibers were prepared using electrospinning apparatus (E Spin Nanotech Pvt. Ltd, India). The spinning solution was transferred to 3 ml of plastic syringe with needle diameter of 21 gauge, by carefully avoiding air bubbles. The syringe was placed horizontally on the syringe pump. The flow rate of the feed solutions were controlled by the syringe pump to ensure homogeneous flow (5 µl/min) throughout the deposition. The electric potential of 12 kV was applied between the tip and the collector from the high voltage power supply, which was kept at a distance of 10 cm. The metal collector was covered with aluminium foil, which was used as a substrate for deposition. The electrospinning process was carried out in the enclosed electrospinning apparatus at 25 °C and 30% relative humidity which was monitored by the digital thermometer and relative humidity sensor (hygrometer) respectively.

3.4.3 Crosslinking of nanofibrous mesh

Electrospun GNF and G-P NF membranes dissolve within few seconds in water, therefore, crosslinking was done by exposing it to saturated vapor of GTA (25% v/v aqueous solution). Both GNF and G-P NF, with and without substrate (i.e., aluminium foil), were cut into 2 × 2 cm^2 sample sizes. These samples were placed inside the closed glass desiccator having 20 ml of GTA solution. Exposure to GTA vapor was performed at room temperature for different time intervals i.e., 2, 4, 6, 8 and 10 min respectively. These crosslinked samples were referred to as GNF CX and G-P NF CX where C referred to crosslinking and X represented the time of crosslinking in minutes.

3.5 *In-vitro* biodegradation study

In accordance with oral delivery systems, pH of release medium was varied as per the gastrointestinal tract (GI) in the human body. The pH of the stomach is pH 1.5-4 due to gastric acids. The pH of the small intestine (duodenum) varies from pH 6-8, where maximum absorption of nutrients takes place. Therefore, pH 1.2, pH 6, pH 7.4 and pH 8 were selected for further *In-vitro* biodegradation as well as release study. *In-vitro* biodegradation study

helped in determining the stability of the cross-linked electrospun mat in different physiological pH solutions. For this study, 5 × 5 cm^2 of electrospun GNF and G-P NF samples, cross-linked over different time intervals, were kept in 25 ml solutions of pH 1.2, pH 6, and pH 7.4, and pH 8 respectively, in a mechanical shaker (Remi RIS-24 plus) for 24 h, at 37 °C and 150 RPM.

Figure 3.2 shows the effect of crosslinking on GNF. Lysine is one of the amino acids present in gelatin, which is responsible for crosslinking with aldehyde group of GTA [133]. After crosslinking, the sample shrinked (Figure 3.2 (b)). Therefore, the membrane was not peeled from the aluminum foil in order to avoid the excessive shrinkage of membrane on crosslinking. Figure 3.2 (a) represents the non-crosslinked GNF membrane with Al foil. The effect of crosslinking and stability of the membrane in aqueous medium is presented in Figure 3.2 (b) and (c) respectively. *In-vitro* biodegradation study was done with the aim to examine the stability of samples up to a period of 24 h. The details of the GNF and G-P NF membranes with different crosslinking time are summarized in Table 3.2. Samples with different crosslinking time (non-cross-linked i.e., 0 min and cross-linked for 2, 4, 6, 8 and 10 min) underwent degradation in different pH (1.2, 6, 7.4 and 8) solutions. Results of the *In-vitro* biodegradation study for electrospun samples cross-linked for 6 min or above were found to be stable even after 24 h in all pH conditions. So, 6 min crosslinking time was selected for further analysis as they were better in comparison to 4 and 8 min crosslinked samples. Although GTA is very effective in crosslinking gelatin and therefore widely used, however, prolonged exposure for up to 24 h as reported in literature [164] may have adverse cytotoxic effects. Here in this work, we exposed gelatin to saturated GTA vapor for crosslinking for only 6 min to achieve the desired stability of the fabric.

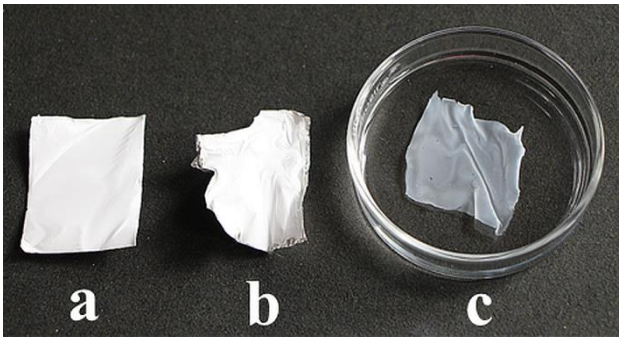

Figure 3.2: Digital images representing, (a) non-crosslinked GNF (b) shrinked GNF C6 and (c) GNF C6 in DI water

Table 3.2: Summary of *In-vitro* biodegradation study for GNF and G-P NF crosslinked over different time interval, in dissolution medium of different pH

pH of dissolution medium	Time of crosslinking with GTA (25% v/v) vapour											
	GNF						G-P NF					
	0	2	4	6	8	10	0	2	4	6	8	10
1.2	-	+	+	+	*	*	-	+	+	*	*	*
6	-	+	*	*	*	*	-	+	*	*	*	*
7.4	-	*	*	*	*	*	-	+	*	*	*	*
8	-	*	*	*	*	*	-	*	*	*	*	*

Where, '-' means completely degraded, '*' means not degraded and '+' refers to partial degradation in the dissolution medium after soaking for 24 h.

3.6 Characterization

3.6.1 Thermal Characterization

Thermogravimetric analysis (TGA) of GNF, GNF C6, G-P NF and G-P NF C6 was carried out using platinum pan in helium atmosphere (pyris 1, Thermogravimetric analyser, Perkin Elmer). The sample weight varied from 5 to 10 mg. Samples were heated from room temperature to 600 °C at a heating rate of 10 °C /min. TGA analysis of electrospun GNF, GNF C6, G-P NF and G-P NF C6 membranes is shown in Figure 3.3. The initial weight loss of 6.6, 7.5, 7.46 and 7.7% for GNF, GNF C6, G-P NF and G-P NF C6 respectively between 35 to 100 °C was due to the elimination of absorbed and bounded water molecules in the membrane. It was very clear that the weight loss is larger in this stage for crosslinked samples (both GNF C6 and G-P NF C6) because of the absorption of water during crosslinking with GTA vapor. However, very interestingly, the difference between weight loss of G-P NF and G-P NF C6 was less because of the presence of hydrophobic drug. The second stage of weight loss, from 250 to 450 °C, corresponded to the thermal degradation of gelatin due to the breakage of the protein chain. For GNF and G-P NF, this was found to be 56.3% and 55.45% respectively, which was later reduced to 43.9% and 46.3% for GNF C6 and G-P NF C6 samples respectively. Thus, crosslinking GNF and G-P NF C6 with GTA vapor, for 6 min, increased the thermal stability and residue percentage as well. Therefore, by improving the water resistive property of GNF and G-P NF mat, GTA increases the thermal stability of GNF and G-P NF membrane.

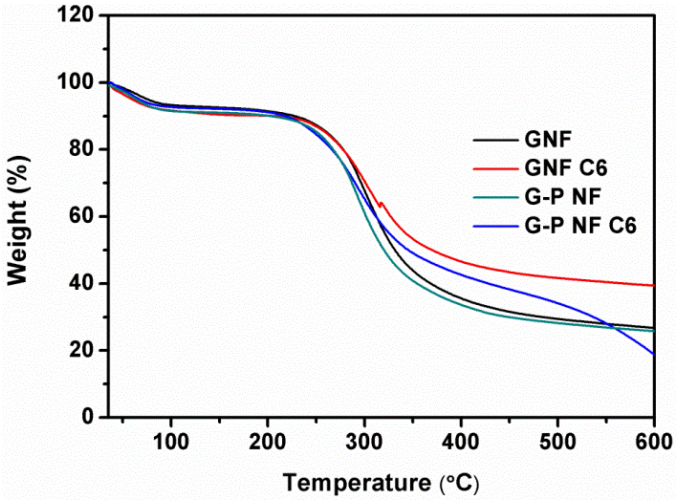

Figure 3.3: Thermogram of GNF, GNF C6, G-P NF, G-P NF C6 membrane

3.6.2 Structural Characterization

The morphology of the GNF and G-P NF, with and without crosslinking samples, were examined using Field Emission Scanning Electron Microscopy (FESEM) (Carl Zeiss, SUPRA 40, Germany) in 10KV. The samples were sputter-coated with gold to reduce the charging effect. The surface morphology of electrospun GNF and G-P NF membrane, with and without crosslinking, is represented in Figure 3.4. SEM micrographs showed continuous, long nanofibers with fiber diameters in the range of 50-200 nm for both GNF and G-P NF as presented in Figure 3.4 (a) and 3.4 (c) respectively.

On crosslinking even for only 6 min, due to its hydrophilic nature, gelatin allows the entry of water molecules along with GTA molecules from the saturated vapor, leading to changes in its morphology. It can be observed that the fibers fuse with one another at contact points (Figure 3.4 (b)), as a result of the partial dissolution of the fiber segments when they come in contact with the moisture-rich GTA vapor [151, 164, 165]. However, in the case of G-P NF, the presence of hydrophobic piperine discourages the interaction between the water molecules of the GTA vapor and the fibers. It leads to relatively less fusing as well as minimal effect on fiber morphology at the point of contact of fibers (Figure 3.4 (d)). Even, from the TGA thermogram results in the range of 35 to 100 °C, it can be observed that the difference between weight loss of G-P NF and G-P NF C6 was less because of the presence of hydrophobic drug. The presence of hydrophobic drug molecules in the matrix repels the water molecules in GTA saturated vapor, and helps to maintain the fibrous structure. Indeed, the

presence of hydrophobic molecules in the polymer matrix protects the nanofiber mesh from unnecessary degradation during its crosslinking with GTA vapor.

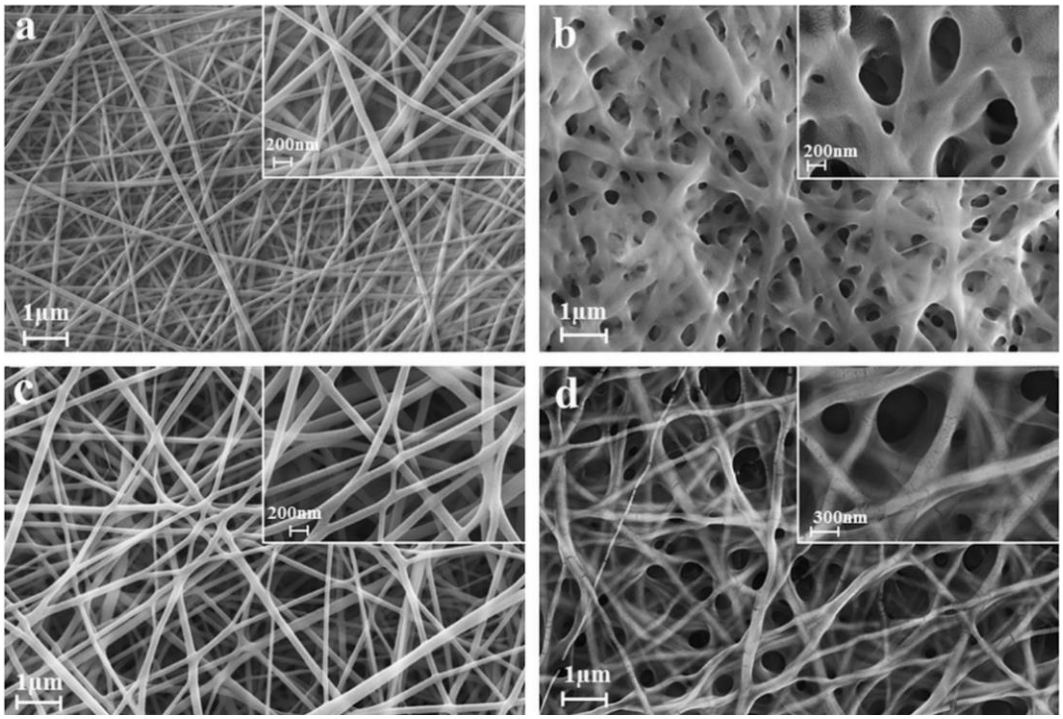

Figure 3.4: FESEM images of electrospun (a) GNF, (b) GNF C6 (c) G-P NF, and (d) G-P NF C6

3.6.3 Specific Surface Area (SSA) measurement and porosity measurements

The Brunauer−Emmett−Teller (BET) surface area of GNF and GNF C6 was determined by N2 physisorption using Micromeritics ASAP 2020 physisorption analyzer (USA). The sample mass was about 100 mg. All samples were degassed at room temperature for 6 h in nitrogen. The SSAs were determined by a multi-point BET measurement with nitrogen as the adsorbate.

To measure the porosity of nanofiber mat, samples were cut in equal pieces (1 × 1 cm^2) and weighed. The thickness of the electrospun mat at a minimum of three different places was measured using digital micrometer (Mitutoyo, Japan). The apparent volume (V_a) was determined using the average thickness of the mat. The volume of the mat (V_g) was determined on the basis of gelatin density (1.41 g cm^{-3}), and piperine (1.193 g cm^{-3}) density and their mass percentage compositions were adapted from [160].

The porosity of the sample was determined using the following equation [160]:

$$\text{Porosity} = [1 - (\frac{V_g}{V_a})] \times 100$$

BET surface area of electrospun GNF was found to be 23.4 ± 1.188 m^2/g. On exposing for 6 min to saturated GTA vapor, the BET surface area decreased to 18.2 ± 1.758 m^2/g. A similar change in the total pore volume was also observed (0.063 ± 0.001 and 0.05 ± 0.001 cm^3/g for electrospun GNF and GNF C6). However, the average pore diameter, as measured by Barrett-Joyner-Halenda (BJH) method, remained almost unchanged to 10.8 ± 0.908 and 10.9 ± 0.551 nm for electrospun GNF and GNF C6 fiber samples respectively. These results reflected in the porosity measurements. For GNF, the porosity was measured to be 89.9 ± 0.336%, which reduced to 83.3 ± 0.984% (with level-p 0.0008) after 6 min of crosslinking. This decrease in surface area, porosity and total pore volume can be explained due to the fusion of fibers in contact with water molecules present along with GTA vapor, as illustrated in Figure 3.4. Similarly as expected for G-P NF, reduction in porosity after crosslinking (6 min) was significantly less (90.2 ± 0.822% to 87.9 ± 0.8% with level-p 0.048) which was also evident from FESEM images in which fiber morphology remained almost intact even after crosslinking. Therefore, the electrospun G-P NF membrane fabricated and used as carrier has a sufficiently large surface area, even after crosslinking with GTA vapor.

3.6.4 Drug-polymer compatibility

Electrospun non-crosslinked and crosslinked GNF and G-P NF were characterized using Fourier Transform Infrared (FTIR) spectrometer (Bruker, Alpha-P, USA). IR spectroscopy was mainly performed using the Attenuated total reflection (ATR) method. Spectra were obtained with 256 scans per sample at a resolution of 4 cm^{-1} between 4000 and 500 cm^{-1}. All the spectra were further processed using OPUS software, which was installed in the instrument system and plotted using Origin Pro 8.

To know the chemical composition, effects of crosslinking, and the interactions between the drug and polymer matrix, FTIR analysis was attempted and represented in Figure 3.5. The absorption bands at 3273 cm^{-1} (N-H stretch), 1631 cm^{-1} (amide I, C=O and C-N stretch), 1536 cm^{-1} (amide II, N-H bend and C-H stretch) and 1237 cm^{-1} (amide III) are the characteristic bands of GNF (Figure 3.5 (a)) [133, 165]. On crosslinking, aldehyde group (-CHO) of GTA reacts with the amino group of lysine, which is present in gelatin, and amino (-NH2) groups interact with the carbonyl groups of GTA to form new covalent (-C=N-) bonds [133]. During the crosslinking, first amide I (C=O and C-N stretching) peak shifts from 1605

cm^{-1} to 1631 cm^{-1} indicating its interaction during crosslinking. Similar trends are also observed in amide II and III peaks of gelatin, which confirm the hydrogen bonding with aldehyde groups of GTA.

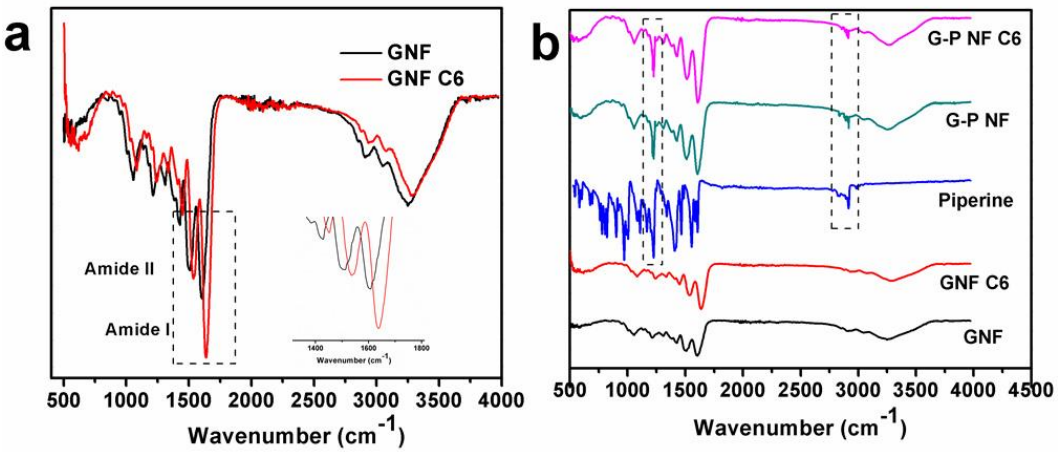

Figure 3.5: FTIR spectra of (a) GNF and GNF C6 (effect of crosslinking). (b) Presence of piperine in polymer matrix and crosslinking effect

Figure 3.5 (b) represents the effect of crosslinking in the presence of piperine. The absorption bands at 2920 cm^{-1} (aliphatic C-H stretching), 1567 cm^{-1} (aromatic stretching of C=C, benzene ring) and 1231 cm^{-1} (asymmetrical stretching of =C-O-C) are the characteristic bands of piperine. The presence of absorption peak due to C-H stretching around 2909 cm^{-1} (G-P NF) and 2919 cm^{-1} (G-P NF C6) are attributed to the presence of piperine in the matrix. Similar peaks are observed due to asymmetric stretching of =C-O- in G-P NF and G-P NF C6 samples. Therefore, one can conclude that piperine was successfully loaded and was found to be stable in both GNF and crosslinked G-P NF samples.

3.7 Drug delivery performance

The release of drug i.e., piperine from electrospun nanofiber mats was measured by placing 5 × 5 cm^2 of drug loaded fiber mat in 10 ml of release medium at different physiological pH levels (1.2, 6, 7.4 and 8). The temperature and the stirring of the system were maintained at 37 °C and at 50 RPM, respectively. An aliquot sample was withdrawn at fixed time intervals, and the same amount of fresh solution was added back to the release medium to maintain the sink condition. The samples were centrifuged (Wise Spin, CF-10) for

2 min at 1300 RPM and analyzed using a UV spectrophotometer (Perkin Elmer Lambda 35, USA) at 342 nm as λ_{max} for piperine. The results were presented in terms of cumulative release as a function of time:

$$\text{Cumulative amount of release (\%)} = \left(\frac{C_t}{C_\infty}\right) \times 100$$

Where, C_t is the amount of piperine released at time t and C_∞ refers to total amount of drug loaded in 5 × 5 cm^2 sample. Standard curve for piperine in PBS is shown in Appendix C.

The release of the drug from a polymer matrix is modulated by the diffusion of the drug and / or degradation of the polymer matrix. Insufficient physical and chemical interactions (as evident in the FTIR study) between the hydrophobic drug molecules and the hydrophilic polymer matrix lead to the sudden release of drug molecules from the surface within few hours. As the crosslinked G-P NF membrane swells, due to presence of water molecules, the osmotic pressure provides the driving force for release of the drug in the release medium. Therefore, after 2 h, there is sustained release of the drug as it diffuses to the release medium through the carrier gradually.

3.7.1 Effect of pH value of release medium

Studying and controlling the drug release at different pH is an important consideration for designing a vehicle for the oral route. As drug molecules need to follow the GI tract and should be absorbed in the small intestine, we need to examine release profiles from harsh acidic conditions to basic environments. In this work, *In-vitro* drug release studies were performed in different pH conditions as per the human GI tract environment i.e., pH 1.2 (stomach), pH 6 (duodenum), pH 7.4 (small intestine) and pH 8 (large intestine) as shown in Figure 3.6. The drug concentration (μg/ml) Vs time (min) data is presented in Appendix B (Table B3).

The various cross-linked G-P NF membranes i.e., 4 min, 6 min and 8 min, were referred to as G-P NF C4, G-P NF C6 and G-P NF C8 respectively. For G-P NF C4, piperine release percentage was 95.7 ± 3.58%, 90.52 ± 3.136%, 82.76 ± 5.96%, 77.76 ± 2.98% (Figure 3.6 (a)) while for (G-P NF C6), drug release percentage was significantly decreased to 87.70 ± 2.08% (with level-p 0.0005) , 85.57 ± 2.94% (with level-p 0.002), 77.56 ± 5.83% (with level-p 0.002) and 72.56 ± 3.439% (with level-p 0.013) for pH 8, pH 7.4, pH 6 and pH 1.2 respectively (Figure 3.6 (b)). We observed that the total amount of drug release was less in

the solution with pH 1.2, compared to higher pH, irrespective of crosslinking time. This may be due to the protonation of hydrophilic groups of the polymer matrix in acidic pH, which discourages formation of H-bonds with water molecules resulting in less swelling of the membrane [166]. If the matrix does not swell much, drug molecules will not get enough osmotic pressure, which help in reducing the drug release amount. However, in alkaline pH, hydrophilic groups form more H-bonds with the release medium, which invites more water molecules inside the carrier, leading to better swelling and more drug release in the dissolution medium. Similarly, when compared to G-P NF C6 and G-P NF C8, after 24 h, the piperine release decreased significantly 72.70 ± 8.15% (with level-p 0.012), 65.51 ± 4.59% (with level-p 0.024), 62.56 ± 0.41% (with level-p 0.008) and 58.56 ± 3.57% (with level-p 0.007), for pH 8, pH 7.4, pH 6 and pH 1.2 respectively, demonstrating the above explanation.

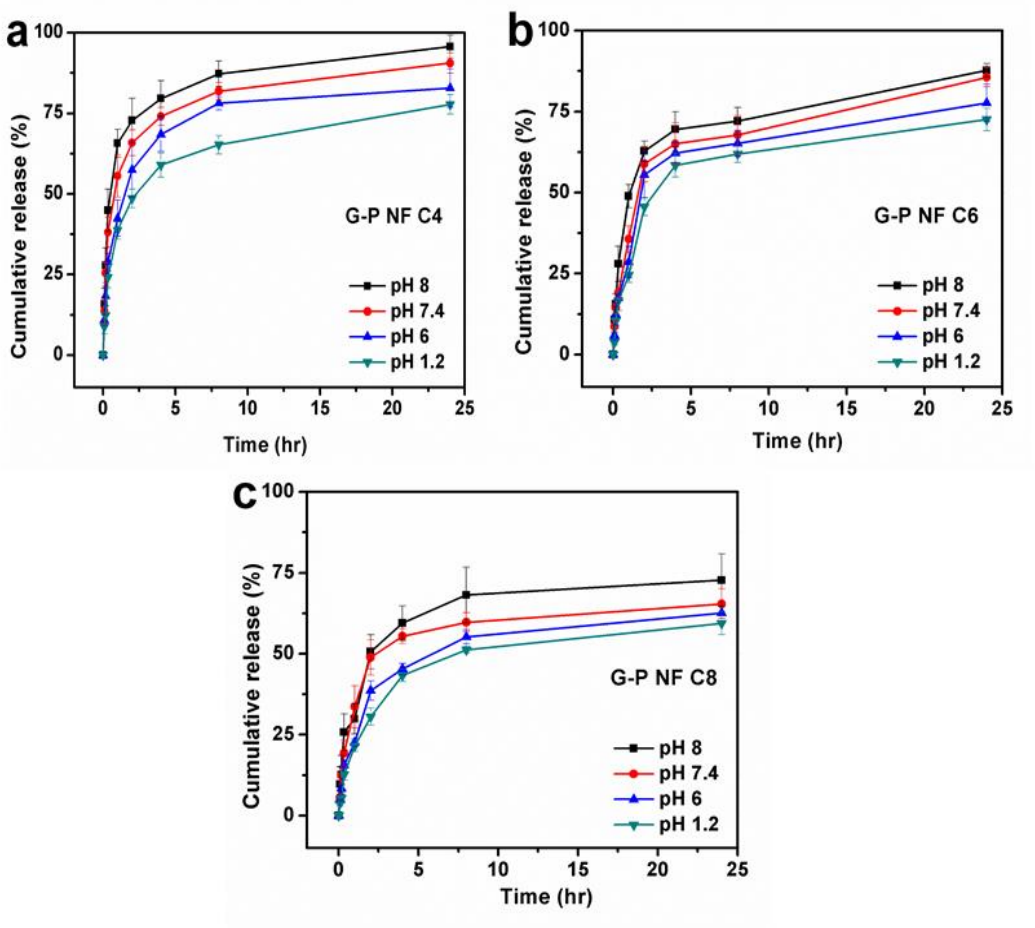

Figure 3.6: Cumulative *In-vitro* release profiles of piperine for (a) G-P NF C4, b) G-P NF C6 and (c) G-P NF C8 in different pH (1.2, 6, 7.4 and 8)

3.7.2 Effect of crosslinking time

With the increase in the crosslinking time from 6 to 8 min, the large amount of drug release in pH 1.2 was controlled. Our main objective was to release the maximum amount of drug in higher pH (7.4, 8) i.e. pH of small intestine, where drug would be absorbed. In the release medium of pH 1.2, the figures for drug release, within 2 h, for G-P NF C4, G-P NF C6 and G-P NF C8 are approximately 48.5 ± 2.92%, 45.5 ± 2.65% and 30.5 ± 2.63% of the total drug respectively (Figure 3.7 (a)). Further, the drug release amount decreases significantly from 72.6 ± 3.43% in G-P NF C6 to 58.5 ± 3.57% (with level-p 0.007) in G-P NF C8, after 24 h release in pH 1.2. Therefore, increasing crosslinking time significantly decreases the release percentage of the drug.

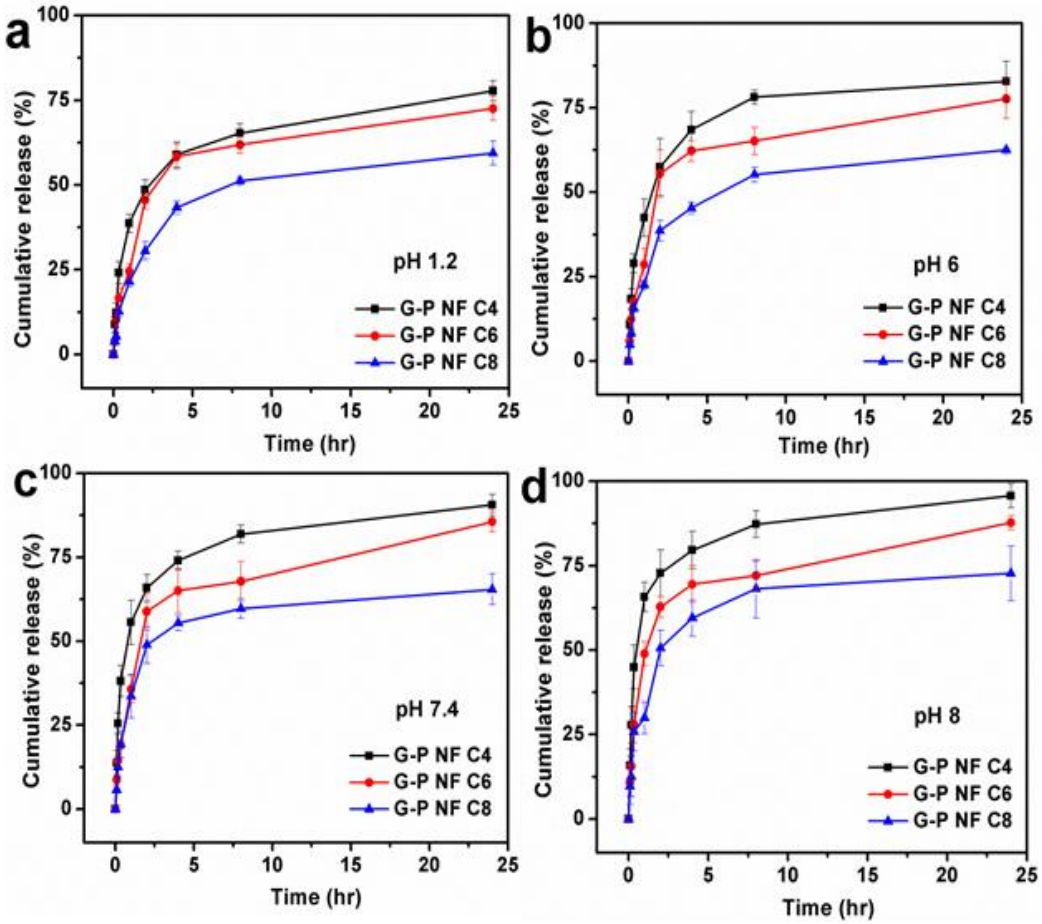

Figure 3.7: Cumulative *In-vitro* release patterns of piperine for different crosslinking time (G-P NF C4, G-P NF C6, and G-P NF C8) in (a) pH 1.2. (b) pH 6 (c) pH 7.4, and (d) pH 8 release medium

Similar control over the release percentage was obtained for pH 6, pH 7.4 and pH 8 for both initial fast release and prolonged sustained release as shown in Figure 3.7 (b)-(d). Therefore, by manipulating the crosslinking exposure time from 4 to 8 min, we can engineer the inter-fibrous porosity, which may result in sustained release of the drug molecules. In addition, from the release study we can conclude that the vehicle is capable of protecting the drug from the harsh conditions (pH 1.2) of the GI tract, and is able to release at the absorption site, i.e., small intestine, in a sustained manner.

3.7.3 Drug release mechanism

To understand the drug release kinetics and the mechanisms, the obtained data from *In-vitro* study was analyzed using mathematical models. The most common equation to describe polymeric DDS is known as Higuchi equation:

$$\frac{M_t}{M_\infty} = k_H\sqrt{t}$$

Where, M_t and M_∞ = absolute cumulative amount of drug released in time t, and final respectively, and k_H is a dissolution constant [134, 135]. The classical Higuchi model and respective Higuchi dissolution constants are presented in Table 3.3. It is a very clear indication that diffusional force plays the major role in drug delivery. K_H is a constant, which indicates the characteristics of polymer matrix network. In addition to that, with the decrease in K_H value the cumulative release of drug deceases. Naturally, when the decrease in K_H values were found for all the cases, this indicates increase in the diffusional barrier means decrease in drug release. The probable reason behind the increased diffusional barrier is the diffused and packed fiber structure, which also reduces the drug molecule penetrability through the matrix. With increase of crosslinking time, K_H value has decreased. Porosity, morphological images, and the release-study data supports these observations. The K_H value can be a good indicator for required drug release profile. The crosslinking can be modified according to required treatment.

Table 3.3: List of drug release co-efficient fitted in Higuchi Model.

Release Model	**Samples (6 min)**				
		pH 1.2	**pH 6**	**pH 7.4**	**pH 8**
Higuchi Model	**K_H**	**0.036**	**0.037**	**0.045**	**0.0588**
	R^2	**0.9776**	**0.9846**	**0.9949**	**0.9892**

3.8 Statistical analysis

Data was analyzed with t-test to compare the difference between two treatment means. The null hypothesis says that the means of the different measurement variables (or populations) are equal (no differences/no effects) for the two treatments. Results were recognized as statistically significant at the level of $p<0.05$. The observations are presented as mean ± standard deviation (SD) of three independent experiments to confirm reproducibility of the findings. All the plots were analyzed using Origin Pro 8 software.

3.9 Discussion

These newly developed electrospun gelatin nanofibers based DDS showed better control on release in different physiological pHs compared to other reports [164-166]. This is summarized in Table 3.4

As mentioned earlier, there is only one report on the release of hydrophobic drug from electrospun gelatin nanofibers. Even in that report [160], the release study was done only at a given pH of 7.4. Additionally, there was either an initial burst release (75% release in first 24 h) or very slow release (35% release in five days with 22% release in first 24 h). Further, as the Table 3.4 shows, all previous reports, based only on electrospun gelatin nanofibers, focus either on the delivery of the hydrophilic drug [161-163], or cross linking is done for prolonged time (up to 24 h) [160-163], or there is a unwanted signature of initial burst release [160-162]. Clearly, the present work addresses most of these challenges as confirmed by *In-vitro* drug release studies discussed above and suggests that controlled crosslinking plays a very important role in the porosity of the matrix with minimal effect on fiber morphology. This in turn essentially helps us to get stable, sustained, and controlled release of the hydrophobic drug, with highly porous electrospun gelatin nanofiber matrix as a delivery vehicle.

Table 3.4: A comparison of the present work with drug release profile from electrospun gelatin nanofibers reported in literature

Crosslinker/time of cross linking	Drug/Nature	Solvent	Remarks	Ref
Polyethylene glycol-diacrylate/ 30 min	**Nystatin/ Hydrophobic**	**HFP**	**(i) Drug release study only at pH 7.4 (ii) Fiber diameter: Few microns (iii) Initial burst release (75% in 24 h)**	**[160]**
Proanthocyanidin , GTA/45 min	**MAP/ Hydrophilic**	**Formic acid**	**(i) PVA is added in gelatin for producing nanofibers (ii) Prolonged exposure to GTA (iii) Initial burst release (65% in 1 h)**	**[161]**
NHS, EDC/24 h	**Cefradine/ Hydrophilic**	**Water and ethanol**	**(i) Use of ethanol as solvent (ii) Prolonged crosslinking (iii) Initial burst release (50% in 4 h)**	**[162]**
GTA/24 h	**Heparin/ Hydrophilic**	**Aqueous acetic acid**	**(i) Prolonged exposure to GTA (ii) Drug release only at pH 7.0 (iii) Slow release**	**[163]**

3.10 Summary

Electrospun gelatin nanofibers were fabricated and exposed to saturated GTA (25% v/v) vapor for crosslinking. Interestingly, only 6 min of exposure was sufficient to control the degradation. Besides increasing water resistivity, crosslinking also improved the thermal stability of the membrane. The presence of hydrophobic drug molecules in the matrix, significantly reduced fiber fusion while crosslinking with saturated vapor of GTA. The electrospun gelatin nanofiber based system showed bi-phasic release profiles such as initial fast release of drug followed by sustained release. This system also showed pH sensitivity, which is favorable in case of orally administration of drug. The drug release was slowed down

in lower pHs which reduced drug loss extensively and the release of maximum drug in intestine (in high pH) was desirable. The pictorial representation of this work is shown in Figure 3.8. In brief, these electrospun gelatin fibers can be considered to be viable drug-carriers for the model hydrophobic drug i.e., piperine.

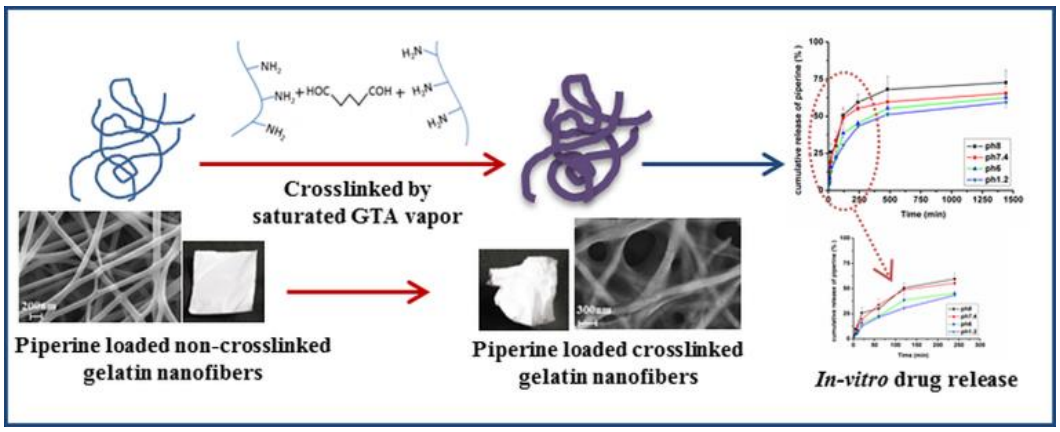

Future 3.8: A pictorial representation of fabrication, crosslinking and *In-vitro* drug release study of gelatin nanofiber based DDS

3.11 Highlights of this work and motivation for the next chapter

Gelatin nanofiber based DDS have the potential to act as an effective DDS due to the following reasons.

1. Piperine is stable in a hydrophilic electrospun GNF carrier, which is similar to GCF.
2. This GNF drug-carrier is crosslinked with saturated vapor of GTA only for 6 min. This certainly reduces the amount of GTA in the vehicle and perhaps reduces the toxic effect associated with it as well. The drug release can be modulated through the duration of crosslinking of the carrier.
3. The *In-vitro* release study shows sustained release of piperine in different physiological pHs over a duration of 24 h. The system exhibits better control over initial fast release control compared to GCF.
4. Electrospun gelatin fiber based DDS is a pH sensitive drug-carrier. Thus, drug release in lower pH is lesser compared to higher pHs, which signifies its potential as a targeted or site-specific drug-carrier.

Despite meeting several points from the main objectives of the thesis mentioned in chapter 1 and section 1.6, this nanofiber based DDS does not show zero-order release of drug. Zero-order drug release, which can maintain the drug concentration within therapeutic window, is highly desirable. Thus, to improve or to reduce the initial fast release of these kinds of biphasic profiles, we have employed different strategies, which have been discussed in the next chapter.

Chapter 4

Fabrication of Multi-layered Gelatin Nanofibers based DDS

4.1 Introduction

Chapter 3 demonstrated the fabrication of the single-layered. piperine loaded, electrospun gelatin nanofibers (GNF) based carrier, and the achievement of sustained release to some extent, as per the gastrointestinal (GI) tract conditions, by controlling the swelling and crosslinking. The high porous structure of nanofibers facilitated in crosslinking the fiber based DDS using saturated vapor of GTA [133]. The GNF based carrier was crosslinked through merely a few minutes of GTA exposure (6 min) instead of a few hours or even days as reported in literature [161-164]. Naturally, this promises a tremendous possibility of reducing the risk of toxicity caused by GTA. In addition, the *In-vitro* drug release study showed a typical biphasic curved profile for all the cases i.e. a sudden release of drugs during initial hours followed by a much slower release during the rest of the observed time scale. The probable reason for this kind of common release pattern could be the penetration of water molecules in the vehicle, which caused swelling of the matrix. This kind of profile can be used for specific treatment purposes where only initial release of the drug is required [90, 140, 167, 168]. However, in general, this type of release profile can potentially cross the toxic drug-

concentration level within the initial hours and sub-therapeutic drug concentration in later part [1, 2, 169]. As a known bio-enhancer, piperine helps in enhancing the bio-availability of other drugs by boosting the absorption from the intestine [128]. Therefore, releasing piperine in the intestine is beneficial. This awareness motivated us to further modify the existing electrospun GNF vehicle by introducing multi-layered sandwiched mesh structure, in order to achieve close to zero-order/controlled release in the intestine. The fabrication and sequence of deposition layers play important roles in the overall mesh thickness and porosity, which may affect the sustained and controlled release profiles [170, 171]. In order to achieve zero-order release profiles, eventually, the concept of multi-layered electrospun fibers was developed. We assumed that, by increasing the diffusional path between the drug and dissolution medium, the system might show better control in release [172, 173].

The idea behind preparing multi-layered electrospun mesh is to get sustained molecular release for a prolonged time by controlling the drug mobility. By sandwiching the drug-loaded layer between two adjacent electrospun layers, the kinetics of water uptake can be controlled, which in turn promotes the sustained release of drug molecules through precise control in both degradation as well as osmotic pressure [172, 173]. However, to the best of our knowledge, there is no such study being performed for hydrophobic drugs, the delivery of which is a challenge for any biodegradable polymer. In this study, piperine was incorporated into a sandwiched GNF mesh with variations in barrier and core layer thicknesses. The effect of drug concentration and sequential crosslinking on the release profile was also investigated. Therefore, the objective of this work is to regulate the release profiles in such way so that we can achieve almost zero-order release (without initial burst release) of piperine for nearly 48 h from this newly developed vehicle.

4.2 Materials and Methods

4.2.1 Materials

Gelatin (Type A, 175 bloom), piperine (98%), hydrochloric acid (ACS, 36.5-38.0%), glutaraldehyde (25% v/v aqueous solution), acetic acid (glacial, ACS, ~99.7%), sodium hydroxide pallets (98%) and phosphate buffer saline (pH 7.4) were purchased from Alfa Aesar. Deionized water (DI) (Milli Q, resistivity 18.1 MΩ.cm) was used throughout the experiments.

4.2.2 Fabrication of nanofiber membrane and crosslinking

Multi-layered meshes were prepared by electrospinning 20% (w/v) of Gelatin (Type A) solution in acetic acid (20% v/v in distilled water) solvent using electrospinning apparatus (Make: E Spin Nanotech Pvt. Ltd, India). Then, a known amount of piperine was added to spinning solution for drug loaded samples (G-P NF). Multi-layered GNF was prepared by sequential electrospinning, with and without the use of drug loaded solutions, on the substrate (aluminium foil). The samples were then crosslinked using saturated vapor of GTA (25% v/v aqueous solution) for a few minutes (6 and 8 min; i.e. G-P NF C6 and G-P NF C8 respectively) following a similar method discussed in chapter 3 section 3.3.3.

4.3 *In-vitro* biodegradation study

In-vitro biodegradation studies were carried out to check the stability of the crosslinked membranes (G-P NF C6 and G-P NF C8) in pH 7.4. Samples were cut (5 × 5 cm^2) and then weighed (M_i). Dried samples were placed in 50 ml of PBS solution (pH 7.4) at 37 ^OC for 48 h. The samples were taken out at a predetermined time interval and dried in a vacuum oven at room temperature and weighed again (M_f). The weight loss (WL %) due to hydrolytic degradation was calculated by using the following equation [160]:

$$\text{Weight loss (WL \%)} = \left(\mathbf{1} - \frac{\mathbf{M_f}}{\mathbf{M_i}}\right) \times \mathbf{100}$$

Where, M_f = Sample mass after an incubation period. M_i = Initial sample mass.

Similarly, swelling study was done in 50 ml of PBS solution (pH 7.4) at 37 ^OC for 48 h. Swelled samples (W_s) were weighed and placed back in the solution. Each time, the samples were dried using tissue paper to remove excessive surface water. Swelling degrees (SD) were calculated using the following equation [160]:

$$\text{Swelling degree (SD \%)} = \left(\frac{\mathbf{W_s - W_d}}{\mathbf{W_d}}\right) \times \mathbf{100}$$

Where, W_s = Weight of swelled sample and W_d = Initial weight of dried sample.

To understand the effect of crosslinking on G-P NF samples; *In-vitro* degradation study and swelling study were performed. Figure 4.1 shows, G-P NF C6 and G-P NF C8 both were quite stable with a time scale of 48 h in pH 7.4. The weight losses (%) of G-P NF C6 and G-P NF C8 in PBS (pH 7.4) solution were 13 ± 2.5% and 10 ± 0.6% respectively, after

24 h. Figure 4.1 shows, the swelling degree for G-P NF C6 and G-P NF C8 were 831.1 ± 23.4 % and 716.2 ± 11.1 % respectively after 24 h. So, with the increase in crosslinking time, naturally the swelling degree decreases [160]. The lower swelling degree and lesser degradation in PBS medium for G-P NF C6 and G-P NF C8 was due to lower porosity because of denser crosslinked matrix [160]. Similarly, stability of 6 min and 8 min crosslinked samples in pH 1.2 for 24 h has already been reported in chapter 3, section 3.4. Results confirmed that as the swelling was less, the degradation was also negligible in pH 1.2. Thus, it can be concluded that 6 min of crosslinking is good enough in terms of stability in aqueous medium which is similar to the case of single-layered nanofiber DDS. So, we finally selected 6 min of crosslinking time for further studies. In addition, this confirmed lower GTA exposure and minimization of potential toxicity.

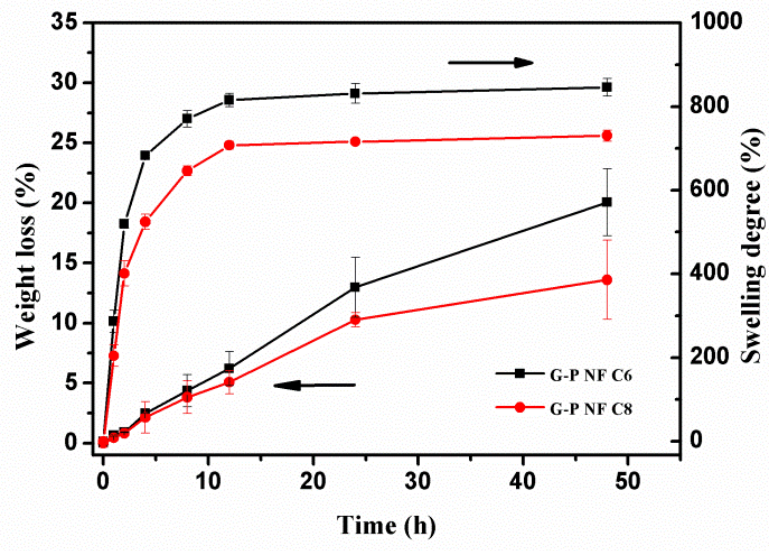

Figure 4.1. Weight loss (%) and swelling degree (%) of G-P NF C6 and G-P NF C8

4.4 Characterization

4.4.1 Thermal characterization

Thermal stability of the vehicle was investigated by thermogravimetric analysis (TGA) (Model: Pyris 1, PerkinElmer Inc., USA) in helium atmosphere in the range from 35 to 600 ^{O}C at a heating rate of 10 ^{O}C /min. The inert gas (helium) in purer form with minimal moisture helped to get perfect thermograms for gelatin. TGA thermograms and its first order derivative curves (DTG) of G-P NF C6 and G-P NF (from 35 to 700 ^{O}C) are presented in Figure 4.2.

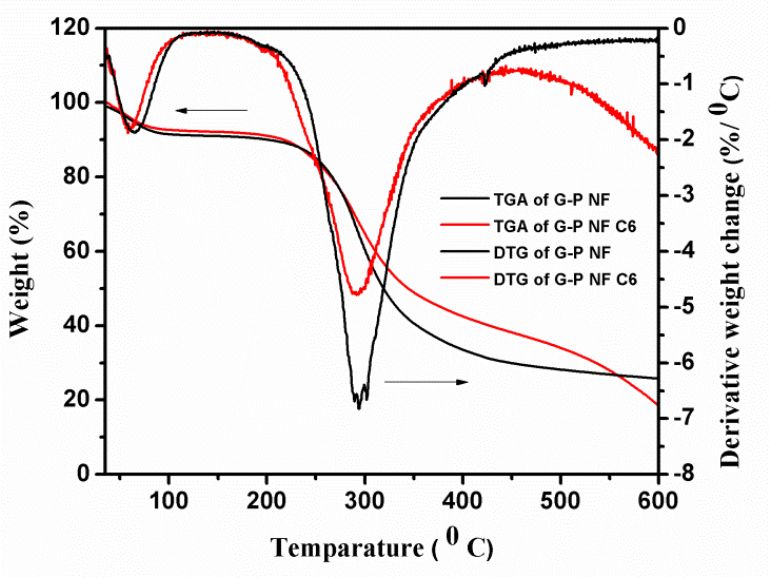

Figure 4.2. TGA and DTG thermogram of G-P NF and G-P NF C6

TGA thermograms of gelatin film showed two stage weight loss in this range which also reflects results similar to the single-layered sample discussed in chapter 3, section 3.5.1. Initial weight loss percent (between 35 to 100 ^{O}C) was less which usually accounted for the presence of moisture in the fiber. A sharp fall of the curve was clearly visible in the range of 250 to 450 ^{O}C which was associated to the decomposition of gelatin due to the breakage of protein chain. While comparing the thermal behavior of G-P NF C6 and G-P NF, weight loss for G-P NF was observed to be higher than the G-P NF C6. This confirmed the thermal stability of the G-P NF C6 sample. DTG thermogram also showed a shift of maximum decomposition in the regions towards higher temperature (290 to 297 ^{O}C) which was a good indication of improved thermal stability upon crosslinking. Weight loss for G-P NF C6 was found to be less in comparison to G-P NF, which was a reflection of improved thermal stability upon crosslinking.

4.4.2 Structural characterization

The morphology of the fibers were examined by table top Scanning Electron Microscopy (SEM) (Make: Phenom world ProX, Netherlands). To reduce the charging effect, samples were coated with thin gold layer using sputter coater (DC Sputtering system, Make: Excel Instruments, India).

The surface morphology of electrospun G-P NF, G-P NF C6, G-P NF C8 samples are represented in Figure 4.3. Randomly oriented continuous piperine loaded GNF are presented in Figure 4.3 (a). Due to the large surface area-to-volume ratio of the GNF mesh, the

hydrophilic matrix were crosslinked with saturated vapor of the GTA solution. Due to the highly porous nanostructured hydrophilic polymer mesh, the mesh tended to immediately dissolve in contact with water molecules. Therefore, the membranes were crosslinked with saturated vapor of GTA for 6 and 8 min, presented in Figure 4.3 (b) and 4.3 (c). Water molecules present in saturated vapor had partially degraded the fibers and fused them together as shown in Figure 4.3 (b) and 4.3 (c) (more compact morphology).

The partial degradation due to swelling of fibers was commonly visible in the case of gelatin nanofibers which has been presented in chapter 3, section 3.5.2. Due to the presence of hydrophobic molecules (piperine in this case) in the gelatin mesh, the fusions of fibres were substantially less. This fused structure of the nanofiber membrane can tailor the release of drug molecules according to the release medium.

From the histogram Figure 4.4, it was evident that with crosslinking, GNF fuse with each other and therefore there was a slight shift towards increased average fiber diameter from non-crosslinked to crosslinked (6 and 8 min) samples respectively.

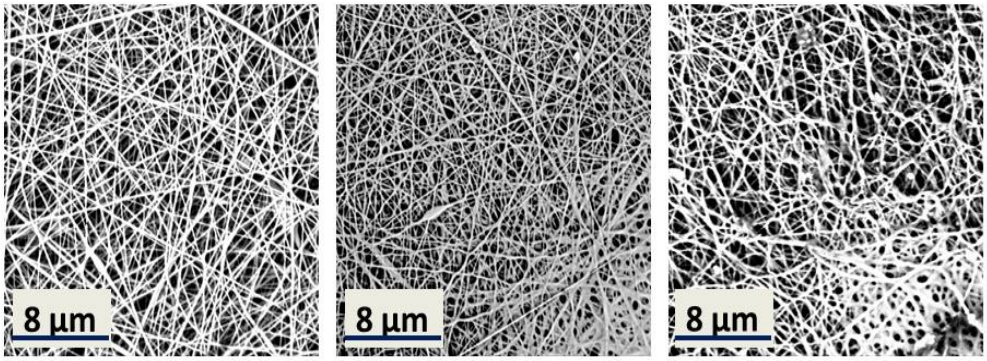

Figure 4.3. Morphology of the electrospun fiber membrane of a) G-P NF, b) G-P NF C6 and c) G-P NF C8

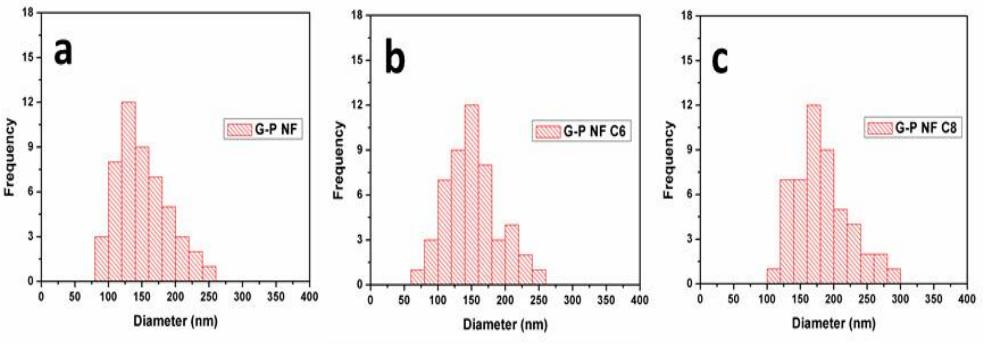

Figure. 4.4. Histograms showing the fiber size distribution of electrospun membrane of a) G-P NF, b) G-P NF C6 and c) G-P NF C8

4.4.3 Drug-polymer compatibility

To investigate the presence of the drug, drug-polymer compatibility and the effect of crosslinking on the mesh, samples were characterized by Fourier transform infra-red spectroscopy (FTIR, Bruker Tensor 37, USA) in the 4000-400 cm^{-1} range with a resolution of 4 cm^{-1} and 256 scans per sample. The crosslinking effects on nanofibers and the co-existence of both drug and polymer with their own characteristic identity were confirmed from Figure 4.5.

The FTIR spectra showed the characteristic absorption bands of gelatin at 3270 cm^{-1} (N-H stretching), 1628 cm^{-1} (amide I, C=O and C-N stretching), 1548 cm^{-1} (amide II, N-H bend and N=C stretch) and 1234 cm^{-1} (amide III, weak N=C stretch, N-H bend) [164]. Absorbance peaks for piperine were at 2920 cm^{-1} (aliphatic C-H stretching), 1567 cm^{-1} (aromatic stretching of C=C, benzene ring) and 1231 cm^{-1} (asymmetrical stretching of =C-O-C). During the crosslinking of fibers using GTA vapor, the first amide (due to C=O and C-N stretching) peak shifted, which was an indication of new covalent bonding. Similar shifting of amide II and III peaks indicated the interaction between the amino group of gelatin and the aldehyde groups of GTA. The presence of piperine peaks in comparison to pure gelatin nanofibers and the preservation of all other characteristic peaks of gelatin have shown the presence of piperine in G-P NF C6 membrane. In a nutshell, the presence of amide peaks of gelatin around 1628 cm^{-1} and aliphatic C-H stretching of piperine around 2920 cm^{-1} proves the presence of piperine in gelatin nanofiber mesh. The results showed that modifying the drug-carrier from single-layered to multi-layered, the properties of drug in the matrix remained intact.

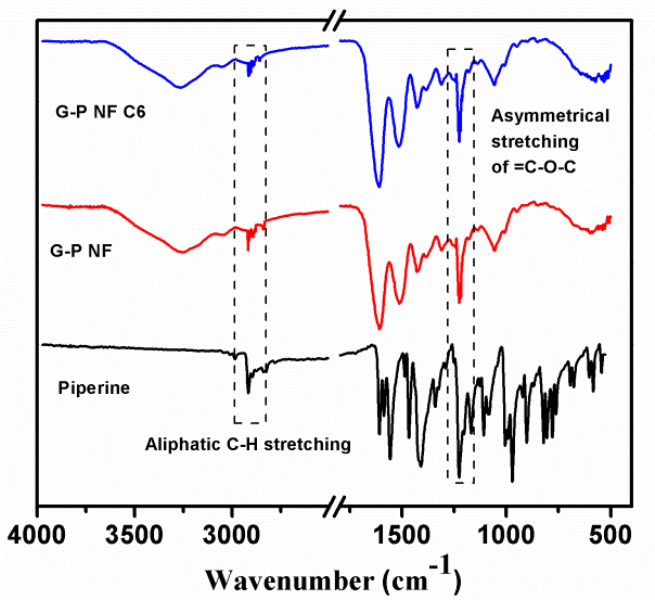

Figure 4.5. FTIR spectra of G-P NF C6, G-P NF and piperine

4.5 Drug release performance

After investigating the different aspects of the vehicles such as the drug-polymer interactions, thermal stability, swelling and degradation study in aqueous medium, *In-vitro* drug release was done in order to design a nanofiber based vehicle which can provide constant drug release for a prolonged period of time. The intention of this study was to develop a drug delivery vehicle, which can provide a near to zero-order release profile in different physiological pH. Thus, we started modifying our existing single-layered vehicle which could successfully circumvent the two stage release profile.

4.5.1 Effect of multi-layer on release profile

First, we attempted to design a vehicle with sufficient diffusional barrier which can exhibit a close to zero-order release without initial fast release of drug molecules. To meet the aforementioned release profile for cases with appreciable drug loading, we fabricated different types of sandwiched structured multi-layered mesh by coating drug loaded layers with two sequential layers of gelatin as shown in Figure. 4.6 and Table 4.1. The drug concentration (µg/ml) Vs time (min) data is presented in Appendix B (Table B4).

Table 4.1: Summary of the configuration of sandwiched electrospun nanofiber membrane

Cases	Composition G-(G+P)-G (layers) (ml)	Remarks based on the drug release profiles (Figure 4.7)
A: G-P NF C6/4/0.5	**(0.5+4+0.5)=5ml**	**1. G Barrier is very less (0.5 ml).** **2. G+P is sufficient (4 ml)**
B: G-P NF C6/3/1	**(1+3+1)=5ml**	**1. G Barrier better than A.**
C: G-P NF C6/2/1.5	**(1.5+2+1.5)=5ml**	**1. G Barrier is improved (1.5 ml)** **2. G+P is less (2 ml)**
D: G-P NF C6/1/2	**(2+1+2)=5ml**	**1. Good diffusional barrier (2 ml)** **2. Very less drug loading (1 ml)**
E: G-P NF C6/4/2	**(2+4+2)=8ml**	**1. Combining A and D** **2. Good amount of drug loading (4ml)** **3.Sufficient diffusional barrier (2ml)**
F: G-P NF C6/4/3	**(3+4+3)=10ml**	**1. Further improved sample E by adding extra diffusional barrier (3ml)** **2. Drug loading is same (4ml)**

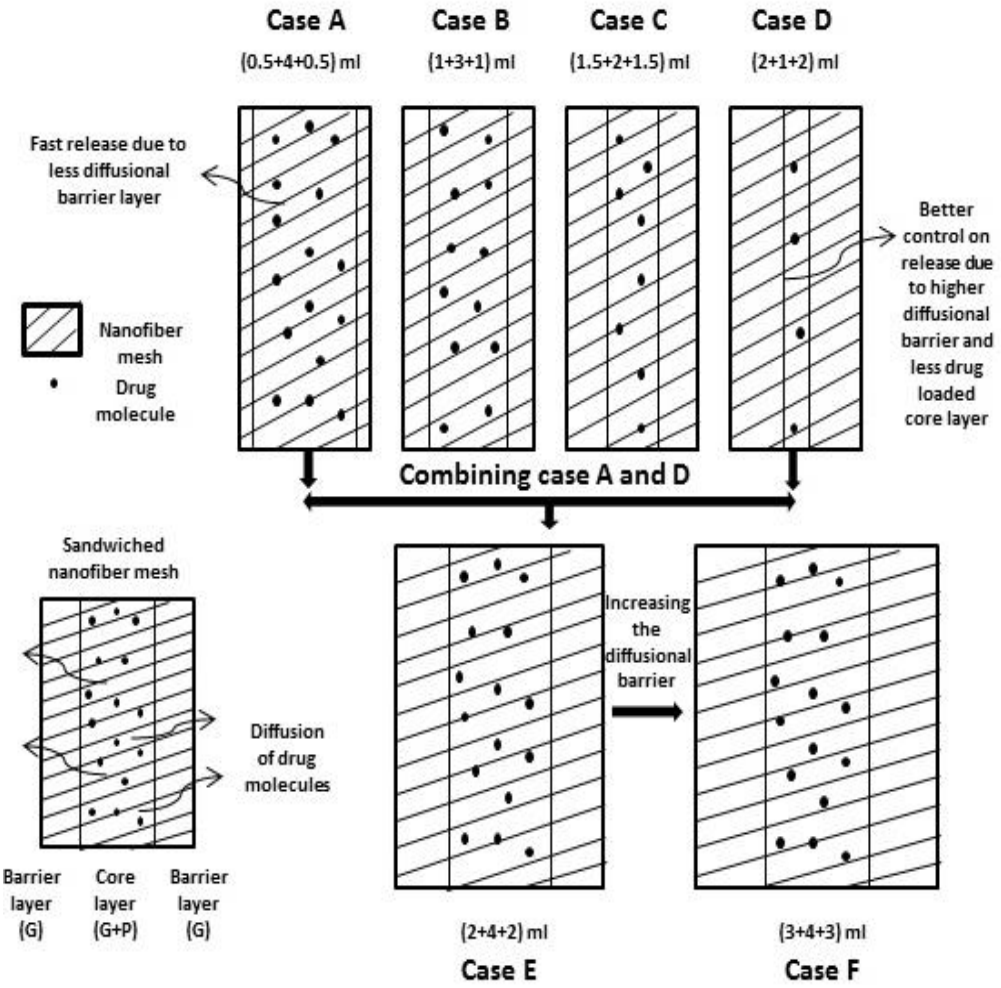

Figure 4.6. Schematic presentation different composition of sandwiched nanofiber mesh

As a starting point, 5 ml of polymer solution was deposited to fabricate four different sandwiched structure i.e. A to D (Table 4.1 and Figure 4.6). Figure 4.7 (a) shows tht the initial fast release of drug (within 4 h) for the first four cases (A to D) decreased (A: 52.0 ± 5.5% to D: 15.6 ± 3.7% within 4 h) drastically with an increase of diffusional barrier from 0.5 ml to 2 ml in both sides of the core layer. On the other hand, the core layer had gradually decreased (4 ml to 1 ml) affecting overall the release profile particularly for case D. Therefore, we combined both A and D formulations to design a new formulation E (total solution 8 ml) shown in Table 4.1 and Fig. 4.6. Thus, the new formation E consist of 4 ml core layer similar to sample A, and 2 ml barrier layers from both sides similar to sample D. More control on the mobility of drug molecules was noticed with this newly fabricated sample E. From Figure 4.7 (a), it was observed that case E had sufficient control over initial release during the first

4h with an appreciable overall release in 24 h. Further, to fine-tune the initial fast release of the drug molecules, additional barrier layers were added to sample E, which resulted in the fabrication of sample F shown in Table 4.1 and Figure 4.6. In that case, a total of 10 ml polymer solution was deposited to fabricate the membrane with enough drug loaded core (4 ml) and good diffusional barrier (3+3 ml) to control the release profile (Sample formulation: F). The sample formulation F is highlighted in the Table 4.1. Figure 4.7 (a) shows that the release profile for sample F exhibited a good control over the mobility of drug molecules and also exhibited sustained drug release (22.5 ± 6.5% in the initial 4 h; total 55.9 ± 2.9 % in 24 h). Thus, further investigation was done with sample F to check the effect of pH (pH 1.2, 6.8 and 7.4; similar pH profile of human GI tract) and the effect of drug concentration (1.5, 2, 2.5, and 3.5 mg/ml) on release profiles.

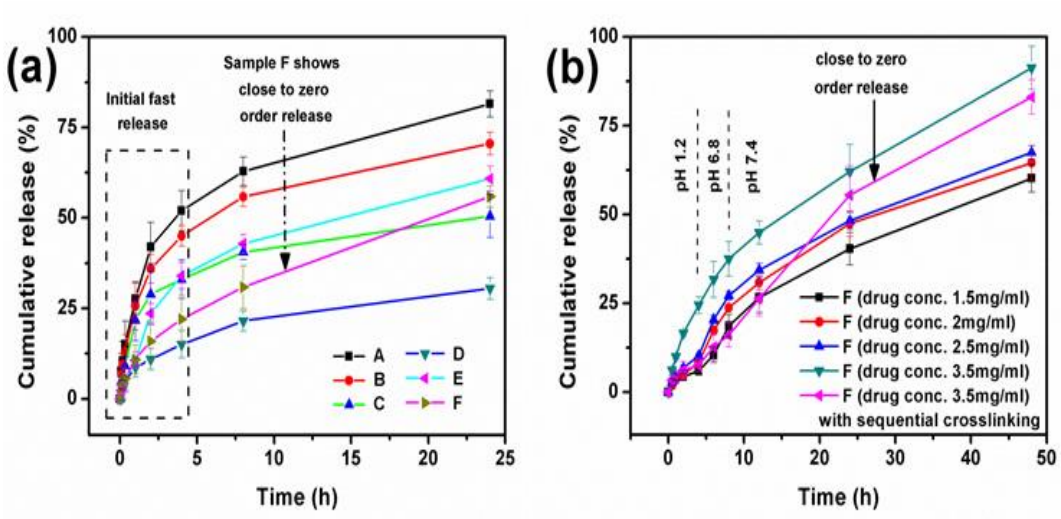

Figure 4.7. a) *In-vitro* cumulative release of piperine from different composition of sandwiched membranes, b) Cumulative release of piperine from F sample with different drug concentration (1.5, 2, 2.5, 3.5 mg/ml) at pH 1.2 for 4 h, then pH 6.8 for 4 h and finally pH 7.4 for 16 h. (results represented are mean ± SD , n=3)

4.5.2 Effect of pH and drug concentration on release profile

To modify the selected vehicle F based on the results discussed above, the *In-vitro* drug release system was designed in such a way so that the vehicle could be exposed to different pH with different retention time, similar to the GI tract [169]. The motivation behind designing such *In-vitro* systems which reflected similar conditions of the GI tract, was to understand the effect of swelling and degradation of the vehicle during drug release. The effect of pH on the release of piperine from sample F with different drug concentration (1.5,

2.0, 2.5 and 3.5 mg/ml) is shown in Figure 4.7 (b). The release of drug molecules accelerated with increase in pH for all the cases which reflects very promising results. This accelerated release can be explained by the increase in swelling degree in higher pH. In higher pH, all the –COOH groups present in gelatin convert into –COO- which results in high anion-anion repulsion and thus high swelling of the polymer matrix. But in acidic pH (<5), due to the high ionic strength of the medium, most of the carboxylate groups are protonated and the anion-anion repulsion forces are minimized [174]. Additionally, the hydrogen bonding between carboxylate and hydroxyl group is also strengthened, which causes overall shrinkage and lesser swelling in acidic pH. Thus, swelling capability increases gradually with increase in pH which promotes better drug release in higher pH conditions [169]. This phenomena can help to minimize the drug loss in the lower pH of the GI tract (pH of stomach is 1.2 and retention time is approx. 4 h), and can effectively swell as well as deliver maximum drug in higher pH region (pH of different parts of intestine are 6.8 and 7.4 respectively). Figure 4.7 (b) reveals that the drug loading in core layers is proportional with drug release. Thus, increase in initial drug release within 4 h was observed with higher drug concentration in core layers: 6.0 ± 1.2%, 8.4 ± 1.1%, 10.3 ± 0.5%, and 24.5 ± 2.3% of cumulative release for 1.5, 2.0, 2.5 and 3.5 mg/ml respectively. The F sample with 3.5 mg/ml drug concentration didn't seem to hold promise in reaching zero-order drug release due to its initial fast release compared to other samples. Although the highest loaded sample showed initial rapid release of drug within 4 h, we had selected the vehicle for further modification to overcome the drawbacks associated with burst release, while still maintaining the higher drug concentration. Our objective is to simultaneously reduce drug loss in the stomach (pH 1.2) within initial hours (approx. 4 h) and to release drug molecules in the intestine (absorption site) in a zero-order manner, with F sample, with the highest possible drug loading, i.e. 3.5 mg/ml. In order to achieve this, we then worked on another strategy, sequential crosslinking, as is discussed further.

4.5.3 Effect of sequential crosslinking on release profile

The next objective was to investigate the effect of different crosslinking methods for the chosen vehicle (3.5 mg/ml drug and sample formulation: F type) in order to overcome the limitations of F sample (sudden release in initial hours with higher drug loading). Thus, sequential crosslinking of the vehicle was attempted as an additional step. To understand this further, we first deposited the barrier layer of gelatin (3.0 ml) nanofibers and then crosslinked it for 2 min with GTA vapor. This was followed by the deposition of a drug loaded core layer (4.0 ml) and crosslinking for 2 min, which was again followed by a deposition of only GNF (3.0 ml) and then again crosslinking for 2 min. The crosslinking was done sequentially

keeping the total crosslinking time the same i.e. 6 min. A comparative study of the release profiles between sequential crosslinked and one time crosslinked sample, both with 3.5 mg/ml F sample, is made in Figure 4.7 (b). The release of the drug from sequential crosslinked sample with 3.5 mg/ml of drug after 4 h was less than 10% (7.6 ± 1.8%), whereas one time crosslinking with same drug concentration, the initial release within 4 h was almost 25% (24.5 ± 2.3%). Results showed that sequentially crosslinked sample F with 3.5 mg/ml of drug successfully toned down the drug loss during initial hours in lower pH conditions. At the same time, it showed controlled and sustained release of piperine (83.0 ± 4.8% of release after 48 h) for rest of the observed time scale.

The probable reason of these observations can be traced to the uniformity of the crosslinking of fibers in the in-between layers of the mesh when done in a sequential manner. The compactness of the vehicle increased due to the layer-by-layer crosslinking strategy which also elevated the water resistivity degree and restricted the drug molecule mobility [172, 173, 175]. Further, to understand the mechanism of drug release, *In-vitro* drug release data for sample F with different drug loading and different crosslinking strategies were fitted with zero-order release, and R^2 values were also listed. The final design gave R^2 as 0.99 for 24 h and 0.97 for 48 h release, which is a signature of a zero-order case for prolonged time. This has been presented in Table 4.2.

Thus, it is worthwhile mentioning that by doing a systematic analysis, the final vehicle design has achieved optimal performance i.e. considerable control over the initial release profile without compromising on the overall drug release along with important advantages like stability and less release in lower pH. Moreover, we also achieved the desired zero-order release profile in higher pH condition for 48 hours, using very cheap biopolymer gelatin based nanofibers.

4.5.4 Drug release mechanism

To investigate the drug release kinetics and drug release mechanisms from multi-layered drug loaded GNF vehicle, the *In-vitro* release data were analysed using mathematical model ie.

$$\text{Zero-order kinetics: } Q_t = Q_0 + K \times t$$

Where, Q_t = Cumulative amount of drug at time t, Q_0= initial amount of drug [169].

Generally, drug release is a process in which drug molecules travel from the core of the polymer matrix to the polymer's outer surface and then finally to the release medium. The release of the drug from a polymer matrix is modulated by diffusion of the drug and/or

degradation of the polymer matrix. To understand the mechanism of drug release, *In-vitro* drug release data for sample F with different drug loading and sequentially crosslinked samples were analyzed with Zero-order kinetics (Table 4.2).

The mechanism of drug release usually consists of three steps [169, 176]. Firstly, water molecules from the release medium diffuse in the polymer matrix through the internal pores and the matrix starts swelling. Swelling starts the degradation of the fiber mesh followed by the enhanced mobility of the drug molecules in the core. Due to the presence of water molecules, the osmotic pressure provides the driving force for the release of drug molecules from the core layer to the release medium. At the same time, the presence of the water molecules in the matrix leads to polymer relaxation and degradation of polymer matrix, which also help in drug release. The drug concentration gradient between the matrix and release medium also plays an important role during the initial hours of the study. In the Table 4.2, sequentially crosslinked F sample with 3.5 mg/ml drug concentration showed good fittings with 0.97 $R^{2,}$ which depicts zero-order release systems for 48 h. The plot fitting is better till 24 h (0.99 R^2) for the same sample as shown in Table 4.2. Thus, the nanofiber based matrix shows the rate of release closer to zero-order release. The compactness of the nanofiber matrix in case of sequentially crosslinked sample can be a possible reason for the increase of diffusional resistance. On the contrary, the increase in drug loading causes higher drug concentration gradient between the matrix and release medium, which enhances the release. As a result, though the mechanism of release is diffusion, close to zero-order release pattern was achieved through the experimental tuning of factors mentioned above. Zero-order release profile is very desirable because of the controllability of drug concentration within the effective safe therapeutic window for a prolonged time [2, 175, 176]. The control on the drug release profile as per the requirement is made possible by varying the thickness of the barrier as well as the core layers and the drug loading of sandwiched membranes [172, 173, 175]. This study concludes that the multi-layered drug loaded gelatin membrane can be a potential drug delivery vehicle with tunable desired drug release profiles.

In a nutshell, in the case of F sample with one time crosslinking, with higher drug concentration (3.5 mg/ml) the release profile was tending towards bi-stage release curve: initial burst release followed by sustained release shown in Figure 4.7 (b). This kind of curve doesn't exhibit close to zero-order release. Thus, decrease in R^2 value is quite evident as shown in Table 4.2. On the other hand, sequential crosslinked F sample with 3.5 mg/ml drug concentration showed close to zero-order release profile. It is evident that initial drug release can be toned down by crosslinking the polymer matrix layer-by-layer. This finally gives a better fitting with the zero-order curves. Although the release profiles are subjected to change

according to the therapeutic requirement, the flexibility of loading more drugs in the vehicle with zero-order signature has been achieved in this work.

Table 4.2: List of drug release co-efficient as fitted in Zero-order kinetic model

Release Model	**Sample F with different drug concentration and sequentially crosslinked sample**						
		1.5 mg/ml	**2 mg/ml**	**2.5 mg/ml**	**3.5 mg/ml**	**3.5 mg/ml sequential**	**3.5 mg/ml sequential (till 24 h)**
Zero-order	**K**	**0.0071**	**0.0092**	**0.00106**	**0.00157**	**0.0131**	**0.0158**
	R^2	**0.93**	**0.87**	**0.83**	**0.74**	**0.97**	**0.99**

4.6 Summary

A biodegradable polymer mesh was fabricated by the electrospinning of the natural polymer gelatin solution with different concentrations of drugs for the assessment of a polymeric DDS containing hydrophobic drug molecules. In order to get close to zero-order drug release, multi-layered membranes with different drug concentrations were used, and different crosslinking strategies were applied. The effect of the crosslinker was investigated in terms of degradation, swelling, chemical stability, and thermal stability. Finally, *In-vitro* release study of the vehicle was done in different physiological pH which mimicked the pH profile of the GI tract. In order to control the initial fast release, different combinations of multi-layered membranes were fabricated and studied extensively. In the next step, by modifying the core as well as the barrier layer and the crosslinking strategies, we have demonstrated the following points:

(a) This fabricated electrospun nanofiber mesh can exhibit better control over the initial fast release of a hydrophobic drug at a substantial level.

(b) It can also achieve close to zero-order release profile for 48 h with flexibility for varying drug-loading capacities as per the therapeutic requirements.

This work lays out the possibility of the systematic designing of multi-layered nanofiber meshes comprised of a cheap biopolymer (gelatin) which can be used as a drug delivery vehicle for hydrophobic drugs, with the desired signature of zero-order release for long hours.

4.7 Highlights of this work and motivation for the next chapter

This newly developed electrospun gelatin nanofiber based DDS shows the potential for a novel DDS for the following reasons:

1. Hydrophobic drug piperine is stable in the hydrophilic matrix.
2. Multi-layers can substantially reduce the initial fast release, which can drastically lessen the drug loss in lower pHs.
3. This device proved itself to be a pH sensitive vehicle as the swelling of the vehicle decreased in lower pHs and increased in higher pHs. This vehicle can successfully release drug molecules at the site of absorption i.e. the intestine.
4. Sequential crosslinking also helped in tuning the burst release in the case of higher drug loaded samples.

Finally, we can conclude that the multi-layered nanofiber based DDS have met all the desirable aspects of a novel drug-carrier and have achieved zero-order drug release for upto 48 h for the hydrophobic drug molecule piperine. A schematic representation of this work is shown in Figure 4.9.

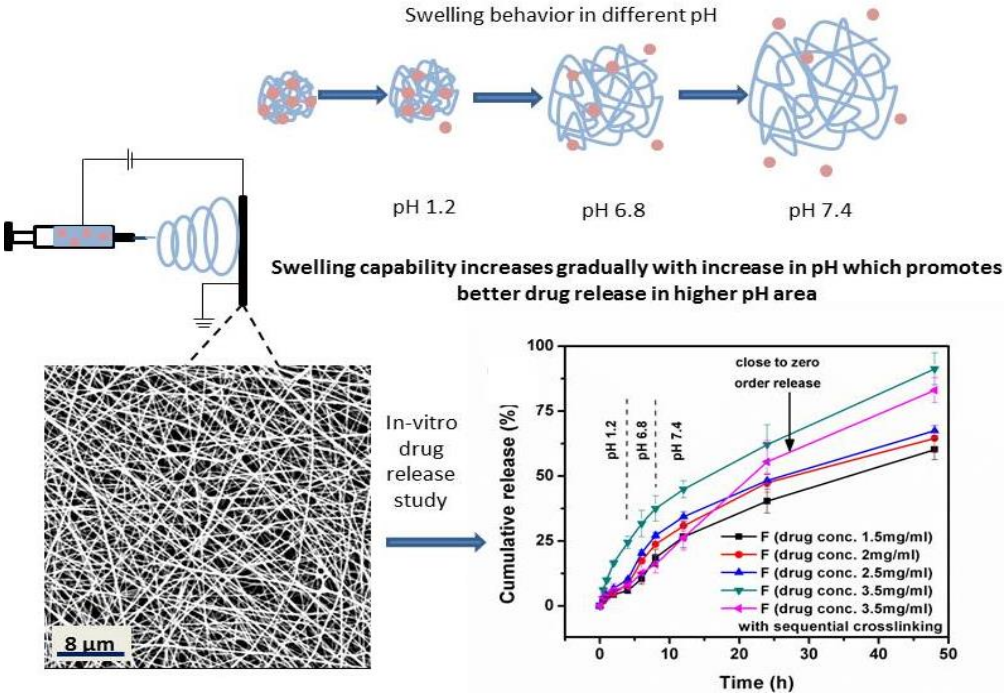

Figure 4.8. A schematic representation of fiber fabrication, swelling behavior and *In-vitro* release profile of multi-layered electrospun gelatin nanofiber based DDS

The results derived from this work indicated the need for further investigation into the role of sequential crosslinking and the requirement for tuning the design of multi-layered mesh to achieve zero-order drug release profiles. Thus, in-depth investigations have been conducted in this direction in the next chapter.

Chapter 5

Fabrication of Sequentially Crosslinked Multi-layered Gelatin Nanofiber based DDS

5.1 Introduction

The focus of this chapter is to investigate the role of crosslinking and developing a multi-layered structure for encapsulation in an attempt to tone down the initial burst release of the drug from the nanofiber based drug-carrier. In chapter 3, single-layered nanofiber based DDS showed a bi-phasic release profile, which helped us in understanding the need for making further modifications to the vehicle in terms of reducing the burst release of drugs. Thus, the concept of multi-layering and sequentially crosslinking of the drug carrier was adopted. This combination contributed to a zero-order drug release with various drug loaded samples for a duration of 48 h. These results from chapter 4 certainly demonstrate the need for a better understanding of the role of crosslinking strategies in multiple layers so that we can fabricate a DDS, which can release drugs according to the required treatment. To design such a carrier, the roles of these two factors need to be investigated thoroughly.

The intention of the present work is to perform a systematic analysis of the vehicle in order to achieve a wide range of release profiles from this nanofiber based DDS. Since we have retained the excipient gelatin, and the drug piperine, as well as the fabrication methods

used previously to design the vehicle, therefore, in this chapter we have mainly focused on the effect of the crosslinking strategies and multi-layered structure on the release profile of the drug. Thus, we have presented a comparative study of three different strategies used for fabricating the drug-carriers based on their drug release profiles. We anticipated that this study might aid in understanding the mechanism better, and this specific knowledge can help us engineer the most viable vehicle for a flexible release profile.

5.2 Materials and Methods

5.2.1 Materials

Gelatin (Type A, 175 bloom), piperine (98%), hydrochloric acid (ACS, 36.5-38.0%), glutaraldehyde (25% v/v aqueous solution), acetic acid (glacial, ACS, ~99.7%), sodium hydroxide pallets (98%), phosphate buffer saline (pH 7.4) were purchased from Alfa Aesar. In addition, deionized water (DI) (Milli Q, resistivity 18.1 MΩ.cm) was used throughout the experiments.

5.2.2 Fabrication of nanofiber membrane and crosslinking

Gelatin nanofiber mesh was prepared by electrospinning 20% (w/v) Gelatin (Type A) solution in acetic acid (20% v/v in distilled water) solvent using an electrospinning apparatus (Make: E Spin Nanotech Pvt. Ltd, India). Piperine was added to the spinning solution for drug loaded samples (G-P NF).

The samples were made using three different strategies:

(a) Single-layered GNF was prepared by electrospinning the drug loaded 5 ml solutions on the substrate (aluminium foil). For crosslinking, the samples (deposited on aluminum foil) were cut into 2 × 2 cm^2 and placed inside the closed glass desiccator with 20 ml of GTA solution (25% v/v aqueous solution) for 6 min. (G-P NF C6).

(b) Single-layered GNF was prepared and was crosslinked in a sequential manner (G-P NF SC6). The drug loaded solution was deposited (1 ml) and further crosslinked for 2 min followed by deposition of fibers from a 3 ml solution with subsequent crosslinking and so on. The total crosslinking time was 6 min.

(c) Multi-layered GNF was prepared by sequential electrospinning of solutions (with and without drug loading) on the substrate (aluminium foil). After that, the sample was crosslinked in the same sequence (2+2+2) min maintaining the total crosslinking time same as before (6 min). In addition to that, 3 ml solution of piperine loaded gelatin fiber layer was sandwiched by only 1 ml solution of gelatin nanofiber layers on both the sides (SG-P NF SC6).

For fabricating these different formulations, the total deposited solution was 5 ml and the total crosslinking time was 6 min. Figure 5.1 shows the deposition and crosslinking strategies through a schematic diagram.

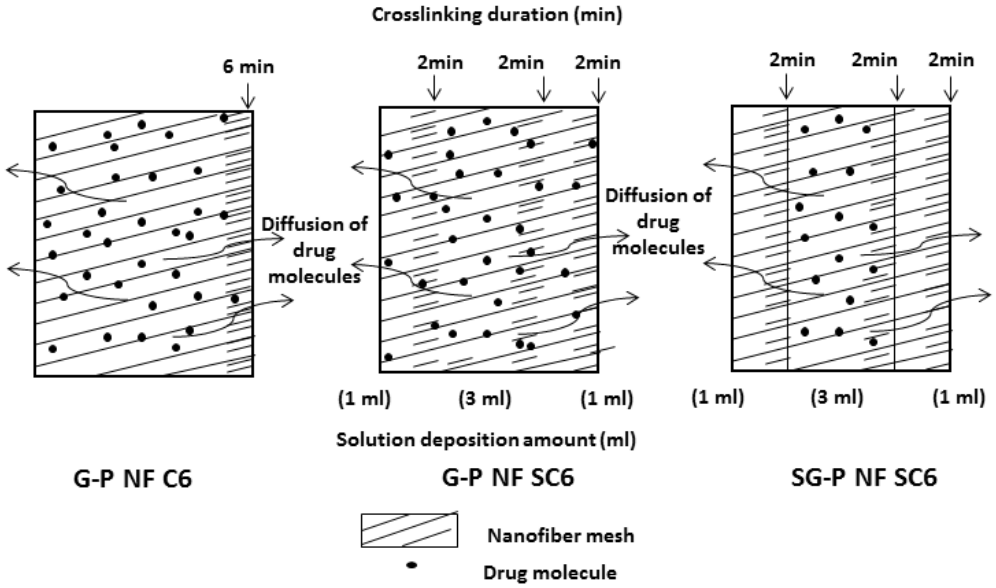

Figure 5.1: A schematic representation of different formulations of fiber based DDS

5.3 *In-vitro* biodegradation study

To understand the effect of different crosslinking mechanisms on the stability of the mesh, *In-vitro* biodegradation was carried out for G-P NF C6, G-P NF SC6 and SG-P NF SC6 in pH 7.4. All the case samples were cut into equal size, weighed (W_i) and placed in 25 ml solution of pH 1.2 for 4 h and in pH 7.4 for another 46 h. As the retention time in the stomach (pH 1.2) is generally 2-4 h, we checked the stability of the vehicle in lower pH for 4 h and then in higher pH (mimicking the pH profile of the human GI tract). At the mentioned fixed time intervals, swelled samples were taken out and dried in a vacuum oven at room temperature and weighed (W_f).

The weight loss (WL) (%) was calculated by using the following equations [160]:

$$\text{Weight loss (\%)} = \left(\mathbf{1} - \frac{\mathbf{W_f}}{\mathbf{W_i}}\right)$$

Where, W_i = Initial sample weight, W_f = Weight after an incubation period.

Figure 5.2 shows that the WL (%) due to hydrolytic degradation in the case of G-P NF C6, G-P NF SC6 and SG-P NF SC6 were 15.2 ± 1.5%, 12.4 ± 1.2% and 12.1 ± 1.6% respectively after 50 h in the solution of pH 1.2 and pH 7.4. The WL (%) was less for the

sample G-P NF SC6 and SG-P NF SC6 as compared to the sample GNF-P C6, which clearly indicates the stability of the nanofiber mesh in an aqueous medium.

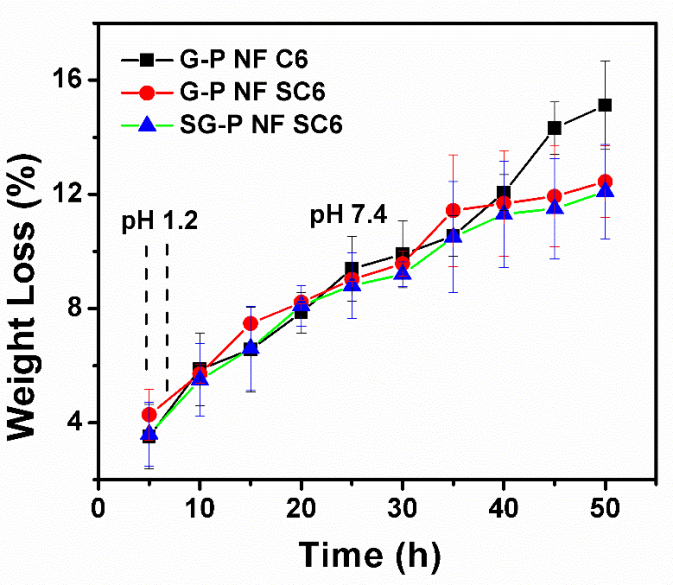

Figure 5.2: Weight Loss (%) for sample G-P NF C6, G-P NF SC6 and SG-P NFSC6 in pH 1.2 for 4 h and in pH 7.4 for 46 h (results represented are mean ± SD , n=3)

5.4 Characterization

Since we have already established the following facts in the previous chapters, we have not repeated them in the discussion in this chapter.

1. The drug-polymer compatibility was studied using FTIR in both chapters 3 and 4. It was found that hydrophobic drug piperine is stable in a gelatin matrix, given that there is no interaction between the drug and the polymer. The effect of crosslinking was also extensively studied in chapters 3 and 4. Naturally, as the polymer system, the drug and the crosslinker are the same as those in previous chapters, we have assumed that the drug is stable in the system.
2. Crosslinking has a major role to play in the thermal stability of the vehicle. As discussed in chapters 3 and 4, we already checked the effect of the crosslinker on the thermal stability of the vehicle, and have therefore not repeated the same experiment in this chapter.
3. Here we have focused on the possible effect of crosslinking as well as different layer formulations on the morphology and biodegradation of the drug-vehicle combination and the consequent release study of the drug.

5.4.1 Structural characterization

The morphology of the nanofiber meshes were captured by a table top scanning electron microscope (SEM) (Phenom world, Model: Pro X). Prior to imaging, the samples were placed on a stub and were also coated with a thin gold layer using a sputter coater (Excel Instruments, India).

The morphology of G-P NF C6, G-P NF SC6 and SG-P NF SC6 are presented in Figure 5.3. As gelatin nanofiber is very sensitive to moisture, and the water molecules present in 25% v/v of GTA saturated vapor damages the outer layer of the mesh by fusing fibers together. The more the exposure time, the more are the instances of fused fiber. Thus the sample G-P NF C6 (Figure 5.3 (a)) showed much more damaged structure in comparison to the samples G-P NF SC6 and SG-P NF SC6. In both G-P NF SC6 and SG-P NF SC6 samples, the exposure time for the top layer is limited to only 2 min and this results in an intact fiber structure (Figure 5.3 (b) and 5.3 (c) respectively).

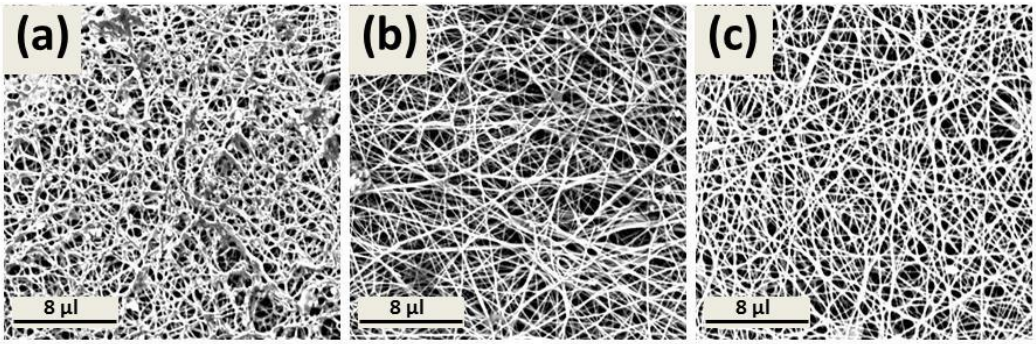

Figure 5.3: SEM images of G-P NF C6, G-P NF SC6 and SG-P NF SC6

5.5 Drug release performance

To study the effect of different crosslinking strategies on controlling the release rate of piperine from a gelatin nanofiber matrix, *In-vitro* release study was performed maintaining the physiological conditions. G-P NF C6, G-P NF SC6 and SG-P NF SC6 were cut into pieces of equal size and placed in a 30 ml release medium with different pH levels (pH 1.2, similar to the pH of stomach and pH 7.4, similar to pH of the intestine) maintaining the temperature and oscillating speed of the mechanical shaker (Remi RIS-24 plus) at 37 ^{O}C and 150 RPM respectively. Adequate amount of samples were taken from the release medium at fixed time intervals and fresh solution was added to maintain the sink condition. The presence of piperine in release medium was detected using a UV spectrophotometer (Perkin Elmer, Lambda 35) at

342 nm as λ_{max} for piperine. The experiment was performed thrice to confirm the accuracy of the results.

Next, *In-vitro* drug release study was performed to investigate the role of different crosslinking strategies on the release study of piperine. Figure 5.4 illustrates the cumulative release (%) of piperine as a function of time (h) for 24 h in different pH. The drug concentration (µg/ml) Vs time (min) data is presented in Appendix B (Table B5). The release (%) of piperine from G-P NF C6, G-P NF SC6 and SG-P NF SC6 meshes in pH 7.4 for 24 h are 67.4 ± 4.5%, 55.2 ± 3.7% and 51.8 ± 4.6% respectively. G-P NF C6 showed initial fast release when compared to the G-P NF SC6 mesh. The initial fast release of piperine within 8 h was successfully tailored by 20% in the case of GNF-P SC6 (40.1 ± 1.2%) as compared to GNF-P C6 (57.7 ± 2.5%) by designing the vehicle through the sequential crosslinking method. Further, we had fabricated a sandwiched mesh consisting of a core layer (with piperine loaded GNF mesh) and two barrier layers (GNF mesh without any drug) on both sides of the core layer. We had also investigated the effect of the barrier layers on the release profiles of piperine. Similarly, sequential crosslinking was performed for sandwiched GNF mesh. The idea was to increase the diffusional barrier between the drug molecules and release medium and also to check the effect of sequential crosslinking (which is discussed in chapter 4 as well to reach a zero-order release profile). Similarly, after 8 h of study, almost 20% of drug release was tailored for SGNF-P SC6 (38.1 ± 2.1% after 8 h) compared to GNF-P C6. Interestingly, sandwiched structure did not show significant control over release than what sequential crosslinking did. The main drawback of direct crosslinking for 6 min (G-P NF C6) is excessive shrinkage of the nanofiber mesh. To overcome this problem associated with non-uniformity of crosslinking in different layers, we tried sequential crosslinking (G-P NF SC6). To increase the diffusional barrier and to overcome the initial fast release of drug, we further fabricated a sandwiched GNF mesh with a similar method of sequential crosslinking with GTA vapor (SGNF-P S-C6). In pH 1.2, after 4 h of release study, the sample formulations G-P NF C6, G-P NF SC6 and SG-P NF SC6 exhibited release of 48.4 ± 2.2 % , 30.2 ± 1.2 % and 25.5 ± 2.2 % respectively. The cumulative release of piperine was less in lower pH for all these samples [169, 174]. The probable reason behind the increased swelling rate in pH 7.4 is the deprotonation of carboxylic group (-COOH) of gelatin chain to carboxylate ion (-COO-), which creates a repulsive force within the polymer chain. This kind of electrostatic repulsion between carboxylate ions would result in polymer relaxation which in turn leads to hydration of the matrix. In addition to that, the hydrophilic nature of the carboxylate ion also leads to remarkable swelling of the matrix at higher pH (pH 7.4). The decrease in swelling degree at lower pH (pH 1.2), can be attributed to the increased number of low-ionized carboxylic group

(-COOH) which form an inter-molecular hydrogen bond. These carboxylic groups can be associated with the intra and/or inter-molecular hydrgen bonds which causes the matrix to collapse. Consequently, a reduction of swelling degree in pH 1.2 takes place [177]. Due to comparatively lower swelling of the mesh, drug molecules do not gather sufficient osmotic pressure to be able to travel from the mesh to release medium. Releasing less drug in lower pH (pH 1.2: similar to stomach) is good as the absorbance site of the drug is usually the intestine [178].

The idea behind performing a comparative analysis of three different kinds of sample formulations was to render a standard platform for comprehending various factors that affect the release profiles of the drug. The aim here was not to achieve zero-order release. The sole reason, then, was to understand which factor played the most important role in controlling drug release. To achieve zero-order release profile, naturally, we had to adopt the final formulation which we had achieved in the previous chapter 4. However, that formulation was made with 10 ml of solution (4 ml solution used for depositing fiber in the core and 3 ml of solution for the fiber on both the sides). Also, the formulation was made for 3.5 mg/ml concentration of drug (formulation F from chapter 4). It is clear from this study that, to achieve zero-order release, it is mandatory to maintain sufficient barrier layers as well as carry out crosslinking in order to achieve zero-order release. The results of this study highlight the importance of sequential crosslinking in controlling the release of molecules. Actually, both the factors play major roles by complementing each other: first, through controlling the swelling and polymer relaxation using an accurate amount of crosslinker, and second, through slow molecular transportation using multi-layer structured mesh. This, consequently, results in a controlled drug release profile. In conclusion, therefore, a sequentially crosslinked multi-layered formulation can achieve zero-order release profiles.

We can conclude that for nanofiber based drug-carrier, choosing the correct crosslinking method is a very important factor. In chapter 3, we had successfully reduced the crosslinking duration from few hours to few mins [163, 164]. Additionally, the reduction of crosslinking time had benefited the system in reducing toxic effects of the GTA crosslinker to a great extent [164]. The extraordinary porous structure of the nanofiber mesh was successfully crosslinked with GTA vapor with a good stability for 24-48 h. In addition to that, while fabricating the system we had selected GTA as crosslinker because of the crosslinking capability for a short span of time and also for its cheap and easily availability [129, 133, 167]. Despite its toxicity, it is still widely used in the pharmaceutical industry. Thus, reduction of crosslinking time can be considered to be an important contribution to this field which can aid the continued use of this toxic crosslinker through minimising its toxicity.

Carrying forward this observation to the next step in order to reduce the immediate release of drug in the initial hours, we found different strategies for crosslinking. The main drawback of using GTA vapor for crosslinking it with a hydrophilic vehicle was the morphological degradation of the exposed layer of the mesh. The water molecules in GTA vapor attaches itself with the gelatin fibers and it starts fusing and swelling. Thus, the topology of the vehicle which is exposed to the GTA vapor starts fusing [164]. In addition, this short span exposure of the fiber to the GTA vapor does not particularly benefit the vehicle in terms of reducing the initial release. The reason for that is that the non-uniformity of the GTA molecules throughout the different layers causes bulk degradation of the system and can cause the fast release of drug molecules [178]. The water molecules attack the less crosslinked hydrophilic fibers (mostly the side of mesh which is attached to the foil) of the mesh which result in early degradation of the polymer matrix. In addition to that, the crosslinking is not uniform in every layer of the fabric and excessive shrinkage of the mesh is also visible. This non-uniformity of the crosslinking leads to reduced water resistivity as compared to sequential crosslinking. In case of sequential crosslinking, the carbonyl group (C=O) of aldehyde can react with amino acid of gelatin in a uniform manner and the compactness of the fabric is better as compared to the one time final crosslinking [133, 164, 178]. It forms strong inter-fibrous bonding, which creates an extra barrier and prevents the diffusion of drug molecules to the release medium. The probable reason behind this observation is the uniformity of crosslinking and the tightly packed structure of intermediate layers of the mesh [178]. This study shows that the compactness of the intermediate layers plays a very important role in terms of water resistivity and the mobility of drug molecules.

Besides the crosslinking strategies, the multi-layer formulation also helps to control the initial drug release. The aim is to increase the diffusional barrier between the drug molecules in the matrix to the release medium. The drug release is heavily dependent on the swelling where crosslinking plays a major role and also, the diffusion of the drug and dissolution medium where multi-layer formulation plays a major role. The drug release process consists of three major steps. First, the dissolution medium penetrates the fibrous structure. The water intake capability is dependent on the nature of the system. In the following steps, polymer relaxation, swelling and degradation start happening due to the retention of water molecules. At this point, crosslinking can confirm the longevity of the system and control the polymer chain relaxation and swelling to a great extent. Finally, the transportation of the drug molecules from the matrix happens due to osmotic pressure. At this stage, the diffusion path between the core layer and the dissolution medium plays an important role. The longer the diffusional barrier the delayed will be the release of drug. The drug molecules start moving

from the core layer and it goes through the barrier layers and finally releases in the dissolution medium [169]. This certainly helps to control the initial fast release of drug. In case of single layered formulation, the drug on the surface starts releasing from the initial moment itself, which causes immediate and fast release. This problem is certainly improved upon a lot by introducing the multi-layered formulation. However, in the comparison between the multi-layered sequential crosslinked sample (SG-P NF SC6) and single layered sequential crosslinked sample (G-P NF SC6), not much difference was noticed. The reason behind this is that the barrier in this multi-layered formulation is not enough to give excellent support or control over the mobility of the drug. However, the uniformity of crosslinking in the intermediate layers can successfully affect control on the transportation of the drug molecules from the vehicle to the release medium. These observations are certainly helpful to us in order to direct our focus to fabricate drug specific or treatment specific release profile.

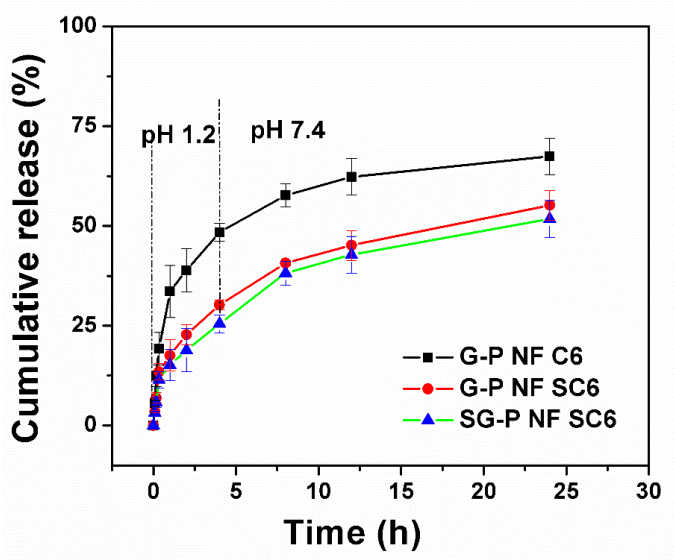

Figure 5.4: The *In-vitro* cumulative release (%) profiles of the sample formulation G-P NF C6, G-P NF SC6 and SG-P NF SC6 (results represented are mean ± SD , n=3)

5.6 Summary

As demonstrated in results, the different strategies of crosslinking certainly play important roles in controlling drug release from GNF based system. Results from the previous chapters demonstrated excellent stability of the mesh in aqueous medium for more than 48 h with only 6 min of crosslinking. In this study, we had focused on further development of the system by addressing the problem of non-uniform crosslinking in between layers in case of one time crosslinking. Thus, sequential layer by layer crosslinking (2+2+2 min) of GNF mesh was done

by keeping the total crosslinking time constant (6 min). As expected, uniformity of crosslinking in different layers was achieved. As a result, strong inter-fibrous bonding was formed because of crosslinking evenly, which in turn controlled the mobility of the drug molecules. Further, sandwiched GNF mesh was fabricated to increase the diffusional barrier between drug molecules and the release medium. Finally, to understand the key factor effecting sequential crosslinking and multi-layer formulation on release study, a comparison among these three fabricated samples was drawn. The results from this study suggested that, in order to achieve zero-order release profiles, the formulation should consist of the perfect barrier support and also uniformly crosslinked layers. In addition, different combinations of these two factors can effectively release the drug molecules in a variable range, which can address different treatment specific requirements.

5.7 Highlights of this work and motivation for the next chapter

This chapter demonstrates the importance of crosslinking methods and barrier layers in the direction of controlling molecular transportation of the drug from the vehicle to the release medium. The main observations of this chapter are as follows:

1. Single-layered one time crosslinking (G-P NF C6) shows fast release of drug in initial hours because of the non-uniformity of the crosslinking throughout the layers. Alternatively single-layered sequentially crosslinked sample (G-P NF SC6) shows better control over the molecular transport than one time crosslinking.
2. Sequential crosslinking not only controls the compactness and uniform distribution of GTA molecules in-between layers of the mesh, but also protects the fiber morphology from fusion by excessive exposure of the mesh to GTA vapor.
3. Multi-layer sequential crosslinking formulation (SG-P NF SC6) has not drastically improved the release profile. However, sequential crosslinking plays a major role during the penetration process of the water molecules in the matrix. Afterwards, the polymer relaxation and the swelling also depend on the uniform crosslinking in the intermediate layers. This influences the drug release process to a large extent.
4. A Multi-layer formulation helps the most in the final stage of the release. The enhanced diffusional barrier can delay the initial release. However, the correct extent of barrier or support needs to be provided to counter the early release of the drug. In brief, the correct combination of multi-layer formulation with sequential crosslinking can achieve a zero-order release profile using nanofiber based DDS.

5. As an endnote of this study, this work can provide the knowledge to help in fabricating a drug-carrier, which can release the drug according to the treatment requirement. For personalized drug treatments, this vehicle can be very useful. With a thorough understanding of its parameters, it is possible to fabricate a drug vehicle with required modifications in order to meet any customization in drug release profiles. This study, therefore, certainly demonstrates huge potential for a novel drug-carrier, which can serve different kinds of treatment specific requirements.

Despite this well-engineered formulation, we aim to achieve even better in order to provide a realistic applicability to this fiber based vehicle. Therefore, our next aim is to fabricate a drug vehicle with higher loading, which can also exhibit a zero-order drug release profile. In addition to that, our final objective of this thesis is to fabricated a novel drug releasing vehicle particularly for low-soluble drugs. In order to achieve that, we have fabricated a drug-carrier which has higher loading capability in addition to being able to deliver different nature of molecules. Thus, in our final step, we fabricated a nanofiber based DDS with amphiphilic molecules (Amphotericin-B: anti-fungal drug) which is discussed in the next chapter.

Chapter 6

Fabrication of a Compressed Nanofiber Oral Tablet

6.1 Introduction

In the previous chapters, we examined the potential of a nanofiber based DDS, particularly for hydrophobic molecules, piperine. Interestingly, different design strategies resulted in different kinds of release profiles i.e. bi-phasic, (when the vehicle was fabricated with single-layered crosslinked mesh), and zero-order release for 48 h (with multi-layered, sequentially crosslinked vehicles). An in-depth examination was performed in order to meet the desired release profiles. The gelatin nanofiber based DDS formulated for the release of piperine showed numerous promising results. Among these were, the reduction of crosslinking time (6 min) and further with the same crosslinking time but through sequential crosslinking, the sample improved release characteristics to a great extent. In addition to that, multi-layers also protected the drug molecules at the core of the matrix providing a longer diffusional path which toned down the initial fast release. In brief, this newly developed GTA crosslinked GNF based DDS showed promising possibilities which led us to perform further investigation in order to engineer a novel DDS, particularly for low-soluble drugs. Despite its positive parameters, this system suffers from the problems of low-drug loading and not so prolonged release of drug.

In this chapter, we took a GNF based drug-carrier and tried to encapsulate another kind of low-soluble drug in order to make it a general drug-carrier for various low-soluble drugs. We have taken anti-fungal drug Amp-B as a model amphiphilic kind of drug. This drug is almost three times bigger than piperine according to the molecular weight and is amphiphilic in nature. In this chapter, we also tried to fabricate (CNOT) with Amp-B and accordingly, different aspects of the tablet have been extensively studied. We attempted to fabricate CNOT in order to load Amp-B with a realistic drug dosage.

The objectives of this chapter are as follows:

1. Fabrication of nanofiber based DDS which can deliver different kinds of drug with different molecular size. To meet this objective, low-soluble anti-fungal drug Amp-B (amphiphilic in nature) was selected for this work.
2. CNOT are fabricated in an attempt to achieve a realistic application with therapeutic dose of Amp-B.
3. To achieve zero-order release for a prolonged period.

6.2 Literature survey of Amp-B drug-carrier

Amp-B is a macrolide polyene antibiotic, which was first derived from Streptomyces Nodosus collected from Venezuela in 1955 [179, 180]. This is known as "gold standard" for anti-fungal treatment since 1950s [179]. In additional to that, it is still considered to be a broad-spectrum anti-fungal drug which can fight against a wide spectrum of systemic fungal diseases [179-181]. Amp-B is amphiphilic in nature because of its hydrophobic (the polyene hydrocarbon chain) and a hydrophilic (the polyhydroxyl chain) domain [179]. Due to this kind of chemical structure, Amp-B shows unfavorable pharmaceutical properties, which includes low solubility and poor bioavailability in case of oral administration [180, 181]. Thus, this drug is administrated parenterally to control severe systemic fungal diseases [180]. Although the drug is very old, recently the use of this drug has increased because of the sudden increase in fungal diseases. Amp-B is widely used for treating patients suffering from invasive fungal infections because of the increased number of cases of AIDS and other immunological diseases, aggressive chemotherapy for cancer patients, organ transplant, implant or prosthetic devices and frequent international travel. Amp-B is also used as an ophthalmic antifungal agent [179, 182]. Amp-B is also used as therapeutics against visceral leishmaniasis (known as Kala-azar) [183-186]. The conventional dose of Amp-B was using colloidal dispersion with sodium deoxycholate, which required daily intravenous administration for a period of 30-40 days. This causes a lot of inconvenience and severe nephrotoxicity as a side effect [179, 181].

Later, lipid-based formulation of Amp-B using liposome, micelle, emulsion was widely used and was available in the market which drastically reduced the treatment duration in 3-5 days [179-181]. However, due to high cost and failure of the drug vehicle, the need for developing a suitable drug-carrier for effective release is still a challenge.

To fight against the deadly systemic fungal diseases, researchers have attempted to develop a suitable drug-carrier for Amp-B, which can improve the delivery process and reduce the side effects associated with this drug. Many investigations on fabricating polymeric micelles, dendrimer-micelles, and liposome with different biocompatible polymers have been reported and are commercially available in order to improve Amp-B release [181, 187-193]. Recently few reports on nanoparticle and nano-suspension based Amp-B DDS have also been reported [182, 193, 194].

Oral administration of Amp-B can reduce the cost associated with hospitalization during administration and this can increase the patient's compliance. An orally administered Amp-B formulation needs to cross the epithelium layer of GI tract. Recently few formulations based on nanoparticle, nano-suspension, micelles, nanofiber and lipid-based oral formulations has been reported [193, 195-199]. Biodegradable and biocompatible polymer based carrier has also been used in different forms like nanoparticles, nanofiber [198, 200-203]. Although few reports on gelatin based nanoparticle for oral administration have been reported but to the best of our knowledge gelatin nanofiber based oral formulation for Amp-B have not explored much except one recent report by Nanda. et. al [200]. Needless to mention, research efforts in the direction of oral administration are still minimal and remain challenging in the field of DDS.

In this chapter, we have selected Amp-B as an amphiphilic model drug in order to deliver it orally using nanofiber based DDS. We have encapsulated Amp-B in the existing GNF based DDS and the release profiles have been studied. Thus, the main objective of this study is to fabricate a nanofiber based drug-carrier encapsulating Amp-B. In furtherance of that, we have also introduced CNOT with the therapeutic dose of AmP-B. Gelatin nanofiber was used as a drug carrier and attempts were made to get prolonged release of Amp-B, which will be extremely beneficial to this field. Based on the previous experience discussed in the prior chapters, we have designed this vehicle aiming to meet the aforementioned objectives of this chapter.

6.3 Materials and Methods

6.3.1 Materials

Gelatin (Type A, 175 bloom), amphotericin-B, hydrochloric acid (ACS, 36.5-38.0%), glutaraldehyde (25% v/v aqueous solution), acetic acid (glacial, ACS, ~99.7%), sodium hydroxide pallets (98%), phosphate buffer saline (pH 7.4), DMSO were purchased from Alfa Aesar. In addition, deionized water (DI) (Milli Q, resistivity 18.1 MΩ.cm) was used throughout the experiments.

6.3.2 Fabrication of the nanofiber membrane

GNF were prepared by electrospinning 20% (w/v) of Gelatin (Type A) solution in acetic acid (10% v/v in distilled water) and DMSO (10% v/v in distilled water) solvent using electrospinning apparatus (Make: E Spin Nanotech Pvt. Ltd, India). 2 mg/ml of amphotericin-b (Amp-B) was added to spinning solution for drug loaded samples (Amp-GNF). Amp-GNF samples were then crosslinked using saturated vapor of GTA (25% v/v aqueous solution) for few minutes in both single and sequentially crosslinking manner (Single 6 min: Amp-GNF C6 and sequentially 6 min: Amp-GNF SC6).

6.3.3 Fabrication of a CNOT

The drug loaded crosslinked GNF mesh was compressed using manual hydraulic press to form a CNOT. The formulation of compressed tablets was done in two different ways: First, Amp-GNF was crosslinked using GTA vapor for 6 min (Amp-GNF C6) and then it was compressed to fabricate CNOT C6 tablets. The other way was to compress sequentially crosslinked sample Amp-GNF SC6 and after compression it formed CNOT SC6 tablet. Later on, we further modified CNOT SC6 by crosslinking the tablet for 2 min which gave the new formulation CNOT SC8. Basically Amp-GNF SC6 mesh was compressed and the tablet (CNOT SC6) was crosslinked for another 2 min which finally gave the fabrication of CNOT SC8.

6.4 *In-vitro* biodegradation study

In-vitro biodegradation studies were carried out to check the stability of the drug loaded crosslinked vehicles (Amp-GNF C6 and Amp-GNF SC6) in pH 7.4. Samples were cut (5 × 5 cm^2) and then weighed (W_d). Dried samples were placed in 50 ml of PBS solution (pH 7.4) at 37 ^{O}C for 72 h. Swelled samples (W_s) were weighed and placed back in the solution. Similarly 50 mg of tablet samples of CNOT C6, CNOT SC6 and CNOT SC8 were taken in order to

check the swelling degree. Each time the samples were dried using tissue paper to remove excess surface water. Swelling degrees (SD) were calculated using the following equation [160]:

$$\text{Swelling degree (SD \%)} = \frac{(W_s - W_d)}{W_d} \times 100$$

Where, W_s = Weight of swelled sample and W_d = Initial weight of dried sample.

Based on our previous experiences, we crosslinked the Amp-B loaded sample (Amp-GNF) in two different strategies as discussed in chapters 4 and 5. The samples were crosslinked with GTA vapor for once for a duration of 6 min for the case of Amp-GNF C6 sample and sequential crosslinking was done for the sample Amp-GNF SC6. We have predicted better control in swelling in the case of Amp-GNF SC6 because of the compactness of the fiber mesh. The uniformity of the concentration of crosslinker within the layers helped to reduce early degradation. Figure 6.1(a) represents the swelling degree of Amp-GNF C6 and Amp-GNF SC6. As the Amp-B molecules consist of hydrophobic and hydrophilic domain in the polymer chain, the hydrophobic chain repels water to keep the fiber matrix safe from hydraulic degradation. The results showed partial degradation of the matrix after 72 h for both the cases. It is interesting to note that again sequential crosslinking reduced the swelling of the matrix in the initial hours drastically for the case with Amp-GNF SC6.

Gathering this knowledge we checked the swelling degree for compressed tablets also. Figure 6.1 (b) shows the swelling degree of CNOT C6 and CNOT SC6. Interestingly, the compressed samples showed excellent stability in PBS and no sign of degradation was noticed even after 72 h. These results explained that the compressed matrix structure creates a diffusional barrier, which leads to less swelling and more stability of the matrix. Further sequential crosslinking of the compressed tablets added even more advantages which led to excellent stability of compressed tablets in PBS for 72 h. These observations led us to check the swelling of CNOT SC8. The modification of CNOT SC6 was done based on the swelling study observation. To reduce the initial swelling degree even further, we crosslinked the CNOT SC6 tablet sample for another 2 more min with GTA vapor (CNOT SC8). This was done to protect the top most layer of the tablet, which resulted in excellent control over swelling in the initial hours. We carried forward the experiment for some more time with the CNOT SC8 sample. We kept the samples for a few more days, maintaining the solution level, temperature and RMP, and took readings in-between. As a result, CNOT SC8 showed surprisingly good stability for a period of almost 10 days. CNOT SC8 was kept for 8 h in pH

1.2 solution and then in PBS (pH 7.4) for 10 days. Figure 6.1 (c) shows that some degradation happened after 6 days, however the overall the matrix was stable for almost 10 days.

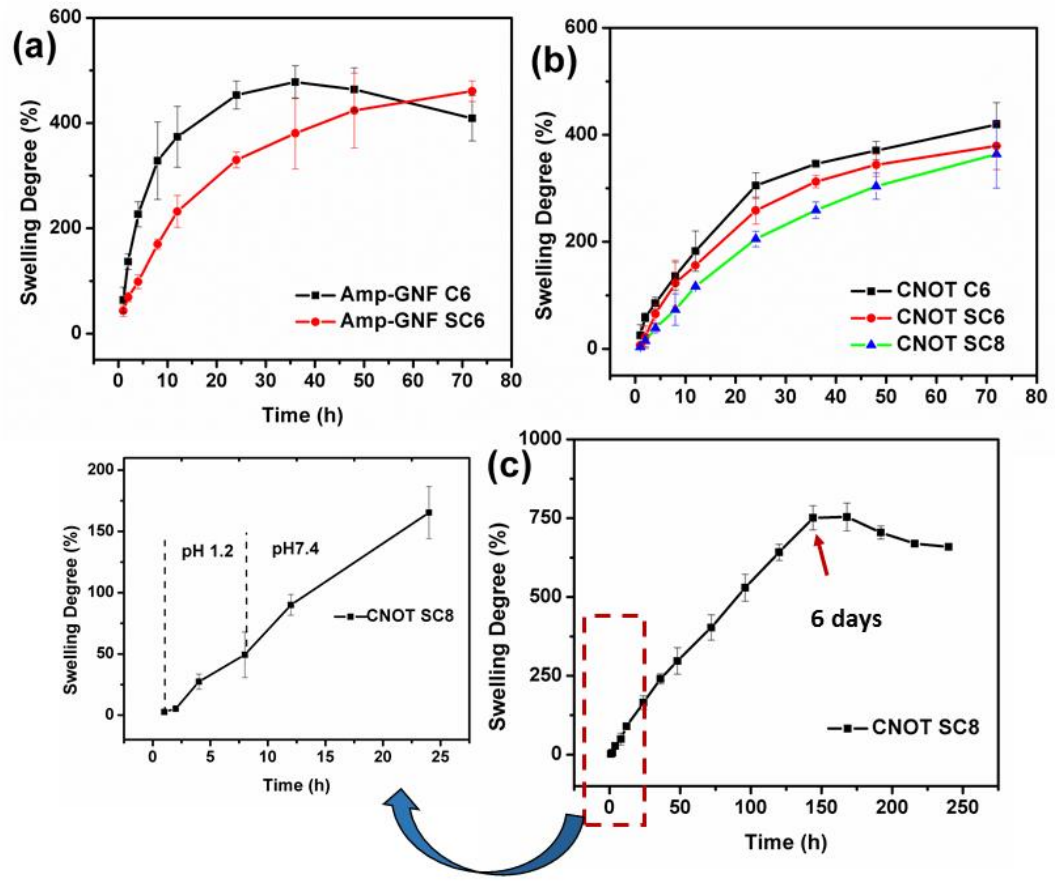

Figure 6.1: Swelling Degree (SD %) of (a) Amp-GNF C6 and Amp-GNF SC6 for 73 h; (b) CNOT C6, CNOT SC6 and CNOT SC8 for 72 h; and (c) CNOT SC8 for 240 h (10days) (results represented are mean ± SD , n=3)

6.5 Characterization

6.5.1 Structural characterization

As mentioned before, Amp-B consists of hydrophobic (the polyene hydrocarbon chain) and a hydrophilic (the polyhydroxyl chain) domain which is shown in Figure 6.2.

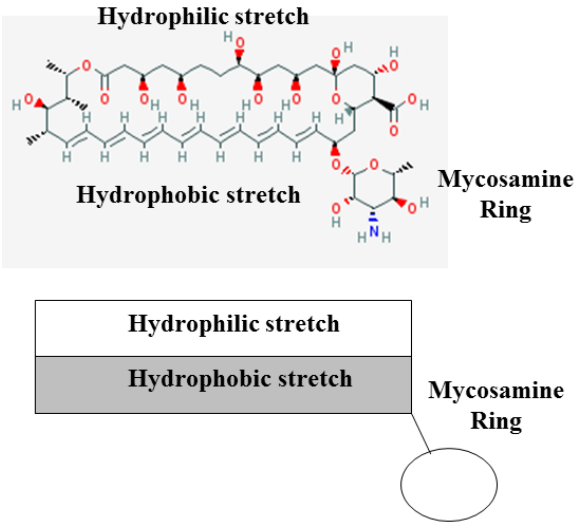

Figure 6.2: Chemical structure of Amphotericin-B [179]

The morphology of the fibers were examined by table top Scanning Electron Microscope (SEM) (Make: Phenom World ProX, Netherlands). To reduce the charging effect, samples were coated with a thin gold layer using a sputter coater (DC Sputtering system, Make: Excel Instruments, India). The optical microscopic image was taken in bright mode with a magnification of 50X.

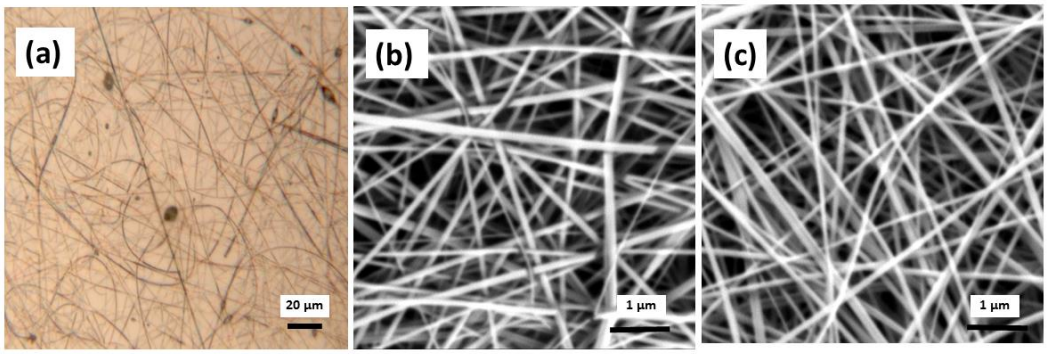

Figure 6.3: (a) Optical microscopic (50X magnification) of Amp-GNF , SEM images of (b) Amp-GNF and (c) Amp-GNF SC6

The optical microscopic and SEM images of Amp-GNF and Amp-GNF SC6 are shown in Figure 6.3. The surface morphology and long continuous fibers are visible in both the optical and SEM images Figure 6.3 (a) and (b). It is anticipated that, the stretched structure of the Amp-B molecules are attached to the surface as well as to the core of the fibers. We have predicted that the hydrophilic stretch of the polymer chain is closely attaching the surface of hydrophilic gelatin nanofibers and the hydrophobic stretch is shielding the fibers. The

alignment of amphiphilic molecules on the surface of the fiber repel the water molecules present in GTA saturated vapor which is presented in Figure 6.3 (c). The top-layer of Amp-GNF SC6 was crosslinked for 2 min with saturated vapor of GTA. It is very evident from Figure 6.3 (c) that Amp-B protected the fiber morphology from unnecessary partial degradation during the crosslinking process. These results can support the observation of degradation study as well. The molecules on the surface take up the role of protecting the fiber morphology from degradation. In addition to that, these long molecules, which are aligned with the fibers, also help in achieving a long and continuous fiber morphology.

6.5.2 Drug-polymer compatibility

To investigate the presence of the drug and the effect of crosslinking on the mesh, samples were characterized by Fourier transform infra-red spectroscopy (FTIR, Bruker Tensor 37, USA) in 4000-400 cm^{-1} range with a resolution of 4 cm^{-1} and 256 scans per samples. Figure 6.4 shows the FTIR peaks of pure drug Amphotericin-B (Amp-B), gelatin nanofibers (GNF) and Amp-B loaded gelatin nanofibers (Amp-GNF).

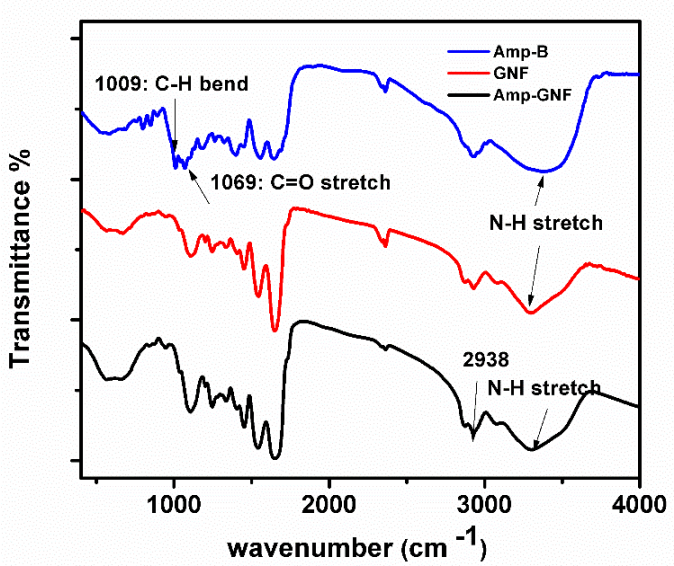

Figure 6.4. FTIR spectra of Amp-B drug, gelatin nanofiber (GNF) and Amp-B loaded gelatin nanofiber (Amp-GNF)

The characteristic peaks of Amp-B are evident from the FTIR plot. The FTIR spectra showed the characteristic absorption bands of gelatin at 3270 cm^{-1} (N-H stretching), 1628 cm^{-1} (amide I, C=O and C-N stretching), 1548 cm^{-1} (amide II, N-H bend and N=C stretch) and 1234 cm^{-1} (amide III, weak N=C stretch, N-H bend) [164]. The major peaks due to the functional groups of Amp-B are clearly visible. The characteristic absorption bands of Amp-

B are secondary amines for N-H stretch (3391 cm^{-1}), alkyl ethers for C-O stretch (1069 cm^{-1}), and C-H bend (trans polyene) in region of 1009 cm^{-1}, are present in the FTIR spectra of Amphotericin B loaded gelatin nanofibers. These results showed that due to electrospinning the drug did not change its characteristic peaks. Thus, it can ben concluded that the chemical integrity of the drug is intact in the gelatin based matrix [200].

6.6 Drug release performance

Based on the swelling study, we had further selected CNOT SC8 sample for the *In-vitro* release study, which was represented in Figure 6.5. The drug concentration (µg/ml) Vs time (min) data and standard curve of Amp-B is presented in Appendix B (Table B6) and Appendix C respectively. The *in-vitro* cumulative study showed controlled release of Amp-B from the well-engineered compressed tablet. From the swelling study, we also derived the idea of the sustainability of the vehicle in PBS (pH 7.4). The swelling rate was very slow which led to less water retention in the system and that in turn helped to keep the compressed tablet intact. As the swelling degree was low for the sample, the mobility of water molecules was very slow. The tablet was also coated with 2 min of crosslinking with GTA vapor, which acted as an added barrier against the entering water molecules in the matrix. The compressed matrix was also sequentially crosslinked, which gave another layer of barricade to the water molecules. Additionally, the drug molecules, which consists of both hydrophobic and hydrophilic stretch, helped the fibers from early degradation. Thus, the water molecules needed to cross three different layers of barriers to enter into the matrix. It took a long time for the water molecules to penetrate the GTA crosslinked extreme outer layer of the tablet, and then they crossed the compressed fiber matrix, which was again sequentially crosslinked and then finally the molecules attacked the fiber where hydrophobic stretch of the Amp-B was shielded the drug. Following this, when enough water had entered into the matrix, due to polymer relaxation and swelling, the drug started to come out from the matrix very slowly. These three layers of protection gave an extraordinarily prolonged release, which almost follows the zero-order release profile.

It is justifiable to mention that, this vehicle is not only capable of higher drug loading but can also release the drug in a very controlled way for almost 10 days. As discussed earlier, fabricating a cheap vehicle which is made of a natural polymer and a simple and scalable fabrication method can make the drug vehicle affordable which is a critical concern till date.

Apart from that, this oral administrative vehicle can release the drug for a longer period, which will again be convenient to patients.

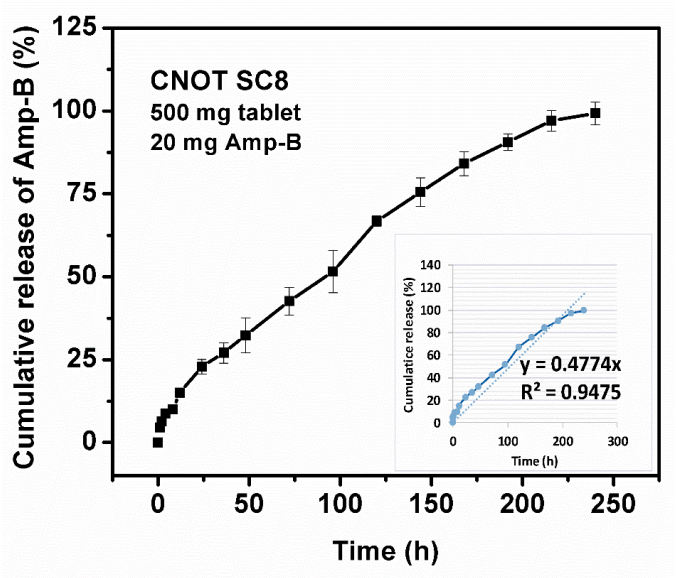

Figure 6.5: *In-vitro* cumulative release of Amp-B from CNOT SC8 tablet for 10 days in PBS (pH 7.4) (results represented are mean ± SD , n=3)

6.7 Summary

The observation from this study reveals interesting features of this newly developed vehicle in order to deliver Amp-B in a zero-order release. The outcome of this research is quite promising in various aspects.

1. First, oral administration of Amp-B is a challenge and scanty research with gelatin nanofibers based drug-carrier for Amp-B exists. An attempt at delivering Amp-B using gelatin nanofibers was reported [200]. However, in the article authors focused on the fabrication of fibers and the release of Amp-B was only for 14 h.
2. To improve the bioavailability and reduce the cytotoxicity of the drug, several research attempts on nano-formulation of new vehicle have been taken up. However, this resulted in increased expenses in most of the cases. In addition, several synthetic polymers and co-polymer were used and the complexity of the vehicle made it more expensive. Thus, in this study we have used gelatin as an excipient, which is natural, cheap and widely acceptable by the pharmaceutical industries. Again, electrospinning is also a very simple and scalable process. These might reduce the overall cost of the formulation.
3. Excellent fiber morphology with Amp-B was seen. We assumed that the hydrophobic and hydrophilic part of the Amp-B molecule helped to form continuous straight fibers while

electrospinning the drug loaded polymer solution. The molecules might have arranged in such way so that it helped the fibers to stretch and get such fine and continuous fibers.

4. In addition to that, compressed nanofiber oral tablet (CNOT) has been formed with 20 mg of Amp-B which gives us a glimpse of a realistic tablet with proper therapeutic doses.

5. Adding to that, the newly fabricated CNOT exhibited excellent stability in PBS for almost 10 days. Although degradation took place after 6 days, it nevertheless showed promising results and great control over the swelling for almost 10 days.

6. The most important outcome of this research was to achieve zero-order release of drug for a prolonged period with an appreciable loading capacity (rare in the most of the DDS research studies). Due to excellent controlled swelling of the vehicle, this new formulation certainly showed fantastic stability as well as zero-ordered release for crosslinked CNOT sample.

These results provide an excellent platform to carry forward the work and to examine the vehicle in all other aspects, so that it be employed for the release of different low-soluble drug molecules in the desired release profile.

6.8 Highlights of this work and future directions

The aim of this work was to fabricate a nanofiber based DDS which can be suitable for Amp-B. We also addressed the fact that, Amp-B is very challenging to deliver orally. Despite different nanoformulations that have existed for the last few decades, oral based DDS is extremely limited. In addition to that, the complex nanoformulation of Amp-B based DDS makes it unaffordable. Given these limitations, gelatin based nanofiber formulation is scalable and affordable.

This CNOT formulation was fabricated with 20 mg of Amp-B, which met the therapeutic dose of the drug. It also showed excellent stability in PBS for almost 10 days and achieved a zero-order release for that duration of time. These results certainly directs us towards the oral formulation of low-soluble drug molecules. Although, this newly developed CNOT formulation showed promising results, extensive research and understanding is required to fabricate oral formulation for Amp-B.

In the end note of this work, the CNOT formulations need to be studied in further detail by performing different microbial assays to check the effectivity of the vehicle along with the cell line studies to check its effect on healthy cells. Natural, cheap polymer gelatin based CNOT certainly showed excellent stability and controlled release for almost 10 days. This feature of the vehicle certainly adds another feather in its cap.

Chapter 7

Summary and Future Directions

7.1 Summary

This thesis details the process of fabricating various polymer based DDSs aimed at delivering drug molecules with low solubility though the oral route. In conclusion, this section revisits the objectives set out in chapter 1 and discusses the respective results achieved in meeting these challenges, chapter-wise. Chapter 1 descibes the historical progression of controlled drug delivery technology, the kinds of DDSs developed over a period in last six decades, the selection of the polymer and drug for our research work followed by the objectives and a layout of the thesis. The literature review discussing the evolution of controlled DDSs from macroscopic to microscopic to the nanoscopic scale across different era provides the justification for the choice of polymer and the nature of drug molecules which bring to the fore the novelty of our present definition.

7.1.1 Revisiting the objectives

- Taking into account our primary objectives of the study mentioned in chapter 1, first, we selected gelatin as an excipient for all different DDS for its biodegradable and bioadhesive nature. Gelatin is a well accepted natural polymer which is FDA approved, cost effective and also widely used in biomedical industries.
- The next objective was to develop a DDS designed to achieve drug molecules with low solubility. The delivery of low-soluble drug molecules is a challenge and we met this

objective by fabricating a polymeric DDS for hydrophobic molecule piperine and amphiphilic molecule Amphotericin-B.

- Next, the fabrication of DDS with zero-order release profiles has also been discussed in the following chapters..
- The subsequent objective was to fabricate polymeric vehicles with zero-order release profile with minimal use of toxic crosslinkers. Formulating nanostructured vehicle reduced the exposure time of crosslinker, thus, reducing the scope of its adverse toxic effect.
- To achieve the next objective, we studied the drug-polymer interactions and checked the chemical, thermal and degradation studies for the vehicle. We took into account the drug-polymer conjugate as a whole system and the performance of this system has been discussed in the chapters.
- Moving to the last point of the objectives, we successfully fabricated a DDS which showed flexible release profiles according to the required treatment. This method takes a general approach to designing such vehicles which in turn can address the need for delivering low-soluble drugs with realistic drug loading.
- Finally, a practical drug with realistic dosage in a compressed tablet form was tested. Results show 10 days long near zero-order release. This humble effort has been emerged from our experimental journey in this area (depicted in the chapters of this thesis). Present research paves the way to take this formulation to the next level of testing with microbial assay and cell line studies before getting elevated for full animal studies.

In this thesis, we have met all of the stated objectives in chapter 1, discussed in detail from chapter 2 onwards till chapter 6. We have presented the development of the different DDS, starting from cast-film to nanofiber based film to compressed tablets through the chapters. Additionally, these chapters also cover the reasons for the modification of the vehicle depending on the release profiles and drug loading mechanism.

7.1.2 Discussion of key results from each chapter

- Chapter 2 discusses the fabrication of cast-film using gelatin as an excipient for the hydrophobic molecule, piperine. We checked its structural characterization, drug-polymer compatibility and drug release performances. We used GTA solution as a crosslinker for 10 mins which yielded good stability in different physiological pHs. The variation of GTA concentration and polymer concentration played a very important role in achieving different release profiles. The variation of the diffusion path according to different concentrations of

polymers and also the entanglement of drug-polymer molecules along with the presence of crosslinker showed a drastic change in the release profiles.

The main outcome of this chapter is the establishment of drug-polymer compatibility and the stability of the vehicle using different concentrations of the polymer and crosslinker. However, the drawback of the present vehicle is the use of GTA solution which is toxic in nature and does not yield a zero-order release profile. In an attempt to reduce the crosslinking time, we decided to fabricate a nanostructured porous vehicle.

- In chapter 3, we continued with the same excipient and drug, and fabricated a nanofiber based mesh in order to deliver piperine in different physiological pHs. We crosslinked the mesh using GTA saturated vapor for 6 to 8 min (instead of exposing it for a few hours or a few days) to achieve increased stability in PBS solution that would last for atleast 24 h. The use of GTA vapor in place of GTA solution not only reduced the unnecessary toxicity but also resulted in better stability in PBS because of the penetration power of GTA in its vapor form through the porous nanofibers. It is worth highlighting that the reduction of exposure time to GTA vapor certainly adds another dimension to the fabrication of this DDS. In this chapter we investigated the effects of different crosslinking time (4 min, 6 min and 8 min) and different pHs (pH 1.2, 6, 7.4 and 8) on release profile to find the controlling key factors in order to achieve the desired release profile. Despite the fact that plenty of research with respect to the use of gelatin nanofiber in drug delivery exist, to the best of our knowledge and with the exception of a recent demonstration of the slow release of nystatin, an anti-fungal reagent, no study of the controlled release of a hydrophobic drug using electrospun gelatin nanofiber has been performed. Mostly, recent reports have either focused on the release of hydrophilic drugs or have used prolonged periods of crosslinking (almost 24 h) or have reported burst-release profiles. Thus, this work, addresses all these challenges and establishes a gelatin nanofiber based system as a potential drug carrier with low soluble drugs.
- Carrying forward the newly developed vehicle to achieve zero-order release profiles, we proposed to increase the diffusional barrier between the drug molecules in the vehicle to the release medium. To accomplish that, a sandwiched-structured fiber mesh was introduced; the process of creating the same as well as the requirement for it was discussed in Chapter 4. The drug loaded core layer was protected by two barrier layers of gelatin nanofiber mesh from both sides. This controls the movement of drug molecules to a great extent. A variety of combinations of barrier and core layers is studied extensively in this chapter to achieve zero-order release profile.

This chapter mainly focuses on the modification of the existing vehicle by adding barrier layers and also through crosslinking strategies. In this chapter, results showed a zero-order

release profile in different pH solutions almost for 48 h. Therefore, the main outcome of this chapter is the modification of the existing gelatin nanofiber based vehicle through the introduction of a multi-layer structure and through sequential crosslinking methods so as to deliver a highly loaded piperine drug in a zero-order manner.

- In chapter 5, we mainly focused on the comparative studies of single crosslinking over sequential crosslinking of single-layered and multi-layered nanofiber mesh. We tried to bring together the idea of a multi-layered fiber mesh and a sequentially crosslinked mesh in this chapter. Moreover, structural characterization, drug-polymer compatibility, and drug release performance were also studied. This section contributes to a better understanding of the crosslinking mechanism employed in enhancing the porous structure of the nanofiber based mesh to reduce diffusion and also tries to identify the key parameters which can control the diffusion of drug molecules from the vehicle to the release medium. This sensitivity study certainly helps in understanding the drug-polymer system as a whole which in turn helps us to apply the system to different kinds of drug molecules possessing different molecular sizes.
- Gathering all this knowledge about the piperine (hydrophobic drug) and gelatin based drug delivery vehicle, we have now moved on to an amphiphilic molecule, Amphotericin B (Amp-B) loaded gelatin based vehicle in chapter 6. Amp-B is almost a three times bigger molecule and is also amphiphilic in nature. The main aim of this chapter is to establish a novel drug delivery vehicle which can be used for different kinds of drug molecules. Thus, we fabricated Amp-B loaded gelatin nanofiber mesh and characterized the vehicle in terms of morphology, drug-polymer compatibility and release performance. We tried to meet the realistic drug dosage of Amp-B and fabricated a compressed nanofiber tablets for the same. Amp-B loaded nanofiber mat was sequentially crosslinked for 6 min and after making the tablet it was again crosslinked for another 2 min. This kind of formulation has shown excellent stability in PBS and almost zero-order release profile for almost 10 days. Therefore, the 500 mg gelatin nanofiber compressed tablet with 20 mg of Amp-B certainly shows promising results and also draws attention toward the need for further research into this newly fabricated polymeric vehicle.

In nut-shell, in this thesis the humble attempt was made to fabricate a general drug carrier which can deliver poor soluble drug molecules. In order to achieve that, we had encapsulated Piperine and Amp-b in the vehicle and delivered in zero order manner. Piperine is poor water soluble drug and Amp-B is amphiphilic in nature. Amphotericin B is three times bigger molecule than piperine. The focus of the study was to design a vehicle by fabricating single or different layered structure mesh or crosslinking the vehicle with different strategies. The modification was done purely based on release study results. The FTIR and release study

depicted the presence of drug molecules in the matrix without reacting with the excipient. In addition to that, the modification or designing of the vehicle did not interfere the molecule or its therapeutic values. Based on the limited data with two drugs as examined in this presented work, it won't be fair to claim that, this drug carrier can be a novel drug delivery vehicle, which can deliver any kinds of drug. However, the aim was on fabrication of the mesh and different crosslinking strategies in order to develop a general drug carrier for particularly low soluble drug molecules. Considering that aim, in this thesis different range of drugs with a wide difference in molecular weights and hydrophobicity were used as model drug to get a glimpse of potential of nanofiber-based carrier as a novel drug carrier.

7.2 Future directions

Based on the key results of this thesis, a number of future possibilities for working with this newly formulated drug delivery vehicle exist. The following are some of them.

1. Multi-layered GNF can be used as dual/multi-drug carrier. Encapsulating different drugs in different layers of the mesh can yield a range of desired release profiles, which can certainly be an interesting study to perform.
2. Although we have drastically reduced the GTA vapor exposure time to 6 min, introducing porous nanofibers could probably increase the penetration capability of the GTA molecules further, which can lead to a considerable reduction of exposure time to GTA vapor. This could play an important role in the diffusion of drug molecules from the matrix to release medium.
3. Core-shell nanofiber based DDS could also form a very interesting study. The core-shell nanofiber based tablet can drastically reduce burst release followed by a prolonged release of drug.
4. Release study of compressed nanofiber based tablets with a range of different molecular size and type of drugs could form a sophisticated area of study. This will help in fabricating a novel drug carrier, which could be modified according to the type of drugs and kind of release profiles.

References

[1] R. Langer. New methods of drug delivery. Science 249 (1990) 1527–33

[2] R.S. Langer, and N. A. Peppas. Present and future applications of biomaterials in controlled drug delivery systems. Biomaterials 2 (1981) 201–214.

[3] K.E. Uhrich, S.M. Cannizzaro, R.S. Langer, and K.M. Shakesheff. Polymeric systems for controlled drug release. Chem. Rev. 99 (1999) 3181–3198.

[4] A.K. Bajpai, S.K. Shukla, S. Bhanu, and S. Kankane. Responsive polymers in controlled drug delivery. Prog. Polym. Sci. 33 (2008) 1088–1118.

[5] P.J. Lef, G. Paolisso, J. Scheen, and J.C. Henquin. Pulsatility of insulin and glucagon release:physiological significance and pharmacological implications. Diabetologia (1987) 443–452.

[6] W. Bensen, A. Frcpc, G.T. Frcpc, J.W. Frcpc, P. Quigley, J. Eisenhoffer, Z.H. Mba, A.C. Darke, A.D. Beaulieu, P.M. Peloso, and B. Haraoui. Once-daily, controlled-release tramadol and sustained-release diclofenac relieve chronic pain due to osteoarthritis: A randomized controlled trial. Pain Res Manage 13 (2008) 103–110.

[7] A. Philip, and B. Philip. Colon Targeted Drug Delivery Systems: A review on primary and novel approaches. Oman Med. J. 25 (2010) 70–78.

[8] K. Park. Controlled drug delivery systems: Past forward and future back. J. Control. Release 190 (2014) 3–8.

[9] W.H. Helfand, and D.L. Cowen. Evolution of pharmaceutical oral dosage forms. Pharm. Hist. 25 (1983) 3–18.

[10] R. Maurya, P.K. Sharma, and R. Malviya. A review on controlled drug release formulation :Spansules. Int J Pharm Sci Res 5 (2014) 78–81.

[11] Ping. I. Lee, and Jian-Xin Li. Evalution of oral controlled release dosage forms. Oral Control. Release Formul. Des. Drug Deliv. Theory to Pract. (2010) 21–31.

[12] J. Folkman, D.M. Long Jr., and R. Rosenbaum. Silicone rubber: a new diffusion property useful for general anesthesia. Science 154 (1966) 148–149.

[13] J. Folkman, and D.M. Long. The Use of silicone rubber as a carrier for Prolonged drug therapy. J. Surg. Res. 4 (1964) 139-142.

[14] A.S. Hoffman. The origins and evolution of “controlled” drug delivery systems. J. Control. Release 132 (2008) 153–163.

[15] E. Lavik, M.H. Kuehn, and Y.H. Kwon. Novel drug delivery systems for glaucoma. Eye 25 (2011) 578–586.

[16] K.L. Macoul, and D. Pavan-Langston. Pilocarpine ocusert system for sustained control of ocular hypertension. Arch Ophthalmol 93 (1975) 587–590.

[17] D. Shoupe, and D.R. Mishell. Norplant: Subdermal implant system for long-term contraception. Am. J. Obstet. Gynecol. 160 (1989) 1286–1292.

[18] A. Zaffaroni, Atherton, and Calif. U. S. Patent 3,797,494, (1974).

[19] M.R. Prausnitz, and R. Langer. Transdermal drug delivery. Nat. Biotechnol. 26 (2009) 1261–1268.

[20] M.R. Prausnitz, S. Mitragotri, and R. Langer, Current status and future potential of transdermal drug delivery. Nat. Rev. Drug Discov. 3 (2004) 115–124.

[21] Aaron C. Anselmo, and Samir Mitragotri. An overview of clinical and commercial impact of drug delivery systems. J. Control. Release. 190 (2014) 15–28.

[22] H. Chuang, D. Ph, M. Trieu, J. Hurley, E.J. Taylor, M.R. England, and S.A. Nasraway. Pilot studies of transdermal continuous glucose measurement during and after cardiac surgery. J. Diabetes Sci Technol 2 (2008) 595–602.

[23] V. Malaterre, J. Ogorka, N. Loggia, and R. Gurny. Oral osmotically driven systems: 30 years of development and clinical use. Eur. J. Pharm. Biopharm 73 (2009) 311–323.

[24] S.A. Rose, and D.J.F. Nelson. A Continuous long-term injection. Austral. J. exp. Biol. 33 (1955) 415–420.

[25] R.A. Keraliya, C. Patel, P. Patel, V. Keraliya, T.G. Soni, R.C. Patel, and M.M. Patel. Osmotic Drug Delivery System as a Part of Modified Release Dosage Form. ISRN Pharm. 2012 (2012) 1–9.

[26] Felix Theeuwes, Los Altos, Calif; Takeru Higuchi, Lawrence, Kans. U. S. Patent 3,845,770 (1976).

[27] F. Theeuwes, D. Swanson, P. Wong, P. Bonsen, V. Place, K. Heimlich, K.C. Kwan. Elementary osmotic pump for indomethacin, J. Pharm. Sci. 72 (3) (1983) 253–258.

[28] M. Weintraub, G. Ginsberg, E.C. Stein, P.R. Sundaresan, B. Schuster, P. O’Connor, and L.M. Byrne. Phenylpropanolamine OROS (Acutrim) vs. placebo in combination with caloric restriction and physician-managed behavior modification. Clin. Pharmacol. Ther 39 (1986) 501–509.

[29] D. Coghill, and S. Seth. Osmotic, controlled-release methylphenidate for the treatment of ADHD. Expert Opin. Pharmacother 7 (2006) 2119–38.

[30] R. Eldor, E. Arbit, A. Corcos, and M. Kidron. Glucose-Reducing Effect of the ORMD-0801 Oral Insulin Preparation in Patients with Uncontrolled Type 1 Diabetes: A Pilot Study, PLOS One. 8 (2013) 4–7.

[31] S. Verma, D. Miles, L. Gianni, I.E. Krop, M. Welslau, J. Baselga, M. Pegram, Do-Youn. Oh, V. Diéras, E. Guardino, L. Fang, M.W. Lu, S. Olsen, and K. Blackwell. Trastuzumab Emtansine for HER2-Positive Advanced Breast Cancer. N. Engl. J. Med. 367 (2012) 1783–1791.

[32] K. Park. Facing the truth about nanotechnology in drug delivery. ACS Nano. 7 (2013) 7442–7447.

[33] Y. Yun, B.K. Lee, and K. Park. Controlled drug delivery systems: The next 30 years. Front. Chem. Sci. Eng. 8 (2014) 276–279.

[34] Brian P. Timko, Kathryn Whitehead, Weiwei Gao, Daniel S. Kohane, Omid Farokhzad, Daniel Anderson,and Robert Langer. Advances in Drug Delivery, J. Chem. Technol. Biotechnol. 90 (2015) 1167–1168.

[35] M. Morishita, and N.A. Peppas. Is the oral route possible for peptide and protein drug delivery?. Drug Discov. Today. 11 (2006) 905–910.

[36] S. Eiamtrakarn, Y. Itoh, J. Kishimoto, Y. Yoshikawa, N. Shibata, M. Murakami, and K. Takada. Gastrointestinal mucoadhesive patch system (GI-MAPS) for oral administration of G-CSF, a model protein. Biomaterials. 23 (2002) 145–152.

[37] J.K. Vasir, K. Tambwekar, and S. Garg. Bioadhesive microspheres as a controlled drug delivery system. Int. J. Pharm. 255 (2003) 13–32.

[38] K. Whitehead, Z. Shen, and S. Mitragotri. Oral delivery of macromolecules using intestinal patches: Applications for insulin delivery. J. Control. Release. 98 (2004) 37–45.

[39] A. Patel, K. Cholkar, V. Agrahari, and A.K. Mitra. Ocular drug delivery systems: an overview. World J. Pharmacol. 2 (2015) 47–64.

[40] V.K. Yellepeddi, and S. Palakurthi. Recent Advances in Topical Ocular Drug Delivery. J. Ocul. Pharmacol. Ther. 32 (2016) 67–82.

[41] S. Türker, E. Onur, and Y. Özer. Nasal route and drug delivery systems. Pharm. World Sci. 26 (2004) 137–142.

[42] L. Casettari, and L. Illum. Chitosan in nasal delivery systems for therapeutic drugs. J Control Release. 190 (2014) 189–200.

[43] D. Paolino, M. Fresta, P. Sinha, and M. Ferrari. Drug delivery system. Encyclopedia

of Medical Devices and Instrumentation. 2nd Edition (2006) 437-496.

[44] M. Kumar, A. Misra, A.K. Babbar, A.K. Mishra, P. Mishra, and K. Pathak. Intranasal nanoemulsion based brain targeting drug delivery system of risperidone. Int. J. Pharm. 358 (2008) 285–291.

[45] H. Brem, and P. Gabikian. Biodegradable polymer implants to treat brain tumors. J. Control. Release. 74 (2001) 63–67.

[46] H.M.Mansour,Y.S.Rhee, and X. Wu.Nanomedicine in pulmonary delivery. Int J Nanomedicine. 4 (2009) 299–319.

[47] K. Vermani and S. Garg. The scope and potential of vaginal drug delivery. Pharm. Sci. Technol. Today.3(2000) 359-365.

[48] V. Muzykantov, S. Muro. Targeting delivery of drugs in the vascular system. Int J Transp Phenom.12(1-2) (2011) 41–49.

[49] V. Muzykantov. Targeted Therapeutics and Nanodevices for Vascular Drug Delivery: Quo Vadis? IUBMB Life 63(8) (2011) 583–585.

[50] E. Koren, and V.P. Torchilin, Drug carriers for vascular drug delivery, IUBMB Life, 63(8) (2011) 586–595.

[51] S. Grund, M. Bauer, and D. Fischer. Polymers in drug delivery-state of the art and future trends. Adv. Eng. Mater. 13 (2011) 61–87.

[52] N.M.D. Siddiqui, G. Garg, and P.K. Sharma. A Short Review on "A Novel Approach in Oral Fast Dissolving Drug Delivery System and Their Patents." Adv. Biol. Res. (Rennes). 5 (2011) 291–303.

[53] Z. Dong, Q. Wang, and Y. Du. Alginate/gelatin blend films and their properties for drug controlled release. J. Memb. Sci. 280 (2006) 37–44.

[54] N. Salamat-Miller, M. Chittchang, and T.P. Johnston. The use of mucoadhesive polymers in buccal drug delivery. Adv. Drug Deliv. Rev. 57 (2005) 1666–1691.

[55] J. H. Kim, S. I. Kim, I.B. Kwon, M. H. Kim, and J. I. Lim. Simple fabrication of silver hybridized porous chitosan-based patch for transdermal drug-delivery system. Mater. Lett. 95 (2013) 48–51.

[56] T. Tsukagoshi, Y. Kondo, and N. Yoshino. Preparation of thin polymer films with controlled drug release. Colloids Surfaces B Biointerfaces. 57 (2007) 219–225.

[57] F. Croisier, C. Jérôme. Chitosan-based biomaterials for tissue engineering, Eur. Polym. J. 49 (2013) 780–792.

[58] E. Calo, and V. V Khutoryanskiy. Biomedical Applications of hydrogels: A review of patent and commercial products. Eur. Polym. J. 65 (2015) 252–267.

[59] T.R. Hoare, and D.S. Kohane. Hydrogels in drug delivery: Progress and challenges.

Polymer 49 (2008) 1993–2007.

[60] M.F. Akhtar, M. Hanif, and N.M. Ranjha. Methods of synthesis of hydrogels . . . A review. Saudi Pharm J. 24 (2016)554–559.

[61] E. M. Ahmed. Hydrogel : preparation , characterization and applications: A review. J. Adv. Res. 6 (2015) 105–121.

[62] Y. Qiu, and K. Park, Environment-sensitive hydrogels for drug delivery, Adv. Drug Deliv. Rev. 53 (2001) 321–339.

[63] U.Bhutani, A.Laha, K.Mitra, and S.Majumdar, Sodium alginate and gelatin hydrogels: Viscosity effect on hydrophobic drug release, Mater. Lett. 164 (2016) 76–79.

[64] A. Samad, Y. Sultana, and M. Aqil, Liposomal Drug Delivery Systems: An Update Review, Curr. Drug Deliv. 4 (2007) 297–305.

[65] K. Tahara, and H.Takeuchi. Liposome-Based Mucoadhesive Formulations, Mucoadhesive Mater. Drug Deliv. Syst. (2014) 297–308.

[66] T. Lian, and R.J. Ho. Trends and developments in liposome drug delivery systems. J. Pharm. Sci. 90 (2001) 667–680.

[67] J.W. Park. Liposome-based drug delivery in breast cancer treatment. Breast Cancer Res. 4 (2002) 95.

[68] J.A. Shabbits, G.N.. C. Chiu, and L.D. Mayer. Development of an in vitro drug release assay that accurately predicts in vivo drug retention for liposome-based delivery systems, J. Control. Release. 84 (2002) 161–170.

[69] A. Sharma, and U. S. Sharma. Liposomes in drug delivery: progress and limitations. Int. J. Pharm. 154 (1997) 123 140.

[70] S. Zununi Vahed, R. Salehi, S. Davaran, and S. Sharifi. Liposome-based drug co-delivery systems in cancer cells, Mater. Sci. Eng. C. 71 (2017) 1327–1341.

[71] J. Gong, M. Chen, Y. Zheng, S. Wang, and Y. Wang. Polymeric micelles drug delivery system in oncology. J. Control. Release. 159 (2012) 312–323.

[72] G. Gaucher, M.H. Dufresne, V.P. Sant, N. Kang, D. Maysinger, and J.C. Leroux. Block copolymer micelles: Preparation, characterization and application in drug delivery. J. Control. Release. 109 (2005) 169–188.

[73] N. Nasongkla, E. Bey, J. Ren, H. Ai, C. Khemtong, J.S. Guthi, S. Chin, A D. Sherry, D. A Boothman, and J. Gao. Multifunctional Polymeric Micelles as Cancer-Targeted, MRI-Ultrasensitive Drug Delivery Systems. Nano Lett. 6 (2006) 2427-2430.

[74] H. Rosen, and T. Abribat. Timeline: The rise and rise of drug delivery. Nat. Rev. Drug Discov. 4 (2005) 381–385.

[75] S. Suri, H. Fenniri, and B. Singh. Nanotechnology-based drug delivery systems, J.

Occup. Med. Toxicol. 2 (2007) 16.

[76] C. Giovino, I. Ayensu, J. Tetteh, and J.S. Boateng. Development and characterisation of chitosan films impregnated with insulin loaded PEG-b-PLA nanoparticles (NPs): A potential approach for buccal delivery of macromolecules. Int. J. Pharm. 428 (2012) 143–151.

[77] V.S. Lin, Y. Zhao, B.G. Trewyn, and I.I. Slowing. Mesoporous Silica Nanoparticle-based Double Drug Delivery System for Glucose Responsive Controlled Release of Insulin and Cyclic AMP. J. Am. Chem. Soc. 131 (2009) 8398–8400.

[78] R. Singh, and L.J. W. Nanoparticle-based targeted drug delivery. Exp. Mol .Pathol. 86 (2009) 215–223.

[79] S. Gelperina, K. Kisich, M.D. Iseman, and L. Heifets. The potential advantages of nanoparticle drug delivery systems in chemotherapy of tuberculosis. Am. J. Respir. Crit. Care Med. 172 (2005) 1487–1490.

[80] S. Zhanga, R. Langer, and G. Traversoa. Nanoparticulate drug delivery systems targeting inflammation for treatment of inflammatory bowel disease. Nano Today 16 (2017) 82–9.

[81] M. Ferrari. Cancer nanotechnology: opportunities and challenges. Nat. Rev. Cancer. 5 (2005) 161–171.

[82] A. Sharma, T. Garg, A. Aman, K. Panchal, R. Sharma, S. Kumar, and T. Markandeywar. Nanogel-An advanced drug delivery tool: Current and future. Artif. Cells, Nanomedicine, Biotechnol. (2014) 1–13.

[83] H. Zhang, Y. Zhai, J. Wang, and G. Zhai. New progress and prospects: The application of nanogel in drug delivery. Mater. Sci. Eng. C. 60 (2016) 560–568.

[84] R.T.Chacko, J.Ventura, J.Zhuang, and S.Thayumanavan. Polymer nanogels: A versatile nanoscopic drug delivery platform. Adv. Drug Deliv. Rev. 64 (2012) 836–851.

[85] A.V.Kabanov, and S.V.Vinogradov. Nanogels as pharmaceutical carriers: Finite networks of infinite capabilities. Angew. Chemie. Int. Ed. 48 (2009) 5418–5429.

[86] Q. Zhang, J. Colazo, D. Berg, S.M. Mugo, and M.J. Serpe. Multiresponsive Nanogels for Targeted Anticancer Drug Delivery. Mol. Pharm. 14 (2017) 2624–2628.

[87] J.-H. Ryu, R.T. Chacko, S. Jiwpanich, S. Bickerton, R.P. Babu, and S. Thayumanavan. Self-Cross-Linked Polymer Nanogels: A Versatile Nanoscopic Drug Delivery Platform. J. Am. Chem. Soc. 3 (2010) 2–10.

[88] D.-G. Yu, L.-M. Zhu, K. White, and C. Branford-White. Electrospun nanofiber-based drug delivery systems. Health 1 (2009) 67–75.

[89] R. Rosic, J. Pelipenko, J. Kristl, P. Kocbeck, and S. Baumgartner. Properties, engineering and applications of polymeric nanofibers: current research and future advances. Chem. Biochem. Eng. Q. 26 (2012) 417–425.

[90] X. Hu, S. Liu, G. Zhou, Y. Huang, Z. Xie, and X. Jing. Electrospinning of polymeric nano fibers for drug delivery applications. J. Control. Release 185 (2014) 12–21.

[91] D.F. Williams. On the nature of biomaterials. Biomaterials 30 (2009) 5897–5909.

[92] D.F. Williams. On the mechanisms of biocompatibility. Biomaterials 29 (2008) 2941–2953.

[93] J. Safari, and Z. Zamegar. Advanced drug delivery systems : Nanotechnology of health design: A review. J. Saudi Chem. Soc. 18 (2014) 85–99.

[94] A.O. Elzoghby. Gelatin-based nanoparticles as drug and gene delivery systems: Reviewing three decades of research. J. Control. Release. 172 (2013) 1075–1091.

[95] A. Bernkop-schnürch, and S. Dünnhaupt. Chitosan-based drug delivery systems. Eur. J. Pharm. Biopharm. 81 (2012) 463–469.

[96] S. Chakraborty, I.C Liao, A. Adler, and K. W. Leong. Electrohydrodynamics: A facile technique to fabricate drug delivery systems. Adv Drug Deliv Rev. 61(12)(2009)1043–1054.

[97] H.H. Tønnesen, and J. Karlsen. Alginate in Drug Delivery Systems. Drug Dev. Ind. Pharm. 28 (2002) 621–630.

[98] J. Necas, L. Bartosikova, P. Brauner, and J. Kolar. Hyaluronic acid (hyaluronan): A review, Vet. Med. 53 (2008) 397–411.

[99] M. Maeda, S. Tani, A. Sano, and K. Fujioka. Microstructure and release characteristics of the minipellet, a collagen-based drug delivery system for controlled release of protein drugs. J. Control. Release. 62 (1999) 313–324.

[100] C. Kojima, S. Tsumura, A. Harada, and K. Kono. A collagen-mimic dendrimer capable of controlled release. J. Am. Chem. Soc. 131 (2009) 6052–6053.

[101] P. Sunny, N. Kumar, D. Ray, and P. Kumar. Hydrolyzed collagen-based hydrogel system design , characterization and application in drug delivery. 4 (1937) 167–177.

[102] D. Olsen, C. Yang, M. Bodo, R. Chang, S. Leigh, J. Baez, D. Carmichael, M. Perälä, E.R. Hämäläinen, M. Jarvinen, and J. Polarek. Recombinant collagen and gelatin for drug delivery. Adv. Drug Deliv. Rev. 55 (2003) 1547–1567.

[103] O. Germershaus, V. Werner, M. Kutscher, and L. Meinel. Deciphering the mechanism of protein interaction with silk fibroin for drug delivery systems. Biomaterials 35 (2014) 3427–3434.

[104] M. Zhang, J. Liu, Y. Kuang, Q. Li, D.W. Zheng, Q. Song, H. Chen, X. Chen, Y. Xu,

C. Li, and B. Jiang. Ingenious pH-sensitive dextran/mesoporous silica nanoparticles based drug delivery systems for controlled intracellular drug release. Int. J. Biol. Macromol. 98 (2017) 691–700.

[105] H. Wang, T. Dai, S. Zhou, X. Huang, S. Li, K. Sun, G. Zhou, and H. Dou. Self-assembly assisted fabrication of dextran-based nanohydrogels with reduction-cleavable junctions for applications as efficient drug delivery systems. Sci. Rep. 7 (2017) 40011.

[106] X.M. Wu, C.J. Branford-White, L.M. Zhu, N.P. Chatterton, and D.G. Yu. Ester prodrug-loaded electrospun cellulose acetate fiber mats as transdermal drug delivery systems. J. Mater. Sci. Mater. Med. 21 (2010) 2403–2411.

[107] K.A.Athanasiou, G.G.Niederauer, and C.M.Agrawal. Sterilization, toxicity, biocompatibility and clinical applications of polylactic acid / polyglycolic acid copolymers. Biomaterials 17 (1996) 93-102.

[108] E.Schlesinger, N. Ciaccio, and T.A Desai. Polycaprolactone thin-film drug delivery systems: empirical and predictive models for device design. Mater Sci Eng C 57 (2015) 232–239.

[109] D. Klose, F. Siepmann, K. Elkharraz, and J. Siepmann. PLGA-based drug delivery systems: Importance of the type of drug and device geometry. Int. J. Pharm. 354 (2008) 95–103.

[110] S. Fredenberg, M. Wahlgren, M. Reslow, and A. Axelsson. The mechanisms of drug release in poly(lactic-co-glycolic acid)-based drug delivery systems - A review. Int. J. Pharm. 415 (2011) 34–52.

[111] E. Khodaverdi, F.S.M. Tekie, S.A. Mohajeri, F. Ganji, G. Zohuri, and F. Hadizadeh. Preparation and investigation of sustained drug delivery systems using an injectable, thermosensitive, in situ forming hydrogel composed of PLGA–PEG–PLGA, AAPS PharmSciTech. 13 (2012) 590–600.

[112] U.D. Bret, N.S. Lakshmi, and C.T. Laurencin. Biomedical Applications of Biodegradable Polymers. J. Polym. Sci. Part B Polym. Phys. 3 (2011) 832–864.

[113] I. Orienti, R. Trere, B. Luppi, F. Bigucci, T. Cerchiara, G. Zuccari, V. Zecchi, Hydrogels formed by crosslinked poly (vinyl alcohol) as sustained drug delivery systems, Arch. Pharm. Pharm. Med. Chem. 335 (2002) 89–93.

[114] H.M.N. El-Din, A.W.M. El-Naggar, and F.I.A. El Fadle. Radiation synthesis of ph-sensitive hydrogels from carboxymethyl cellulose/poly(ethylene oxide) blends as drug delivery systems. Int. J. Polym. Mater. Polym. Biomater. 62 (2013) 711–718.

[115] A. Kumari, S.K. Yadav, and S.C. Yadav. Biodegradable polymeric nanoparticles

based drug delivery systems. Colloids Surfaces B Biointerfaces. 75 (2010) 1–18.

[116] G. Tiwari, R. Tiwari, S. Bannerjee, L. Bhati, S. Pandey, P. Pandey, and B. Sriwastawa. Drug delivery systems: An updated review. Int. J. Pharm. Investig. 2 (2012) 2-11.

[117] L. Plapied, N. Duhem, A. des Rieux, and V. Préat. Fate of polymeric nanocarriers for oral drug delivery. Curr. Opin. Colloid Interface Sci. 16 (2011) 228–237.

[118] J.O. Morales, and J.T. McConville. Manufacture and characterization of mucoadhesive buccal films. Eur. J. Pharm. Biopharm. 77 (2011) 187–199.

[119] R. Shamma, and N. Elkasabgy. Design of freeze-dried Soluplus/polyvinyl alcohol-based film for the oral delivery of an insoluble drug for the pediatric use. Drug Deliv. 23(2) (2016) 489-99.

[120] M. Nishimura, K. Matsuura, T. Tsukioka, H. Yamashita, N. Inagaki, T. Sugiyama, and Y. Itoh. In vitro and in vivo characteristics of prochlorperazine oral disintegrating film. Int. J. Pharm. 368 (2009) 98–102.

[121] L.F. Siew, a W. Basit, and J.M. Newton. The potential of organic-based amylose-ethylcellulose film coatings as oral colon-specific drug delivery systems. AAPS PharmSciTech. 1 (2000) 22.

[122] M. Foox, and M. Zilberman. Drug delivery from gelatin-based systems. Expert Opin. Drug Deliv. 12 (2015) 1547–1563.

[123] N.C. Ngwuluka, N.A. Ochekpe, and O.I. Aruoma. Naturapolyceutics: The science of utilizing natural polymers for drug delivery. Polymers 6 (2014) 1312–1332.

[124] R.P. Dixit, and S.P. Puthli. Oral strip technology: Overview and future potential. J. Control. Release. 139 (2009) 94–107.

[125] K. Yamamura, S. Ohta, K. Yano, T. Yotsuyanagi, T. Okamura, and T. Nabeshima. Oral mucosal adhesive film containing local anesthetics: In vitro and clinical evaluation. J. Biomed. Mater. Res. 43 (1998) 313–317.

[126] Z.A. Nur Hanani, J. McNamara, Y.H. Roos, and J.P. Kerry. content on the functional properties of extruded gelatin-based composite films. Food Hydrocoll. 31 (2013) 264–269.

[127] N. Ahmad, H. Fazal, B.H. Abbasi, S. Farooq, M. Ali, and M.A. Khan. Biological role of Piper nigrum L. (Black pepper): A review. Asian Pac. J. Trop. Biomed. 2 (2012) S1945–S1953.

[128] G. Shoba, D. Joy, T. Joseph, M. Majeed, R. Rajendran, and P. Srinivas. Influence of piperine on the harmacokinetics of curcumin in animals and human volunteers. Planta Med. 64 (1998) 353–356.

[129] A. Bigi, G. Cojazzi, S. Panzavolta, K. Rubini, and N. Roveri. Mechanical and thermal

properties of gelatin film at different degrees of glutaraldehyde crosslinking. J. Biomed. Mater. Res. 22 (2001) 3–8.

[130] M.G. Cascone, B. Sim, and S. Downes. Blends of synthetic and natural polymers as drug delivery systems for growth hormone. Biomaterials. 16 (1995) 569–74.

[131] A. Bigi, G. Cojazzi, S. Panzavolta, N. Roveri, and K. Rubini. Stabilization of gelatin films by crosslinking with genipin. Biomaterials 23 (2002) 4827–4832.

[132] R.A. De Carvalho, and C.R.F. Grosso. Characterization of gelatin based films modified with transglutaminase, glyoxal and formaldehyde. Food Hydrocoll. 18 (2004) 717–726.

[133] S. Farris, J. Song, and Q. Huang. Alternative reaction mechanism for the cross-linking of gelatin with glutaraldehyde. J. Agric. Food Chem. 58 (2010) 998–1003.

[134] S. Dash, P.N. Murthy, L. Nath, and C. Prasanta. Review kinetic modeling on drug release from controlled drug delivery systems. Acta Pol. Pharm. Res. 67 (2010) 217–223.

[135] T. Higuchi, Rate of release of medicaments from ointment bases containg drug in suspension, J. Pharm. Sci. 50 (1961) 874–875.

[136] J. Xie, and C.H. Wang. Electrospun micro- and nanofibers for sustained delivery of paclitaxel to treat C6 glioma in vitro. Pharm. Res. 23 (2006) 1817–1826.

[137] J. Han, H.T. Zhang, L.M. Zhu, and C.J. Branford-White. Electrospun biodegradable nanofiber mats for controlled release of herbal medicine. 3rd Int. Conf. Bioinforma. Biomed. Eng. ICBBE 2009. (2009) 1–4.

[138] J.H. Ko, H. Yin, J. An, D.J. Chung, J.H. Kim, S.B. Lee, and D.G. Pyun. Characterization of cross-linked gelatin nanofibers through electrospinning. Macromol. Res. 18 (2010) 137–143.

[139] F. Ignatious, L. Sun, C.-P. Lee, and J. Baldoni. Electrospun Nanofibers in Oral Drug Delivery. Pharm. Res. 27 (2010) 576–588.

[140] A. Akhgari, Z. Shakib, and S. Sanati. A review on electrospun nanofibers for oral drug delivery. Nanomedicine J. 4 (2017) 197–207.

[141] DC Aduba, JA Hammer, Q Yuan, WA Yeudall, GL Bowlin, and H. Yang. Semi-interpenetrating network (sIPN) gelatin nanofiber scaffolds for oral mucosal drug delivery. Acta Biomater 9(5) (2013) 6576-6584.

[142] F. Ignatious. Nanofibers: electrospun, oral drug delivery. Encycl. Biomed. Polym. Polym. Biomater. (2015) 5226–5238.

[143] G.L. Bowlin, G. Simpson, E.H. Sanders, and G.E. Wnek. Release of tetracycline hydrochloride from electrospun poly (ethylene-co- vinylacetate), poly (lactic acid),

and a blend Release of tetracycline hydrochloride from electrospun poly (ethylene-co-vinylacetate), poly (lactic acid), and a blend, J. Control. Release 81 (2002) 57–64.

[144] E.-R. Kenawy, F.I. Abdel-Hay, M.H. El-Newehy, and G.E. Wnek. Processing of polymer nanofibers through electrospinning as drug delivery systems. Mater. Chem. Phys. 113 (2009) 296–302.

[145] S.K. Bhullar, and H.S. Buttar. Nanofiber devices for the targeted-delivery of therapeutically active plant and herbal ingredients. Biomed. Rev. 26 (2015) 37–42.

[146] M. Zamani, M.P. Prabhakaran, and S. Ramakrishna. Advances in drug delivery via electrospun and electrosprayed nanomaterials. Int. J. Nanomedicine. 8 (2013) 2997–3017.

[147] S. Ramakrishna, K. Fujihara, W. Teo, T. Yong, and R. Ramaseshan. Electrospun nanofibers: solving global issues. Mater. Today 9 (2006) 40–50.

[148] R. Sridhar, R. Lakshminarayanan, K. Madhaiyan, V. Amutha Barathi, K.H.C. Lim, and S. Ramakrishna. Electrosprayed nanoparticles and electrospun nanofibers based on natural materials: applications in tissue regeneration, drug delivery and pharmaceuticals. Chem. Soc. Rev. 44 (2015) 790–814.

[149] K.P. Chellamani, R.S.V. Balaji, D. Veerasubramanian, and J. Sudharsan. Wound Healing Ability of Herbal Drug Incorporated PCL (Poly (ε -caprolactone)) Wound Dressing, J. Acad. Ind. Res. 2 (2014) 622–626.

[150] P. Sikareepaisan, A. Suksamrarn, and P. Supaphol. Electrospun gelatin fiber mats containing a herbal— *Centella asiatica* —extract and release characteristic of asiaticoside. Nanotechnology 19 (2008) 15102.

[151] D.N. Heo, D.H. Yang, J.B. Lee, M.S. Bae, J.H. Kim, S.H. Moon, H.J. Chun, C.H. Kim, H.N. Lim, and I.K. Kwon. Burn-wound healing effect of gelatin/polyurethane nanofiber scaffold containing silver-sulfadiazine. J. Biomed. Nanotechnol. 9 (2013) 511–515.

[152] W. Cui, Y. Zhou, and J. Chang. Electrospun nanofibrous materials for tissue engineering and drug delivery. Sci. Technol. Adv. Mater. 11 (2010) 14108.

[153] G.B. Yin, Y.Z. Zhang, S.D. Wang, D.B. Shi, Z.H. Dong, and W.G. Fu. Study of the electrospun PLA/silk fibroin-gelatin composite nanofibrous scaffold for tissue engineering. J. Biomed. Mater. Res. - Part A. 93 (2010) 158–163.

[154] M.S. Kim, I. Jun, Y.M. Shin, W. Jang, S.I. Kim, and H. Shin. The development of genipin-crosslinked poly(caprolactone) (PCL)/gelatin nanofibers for tissue engineering applications. Macromol. Biosci. 10 (2010) 91–100.

[155] Y. Zhang, Z. Huang, X. Xu, C.T. Lim, and S. Ramakrishna. Preparation of core - shell

structured PCL-r-Gelatin bi-component nanofibers by coaxial electrospinning. 12 (2004) 3406–3409.

[156] U. Paaver, J. Heinämäki, I. Laidmäe, A. Lust, J. Kozlova, E. Sillaste, K. Kirsimäe, P. Veski, and K. Kogermann. Electrospun nano fibers as a potential controlled-release solid dispersion system for poorly water-soluble drugs. Int. J. Pharm. 479 (2015) 252–260.

[157] S. Ramakrishna, K. Fujihara, W.E Teo, T.C Lim and Z. Ma. An Introduction to Electrospinning and Nanofibers, 2005.

[158] J. Zeng, X. Xu, X. Chen, Q. Liang, X. Bian, L. Yang, and X. Jing. Biodegradable electrospun fibers for drug delivery. J. Control. Release. 92 (2003) 227–231.

[159] T.J. Sill, and H.A. von Recum. Electrospinning: Applications in drug delivery and tissue engineering. Biomaterials. 29 (2008) 1989–2006.

[160] D.C. Aduba, J.A. Hammer, Q. Yuan, W. Andrew Yeudall, G.L. Bowlin, and H. Yang. Semi-interpenetrating network (sIPN) gelatin nanofiber scaffolds for oral mucosal drug delivery. Acta Biomater. 9 (2013) 6576–6584.

[161] C.H. Huang, C.Y. Chi, Y.S. Chen, K.Y. Chen, P.L. Chen, and C.H. Yao. Evaluation of proanthocyanidin-crosslinked electrospun gelatin nanofibers for drug delivering system. Mater. Sci. Eng. C. 32 (2012) 2476–2483.

[162] H. Nie, J. Li, A. He, S. Xu, Q. Jiang, and C.C. Han. Carrier system of chemical drugs and isotope from gelatin electrospun nanofibrous membranes. Biomacromolecules. 11 (2010) 2190–2194.

[163] A.L. H. Wang, Y. Feng, H. Zhao, J.Lu, J. Guo, M. Behl, Controlled heparin release from electrospun gelatin fibers, J. Control. Release. 152 (2011) e26-8.

[164] Y.Z. Zhang, J. Venugopal, Z.M. Huang, C.T. Lim, and S. Ramakrishna. Crosslinking of the electrospun gelatin nanofibers, Polymer. 47 (2006) 2911–2917.

[165] M.A. Oraby, A.I. Waley, A.I. El-dewany, E.A. Saad, and M.A. El-hady. Electrospun gelatin nanofibers : effect of gelatin concentration on morphology and fiber diameters. Journal of Applied Sciences Research, 9(1) (2013) 534-540,

[166] K. Jalaja, P.R.A. Kumar, T. Dey, S.C. Kundu, and N.R. James. Modified dextran cross-linked electrospun gelatin nanofibres for biomedical applications. Carbohydr. Polym. 114 (2014) 467–475.

[167] D. Yang, Y. Li, and J. Nie. Preparation of gelatin/PVA nanofibers and their potential application in controlled release of drugs. Carbohydr. Polym. 69 (2007) 538–543.

[168] Y.J. Son, W.J. Kim, and H.S. Yoo. Therapeutic applications of electrospun nanofibers for drug delivery systems. Arch. Pharm. Res. 37 (2014) 69–78.

[169] D. Das, R. Das, P. Ghosh, S. Dhara, A.B. Panda, and S. Pal. Dextrin cross linked with poly(HEMA): a novel hydrogel for colon specific delivery of ornidazole, RSC Adv. 3 (2013) 25340.

[170] L. Moroni, R. Licht, J. de Boer, J.R. de Wijn, and C.A. van Blitterswijk. Fiber diameter and texture of electrospun PEOT/PBT scaffolds influence human mesenchymal stem cell proliferation and morphology, and the release of incorporated compounds. Biomaterials 27 (2006) 4911–4922.

[171] K. Nayani, H. Katepalli, C.S. Sharma, A. Sharma, S. Patil, and R. Venkataraghavan. Electrospinning combined with nonsolvent-induced phase separation to fabricate highly porous and hollow submicrometer polymer fibers. Ind. Eng. Chem. Res. 51 (2012) 1761–1766.

[172] A.P.S. Immich, M.L. Arias, N. Carreras, R.L. Boemo, and J.A. Tornero. Drug delivery systems using sandwich configurations of electrospun poly(lactic acid) nanofiber membranes and ibuprofen. Mater. Sci. Eng. C. 33 (2013) 4002–4008.

[173] T. Okuda, K.Tominaga, and S.Kidoaki.Time-programmed dual release formulation by multilayered drug-loaded nanofiber meshes. J. Control. Release. 143 (2010) 258–264.

[174] T.S. Anirudhan, and A.M. Mohan. Novel pH switchable gelatin based hydrogel for the controlled delivery of the anti cancer drug 5-fluorouracil. RSC Adv. 4 (2014) 12109.

[175] B. Dekyndt, J. Verin, C. Neut, F. Siepmann, and J. Siepmann. How to easily provide zero order release of freely soluble drugs from coated pellets. Int. J. Pharm. 478 (2015) 31–38.

[176] F. Yao, and J.K. Weiyuan. Drug release kinetics and transport mechanisms of non-degradable and degradable polymeric delivery systems. Expert Opin. Drug Deliv. 7 (2010) 429–444.

[177] A.I. Raafat. Gelatin based pH-sensitive hydrogels for colon-specific oral drug delivery: synthesis, characterization, and in vitro release study. J. of Applied Polymer Sci. 118 (2010) 2642–2649.

[178] W. Lu, M. Ma, H. Xu, B. Zhang, X. Cao, and Y. Guo. Gelatin nano fibers prepared by spiral-electrospinning and cross-linked by vapor and liquid-phase glutaraldehyde. 140 (2015) 1–4.

[179] A.M. Hillery. Supramolecular lipidic drug delivery systems: From laboratory to clinic A review of the recently introduced commercial liposomal and lipid-based formulations of amphotericin B. Adv. Drug Deliv. Rev. 24 (1997) 345–363.

[180] S. Hartsel, and J. Bolard. Amphotericin B: new life for an old drug. Trends Pharmacol Sci. 17 (1996) 445–449.

[181] C. Gates, and R.J. Pinney. Amphotericin B and its delivery by liposomal and lipid formulations. J. Clin. Pharm. Ther. 18 (1993) 147–153.

[182] S. Das, and P.K. Suresh. Nanosuspension: A new vehicle for the improvement of the delivery of drugs to the ocular surface. Application to amphotericin B, Nanomed Nanotech, Biol. Med. 7 (2011) 242–247.

[183] D.A. Kafetzis, I.M. Velissariou, S. Stabouli, M. Mavrikou, D. Delis, and G. Liapi, Treatment of paediatric visceral leishmaniasis: Amphotericin B or pentavalent antimony compounds?, Int. J. Antimicrob. Agents. 25 (2005) 26–30.

[184] Ş. Köse, S.Ö. Töz, İ.C. Balcioğlu, A. Olut, M. Korkmaz, and Y. Özbel. Case Report : Treatment of Kala-Azar by Amphotericin B Lipid Complex (ABELCET ®). 28 (2004) 126–128.

[185] C. Thakur. Impact of Amphotericin B in the Tx of VL on the incidence of PKDL in India, Indian J Med Res. 128 (2008) 38–44.

[186] J. Seaman, C. Boer, R. Wilkinson, J. D. Jong, E.D. Wilde, E. Sondorp, and R. Davidson. Liposomal Amphotericin B (AmBisome) in the Treatment of Complicated Kala-Azar Under Field Conditions. Clin. Infect. Dis. 21 (1995) 183-193.

[187] B.G. Yu, T. Okano, K. Kataoka, and G. Kwon. Polymeric micelles for drug delivery: Solubilization and haemolytic activity of amphotericin B. J. Control. Release. 53 (1998) 131–136.

[188] A.V. Ambade, E. N. Savariar, and S. Thayumanavan. Dendrimeric micelles for controlled drug release and targeted delivery. Mol Pharm. 2005 ; 2(4): 264–272

[189] A. Safdar, J. Ma, F. Saliba, B. Dupont, J.R. Wingard, R.Y. Hachem, G.N. Mattiuzzi, P.H. Chandrasekar, D.P. Kontoyiannis, K. V. Rolston, T.J. Walsh, R.E. Champlin, and I.I. Raad. Drug-Induced Nephrotoxicity Caused by Amphotericin B Lipid Complex and Liposomal Amphotericin B. Medicine 89 (2010) 236–244.

[190] K. Sau, S.S. Mambula, E. Latz, P. Henneke, D.T. Golenbock, and S.M. Levitz. The antifungal drug amphotericin B promotes inflammatory cytokine release by a toll-like receptor- and CD14-dependent mechanism. J. Biol. Chem. 278 (2003) 37561–37568.

[191] H.G. Prentice, I.M. Hann, R. Herbrecht, M. Aoun, S. Kvaloy, D. Catovsky, C.R. Pinkerton, S.A. Schey, F. Jacobs, A. Oakhill, others, R.F. Stevens, P.J. Darbyshire, and B.E. Gibson. A randomized comparison of liposomal versus conventional amphotericin B for the treatment of pyrexia of unknown origin in neutropenic patients. Br. J. Haematol. 98 (1997) 711–718.

[192] A. Lavasanifar, J. Samuel, and G.S. Kwon. The effect of fatty acid substitution on the in vitro release of amphotericin B from micelles composed of poly (ethylene oxide)-

block-poly (N-hexyl stearate-L-aspartamide). J. Control. Release. 79 (2002) 165–172.

[193] W. Tiyaboonchai, and N. Limpeanchob. Formulation and characterization of amphotericin B-chitosan-dextran sulfate nanoparticles. Int. J. Pharm. 329 (2007) 142–149.

[194] H. Van De Ven, C. Paulussen, P.B. Feijens, A. Matheeussen, P. Rombaut, P. Kayaert, G. Van Den Mooter, W. Weyenberg, P. Cos, L. Maes, and A. Ludwig. PLGA nanoparticles and nanosuspensions with amphotericin B: Potent in vitro and in vivo alternatives to Fungizone and AmBisome. J. Control. Release. 161 (2012) 795–803.

[195] B.T. AL-Quadeib, M.A. Radwan, L. Siller, B. Horrocks, and M.C. Wright. Stealth Amphotericin B nanoparticles for oral drug delivery: In vitro optimization. Saudi Pharm. J. 23 (2014) 290–302.

[196] K.M. Wasan, E.K. Wasan, P. Gershkovich, X. Zhu, R.R. Tidwell, K. a Werbovetz, J.G. Clement, and S.J. Thornton. Highly effective oral amphotericin B formulation against murine visceral leishmaniasis. J. Infect. Dis. 200 (2009) 357–360.

[197] J.L. Italia, M.M. Yahya, D. Singh, M.N. and V Ravi Kumar. Biodegradable nanoparticles improve oral bioavailability of amphotericin B and show reduced nephrotoxicity compared to intravenous fungizone®. Pharm. Res. 26 (2009) 1324–1331.

[198] G. Buschle-Diller, J. Cooper, Z. Xie, Y. Wu, J. Waldrup, and X. Ren. Release of antibiotics from electrospun bicomponent fibers. Cellulose. 14 (2007) 553–562.

[199] M. Sedlák, M. Pravda, F. Staud, L. Kubicová, K. Týčová, and K. Ventura. Synthesis of pH-sensitive amphotericin B-poly(ethylene glycol) conjugates and study of their controlled release in vitro. Bioorganic Med. Chem. 15 (2007) 4069–4076.

[200] H. Sekhar Nanda, and N. Chandra Mishra "Amphotericin B" Loaded Natural Biodegradable Nanofibers as a Potential Drug Delivery System against Leishmaniasis. Curr. Nanosci. 7 (2011) 943–949.

[201] M. Nahar, D. Mishra, V. Dubey, and N.K. Jain. Development, characterization, and toxicity evaluation of amphotericin B-loaded gelatin nanoparticles. Nanomedicine Nanotechnology, Biol. Med. 4 (2008) 252–261.

[202] S. Jain, P.U. Valvi, N.K. Swarnakar, and K. Thanki. Gelatin Coated Hybrid Lipid Nanoparticles for Oral Delivery of Amphotericin B. Mol. Pharm. 9 (2012) 2542–2553.

[203] S. Panzavolta, M. Gioffrè, M.L. Focarete, C. Gualandi, L. Foroni, and A. Bigi. Electrospun gelatin nanofibers: Optimization of genipin cross-linking to preserve fiber morphology after exposure to water. Acta Biomater. 7 (2011) 1702–1709.

[204] Pachauri M, Gupta ED, Ghosh PC. Piperine loaded PEG-PLGA nanoparticles: preparation, characterization, and targeted delivery for adjuvant breast cancer chemotherapy. J Drug Delivery Sci Technol. 29 (2015) 269–82.

[205] Elnaggar YS, Etman SM, Abdelmonsif DA, Abdallah OY. Intranasal piperine-loaded chitosan nanoparticles as brain-targeted therapy in Alzheimer's disease: optimization, biological efficacy, and potential toxicity. J Pharm Sci. 104 (2015) 3544–56.

[206] Yusuf M, Khan M, Khan RA, Ahmed B. Preparation, characterization, *in vivo*, and biochemical evaluation of brain targeted Piperine solid lipid nanoparticles in an experimentally induced Alzheimer's disease model. J Drug Targeting. 21 (2013) 300–11.

[207] Veerareddy P, Vobalaboina V. Pharmacokinetics and tissue distribution of piperine lipid nanospheres. Die Pharmazie- Int J Pharmac Sci. 63 (2008) 352–5.

[208] Pentak D. *In vitro* spectroscopic study of piperine-encapsulated nanosize liposomes. Eur Biophys J. 45 (2016) 175–86.

[209] Jain S, Meka SRK, Chatterjee K. Engineering a piperine eluting nanofibrous patch for cancer treatment. ACS Biomater Sci Eng. 2 (2016) 1376–85.

[210] Shao B, Cui C, Ji H, Tang J, Wang Z, Liu H, Qin M, Li X, Wu L. Enhanced oral bioavailability of piperine by self-emulsifying drug delivery systems: *in vitro, in vivo* and *in situ*intestinal permeability studies. Drug Deliv. 22 (2015) 740–7.

[211] Boddupalli BM, Ramani R, Subramaniam B, Anisetti RN. *In vitro* and *in vivo* evaluation of hepato-protection and anti-ulcer activities of piperine gastro retentive micropspheres. Asian Pac J Trop Biomed 2 (2012) 1237–40.

[212] Ashour EA, Majumdar S, Alsheteli A, Alshehri S, Alsulays B, Feng X, Gryczke A, Kolter K, Langley N, Repka MA. Hot melt extrusion as an approach to improve solubility, permeability, and oral absorption of a psychoactive natural product, piperine. J Pharm Pharmacol. 68 (2016) 989–98.

Appendix A

Table A1: Piperine loaded different drug delivery vehicles with various kinds of excipients

	DSSs	Excipients	References
1	**Nanoparticle**	**Poly (ethylene glycol)-poly (lactic-co-glycolic acid)**	**[204]**
2	**Nanoparticle**	**Chitosan**	**[205]**
3	**Solid-lipid Nanoparticles**	**Polysorbate-80 coated piperine solid-lipid nanoparticles (PS-80-PIP-SLN)**	**[206]**
4	**Lipid Nanospheres**	**Positively charged stearylamine (LN-P-SA) and pegylated lipid nanospheres (LN-P-PEG)**	**[207]**
5	**Nanosize Liposomes**	**L-α-phosphatidylcholine dipalmitoyl (DPPC)**	**[208]**
6	**Nanofiber patch**	**poly(ε-caprolactone) (PCL) and gelatin (GEL) blends**	**[209]**
7	**Self-emulsifying drug delivery systems (SEDDS)**	**Ethyl oleate, Transcutol P, and Tween 80 were used as the oil phase, co-surfactant, and surfactant, respectively**	**[210]**
8	**Floating microspheres, Mucoadhessive microspheres**	**In floating microspheres, ethyl cellulose, hydroxy propyl methyl cellulose and calcium carbonate were used as polymers. In mucoadhessive microspheres ethyl cellulose, hydroxy propyl methyl cellulose and carbopal were used.**	**[211]**
9	**Hot melt extrusion (HME)**	**Soluplus®, polyvinylpyrrolidone-co-vinylacetate 64 (Kollidon® VA 64), and Eudragit® EPO**	**[212]**
10	**Hydrogel**	**Sodium alginate/gelatin**	**[63]**

Appendix B

Chapter 2

Table B1: Drug concentration Vs Time for release profile of piperine (pH 7.4) from gelatin cast-film (Section 2.5, Figure: 2.6 (a), Page number: 32)

Concentration vs time for release profile of piperine (pH 7.4)						
Time (min)	**A2 (µg/ml)**	**A3 (µg/ml)**	**A4 (µg/ml)**	**B2 (µg/ml)**	**B3 (µg/ml)**	**B4 (µg/ml)**
0	**0**	**0**	**0**	**0**	**0**	**0**
5	**16.9**	**11.4**	**8.8**	**12.9**	**12.9**	**10.6**
10	**32.9**	**28.5**	**25.1**	**22.7**	**22.7**	**23.7**
20	**58.6**	**43.4**	**34.4**	**34.7**	**34.7**	**31.3**
60	**85.5**	**86.9**	**77.7**	**59.3**	**59.3**	**57.2**
120	**116.4**	**98.8**	**83.3**	**77.3**	**77.3**	**76.4**
240	**163.3**	**162.7**	**138.8**	**116.8**	**116.8**	**102.1**
480	**184.4**	**177.6**	**168.9**	**159.9**	**159.9**	**140.5**
1440	**190.5**	**188.1**	**179.7**	**176.8**	**174.4**	**159.9**
Concentration vs time for release profile of piperine (pH 7.4)						
Time (min)	**C2 (µg/ml)**	**C3 (µg/ml)**	**C4 (µg/ml)**	**D2 (µg/ml)**	**D3 (µg/ml)**	**D4 (µg/ml)**
0	**0**	**0**	**0**	**0**	**0**	**0**
5	**11.9**	**10.7**	**11.6**	**8.1**	**6.2**	**4.1**
10	**22.1**	**16.3**	**17.9**	**15.7**	**10.8**	**7.7**
20	**37.1**	**35.2**	**31.7**	**25.6**	**16.9**	**15.1**
60	**46.9**	**43.5**	**41.7**	**33.1**	**25.0**	**19.1**
120	**72.9**	**55.3**	**59.8**	**57.7**	**43.1**	**35.7**
240	**106.0**	**97.6**	**88.3**	**95.0**	**66.3**	**61.1**
480	**131.2**	**128.6**	**124.1**	**116.8**	**97.3**	**86.7**
1440	**149.6**	**147.7**	**136.4**	**127.6**	**115.3**	**109.3**

Table B2: Drug concentration Vs Time for release profile of piperine (pH 1.2) from gelatin cast-film (Section 2.5, Figure: 2.7 (a), Page number: 32)

Concentration vs time for release profile of piperine (pH 1.2)						
Time (min)	**A2 (µg/ml)**	**A3 (µg/ml)**	**A4 (µg/ml)**	**B2 (µg/ml)**	**B3 (µg/ml)**	**B4 (µg/ml)**
0	**0**	**0**	**0**	**0**	**0**	**0**
5	**5.1**	**6.2**	**3.9**	**3.8**	**3.8**	**3.1**
10	**13.4**	**10.3**	**6.5**	**7.6**	**5.7**	**5.0**
20	**20.1**	**16.2**	**11.9**	**9.7**	**7.5**	**9.5**
60	**31.8**	**23.9**	**17.7**	**18.1**	**12.9**	**12.9**
120	**36.6**	**38.5**	**30.5**	**23.5**	**18.4**	**18.5**
240	**42.3**	**41.7**	**39.9**	**32.8**	**26.5**	**30.9**
480	**49.5**	**44.8**	**40.6**	**36.9**	**35.5**	**42.1**
Concentration vs time for release profile of piperine (pH 1.2)						
Time (min)	**C2 (µg/ml)**	**C3 (µg/ml)**	**C4 (µg/ml)**	**D2 (µg/ml)**	**D3 (µg/ml)**	**D4 (µg/ml)**
0	**0**	**0**	**0**	**0**	**0**	**0**
5	**3.3**	**4.0**	**4.0**	**2.4**	**2.4**	**2.4**
10	**5.0**	**7.3**	**7.0**	**7.6**	**7.1**	**7.1**
20	**11.8**	**9.8**	**12.9**	**12.5**	**12.5**	**11.5**
60	**13.1**	**12.1**	**13.3**	**14.5**	**11.3**	**11.3**
120	**18.7**	**18.4**	**18.7**	**21.3**	**18.9**	**18.9**
240	**40.1**	**31.9**	**28.6**	**27.3**	**24.5**	**22.6**
480	**44.0**	**43.5**	**42.1**	**33.7**	**33.0**	**28.8**

Chapter 3:

Table B3: Drug concentration Vs Time for release profile of piperine from G-P NFCX based DDS (Section: 3.7.1, Figure 3.6, Page number: 51)

Concentration vs time for release profile of piperine (sample: G-PNFC4)				
Time (min)	**pH 8 (µg/ml)**	**pH 7.4 (µg/ml)**	**pH 6.8 (µg/ml)**	**pH 1.2 (µg/ml)**
0	**0**	**0**	**0**	**0**
5	**9.4**	**8.2**	**6.5**	**5.2**
10	**16.6**	**15.3**	**11.0**	**7.3**
20	**26.9**	**22.8**	**17.3**	**14.4**
60	**39.4**	**33.3**	**25.4**	**23.2**
120	**43.6**	**39.5**	**34.4**	**29.1**
240	**47.7**	**44.4**	**41.0**	**35.3**
480	**52.3**	**49.1**	**46.8**	**39.1**
1440	**57.4**	**54.3**	**49.6**	**46.6**
Concentration vs time for release profile of piperine (sample: G-PNFC6)				
Time (min)	**pH 8 (µg/ml)**	**pH 7.4 (µg/ml)**	**pH 6.8 (µg/ml)**	**pH 1.2 (µg/ml)**
0	**0**	**0**	**0**	**0**
5	**6.4**	**5.2**	**3.5**	**2.2**
10	**9.3**	**8.6**	**7.4**	**6.2**
20	**16.7**	**11.4**	**10.5**	**9.9**
60	**29.3**	**21.4**	**17.1**	**14.7**
120	**37.6**	**35.2**	**33.2**	**27.3**
240	**41.6**	**39.0**	**37.3**	**35.0**
480	**43.2**	**40.6**	**39.0**	**37.1**
1440	**52.6**	**51.3**	**46.5**	**43.5**
Concentration vs time for release profile of piperine (sample: G-PNFC8)				
Time (min)	**pH 8 (µg/ml)**	**pH 7.4 (µg/ml)**	**pH 6.8 (µg/ml)**	**pH 1.2 (µg/ml)**
0	**0**	**0**	**0**	**0**
5	**5.8**	**3.3**	**2.8**	**2.2**
10	**7.5**	**7.4**	**5.0**	**3.2**
20	**15.4**	**11.5**	**9.4**	**7.6**
60	**17.9**	**20.1**	**13.5**	**12.8**
120	**30.3**	**29.3**	**23.1**	**18.3**
240	**35.6**	**33.2**	**27.1**	**25.9**
480	**40.8**	**35.8**	**33.1**	**30.7**
1440	**43.6**	**39.2**	**37.5**	**35.6**

Chapter 4:

Table B4: Drug concentration Vs Time for release profile of piperine from sample F with different piperine concentrations (Section: 4.5.1, Figure 4.7, Page number: 67)

Concentration vs time for release profile of piperine (sample: F)					
Time (h)	**(1.5mg/ml drug) (µg/ml)**	**(2 mg/ml drug) (µg/ml)**	**(2.5mg/ml drug) (µg/ml)**	**(3.5mg/ml drug) (µg/ml)**	**(3.5mg/ml drug) with sequential crosslinking (µg/ml)**
0	**0**	**0**	**0**	**0**	**0**
0.5	**1.1**	**1.1**	**1.8**	**4.2**	**2.3**
1	**2.0**	**1.9**	**2.6**	**6.9**	**2.9**
2	**2.1**	**2.8**	**4.3**	**11.6**	**4.3**
4	**3.0**	**4.8**	**6.6**	**17.1**	**5.3**
6	**5.2**	**10.0**	**13.1**	**22.2**	**8.9**
8	**9.3**	**13.8**	**17.4**	**26.7**	**11.2**
12	**13.3**	**17.9**	**22.1**	**31.4**	**18.4**
24	**20.2**	**27.6**	**31.1**	**43.4**	**38.8**
48	**30.2**	**37.6**	**43.4**	**63.8**	**58.1**

Chapter 5:

Table B5: Drug concentration Vs Time for release profile of piperine (Section: 5.5, Figure 5.4, Page number: 82)

Concentration vs time for release profile of piperine			
Time (h)	**(G-P NF C6) (µg/ml)**	**(G-P NF SC6) (µg/ml)**	**(SG-P NF SC6) (µg/ml)**
0	**0**	**0**	**0**
0.0833	**3.3**	**2.1**	**1.9**
0.1667	**7.4**	**4.1**	**3.4**
0.3333	**11.5**	**8.1**	**6.9**
1	**20.1**	**10.5**	**9.1**
2	**23.3**	**13.6**	**11.3**
4	**29.0**	**18.1**	**15.3**
8	**34.6**	**24.4**	**22.9**
12	**37.3**	**27.1**	**25.6**
24	**40.4**	**33.1**	**31.1**

Chapter 6:

Table B6: Drug concentration Vs Time for release profile of Amphotericin B from CNOT SC8
(Section: 6.6, Figure 6.5, Page number: 94)

Concentration vs time for release profile of Amphotericin B	
Time (h)	**Sample: CNOT SC8 (µg/ml)**
0	**0**
1	**22.6**
2	**32.4**
4	**44.0**
8	**50.4**
12	**75.2**
24	**114.4**
36	**135.3**
48	**161.7**
72	**213.3**
96	**257.7**
120	**333.7**
144	**377.6**
168	**420.5**
192	**452.9**
216	**485.2**
240	**496.4**

Appendix C

Table C1: Standard curve for piperine in PBS (pH 7.4)

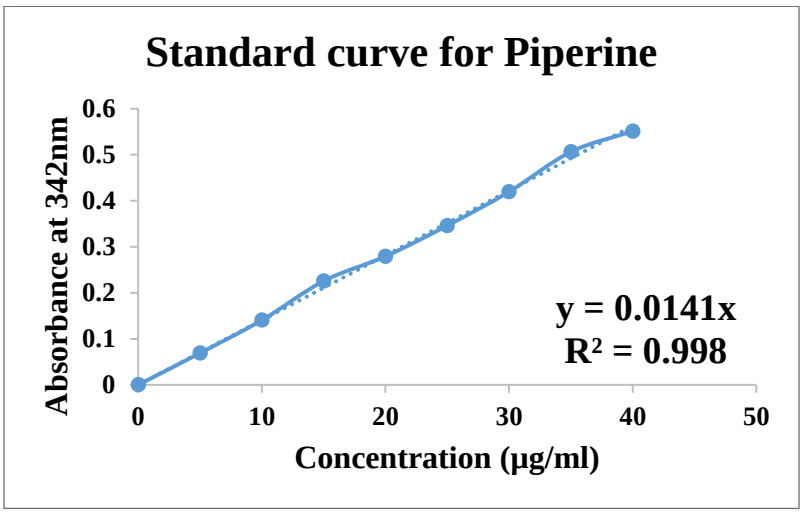

Table C2: Standard curve for Amphotericin-B in PBS (pH 7.4)